



I L L I N O I S

UNIVERSITY OF ILLINOIS AT URBANA-CHAMPAIGN

-

PRODUCTION NOTE

University of Illinois at
Urbana-Champaign Library
Large-scale Digitization Project, 2007.

UNIVERSITY OF ILLINOIS
COLLEGE OF ENGINEERING

ENGINEERING EXPERIMENT STATION
BULLETIN 468

**SURFACE FAILURE OF
BEARINGS AND OTHER
ROLLING ELEMENTS**

By

G. J. MOYAR

Formerly Assistant Professor*

JoDEAN MORROW

Associate Professor

ENGINEERING EXPERIMENT STATION
BULLETIN 468

**SURFACE FAILURE OF
BEARINGS AND OTHER
ROLLING ELEMENTS**

By

G. J. MOYAR

Formerly Assistant Professor*

JO DEAN MORROW

Associate Professor

*Presently with Knolls Atomic Power Laboratory,
General Electric Company, Schenectady, New
York

Price: \$2.00

Edited by

R. Alan Kingery

UNIVERSITY OF ILLINOIS BULLETIN

Volume 62, Number 35; November, 1964. Published nine times each month by the University of Illinois. Entered as second-class matter December 11, 1912, at the post office at Urbana, Illinois, under the Act of August 24, 1912. Office of Publication, 114 Altgeld Hall, Urbana, Illinois.

PREFACE

This bulletin represents a summary of research into the failure of surfaces in rolling contact conducted in the Department of Theoretical and Applied Mechanics from 1957 to 1962. Two theses and several unpublished departmental and industrial research reports were prepared during this period which are no longer available. The purpose of this bulletin is to bring the past work together into one publication which is easily available to the engineer and researcher interested in rolling contact. It should serve as an introduction to the mechanics of surface failures in rolling elements and as a model for the systematic treatment of some of the problem areas involved.

ACKNOWLEDGEMENT

Correspondence and visits with the following persons have been stimulating and helpful:

J. Lawrence and T. Tallian, SKF Industries, Inc.
H. R. Neifert and O. J. Horger, Timken Roller Bearing Company
E. N. Bamberger and R. A. Baughman, Flight Propulsion Division, General Electric Company
W. J. Greenert and W. V. Smith, U.S. Naval Engineering Experiment Station
M. E. Otterbein, Hyatt Bearings Division
B. Kelley, Caterpillar Tractor Co.
C. M. Allen, Battelle Memorial Institute

Some of the initial rolling contact research was supported by the University of Illinois Engineering Experiment Station. The Timken Roller Bearing Company contributed specimens during this phase, and SKF Industries supported part of the work through a research grant in 1960.

We acknowledge the advice and assistance of Prof. G. M. Sinclair of the H. F. Moore Fracture Research Laboratory throughout the research program. Discussions with Prof. T. J. Dolan, Head of the Department, Prof. J. O. Smith and other members of the Theoretical and Applied Mechanics Department Staff, as well as Prof. E. I. Radzimovsky of the Mechanical Engineering Department, have contributed greatly to this research. We greatly appreciate the help of Mrs. Ruth Moyer and Mrs. H. Corray in preparing the manuscript.

ABSTRACT

TWO MODES OF SURFACE FAILURE IN ROLLING ELEMENTS, FATIGUE PITTING AND CUMULATIVE PLASTIC DEFORMATION, ARE CONSIDERED IN THIS PUBLICATION. SPECIAL ATTENTION IS GIVEN TO THE DEVELOPMENT OF RATIONAL METHODS OF DATA CORRELATION AND TO THE ELIMINATION OF SIZE AND CONFIGURATION EFFECTS IN STANDARD LABORATORY, BENCH RIG, AND FULL SCALE BEARING TESTS. AN EXAMINATION OF THE COMPLEX LOADING CYCLE INDUCED IN THE ELEMENTS BY THE ROLLING ACTION, AND ITS SIGNIFICANCE WITH REGARD TO THE FATIGUE AND CYCLE-DEPENDENT STRESS-STRAIN MATERIAL CHARACTERISTICS, IS MADE FOR BOTH PHENOMENA.

INCLUDED IS A CLASSIFICATION OF RESEARCH AND AN EXPANDED LITERATURE REVIEW PERTINENT TO THESE FAILURES, AS WELL AS EXCESSIVE ROLLING RESISTANCE. EMPHASIS IS PLACED ON THE NEED FOR ROLLING CONTACT TESTS IN WHICH FORCES AND RELATIVE MOTIONS ARE KNOWN AND CONTROLLED.

CONTENTS

I. INTRODUCTION	1
II. ANALYSIS OF THE PITTING MODE OF FAILURE	4
A. Effect of Rolling Element Configuration on Pitting	4
B. Analysis of Critical Stress in Pure Rolling	7
C. Discussion of the Mechanism of Pitting	9
D. Statistical Considerations in Fatigue Pitting	11
E. Consideration of Plastic Deformation	12
III. CORRELATION OF PITTING FAILURES	14
A. Correlation of Pitting and Torsion Fatigue Strength	14
B. Correlation of Bench Rig Life Data	19
C. Correlation of Bench Rig and Full Scale Bearing Data	20
IV. ANALYSIS OF CUMULATIVE DEFORMATION	25
A. Preliminary Consideration of Externals	25
B. Plastic Deformation in Rolling Contact	28
C. Associated Phenomena	33
V. SUMMARY AND CONCLUSIONS	36
A. Review	36
B. Analysis	37
VI. RECOMMENDATIONS	39
A. Pitting	39
B. Cumulative Deformation	39
C. Excessive Rolling Resistance	40
D. General	40
VII. APPENDIX A (RESEARCH CLASSIFICATION)	41
A. Modes of Failure	41
B. Phases of Research	42
VIII. APPENDIX B (LITERATURE REVIEW)	44
A. Pitting	44
B. Cumulative Deformation	58
C. Excessive Rolling Resistance	64
IX. REFERENCES CITED	70
X. INDEX	81

FIGURES

1. Schematic Illustration of Various Rolling Contact Rig Types
2. Contact Fatigue Data for Several Geometries
3. Effect of Rig Types and Rolling Element Configuration on Pitting Endurance for Three Steels
4. Rolling Contact Rig Used in Cumulative Deformation and Pitting Experiments
5. Rolling Elements Used in Pitting Endurance Test
6. Typical Pitting Failures
7. Range of Orthogonal Shear Stress as a Function of Rolling Element Configuration, e
8. Surface Tensile Stress at Leading Edge of Contact Ellipse as a Function of Rolling Element Configuration, e
9. Incipient Flake on Toroid Specimen A-2
10. Increase in Track Width
11. Geometric Definitions
12. Factor for Track Width Calculation
13. Depth of Maximum Orthogonal Shear Stress
14. Effect of Hydrostatic Pressure on Fatigue (Crossland)
15. S-N Curves for Torsion and Rotating Beam Tests of Hard 52100 Steel (Styri)
16. Successive Steps in Correlation of Data
17. Ratio of Normal to Shear Stress on Plane of Maximum Orthogonal Shear Stress
18. Weibull Plot of Unadjusted Annapolis Data
19. Log-Log Plot of RC Data Showing Slope to be $-1/9$ th
20. Thrust Ball Bearing Data
21. Gel 202K Radial Bearing Data
22. 202S MRC Radial Bearing Data
23. Ideal Pronounced Plastic Deformation

24. Comparison of Theory and Experiment for Pronounced Plastic Deformation
25. Radial Deformation for Elastically Restrained Plastic Blunting
26. Reduction of Contact Stress in Pronounced Plastic Blunting
27. Dimensionless Presentation of Drutowski's Grooving Data
28. Superimposed Traces of Flat Plate Grooved by Rolling Ball
29. Dimensionless Summary of Kraupner and Niemann's Blunting Data and Comparison to Actual Experimental Results
30. Rolling Elements Used in Cumulative Deformation Tests
31. Cyclic Growth of Track Width for Pronounced Plastic Deformation of Brass
32. Cyclic Increase of Radial Deformation for Pronounced Plastic Deformation of Brass
33. Variation of Deviator Stresses at Depth of Maximum Reversing Shear Stress
34. Axial Stress-Plastic Strain Locus for Combined Tension Tests with Annealed Brass
35. Thin Wall Tube Data
36. Kinetics of Lubricated Rolling Disks
37. Effect of Asymmetric Contact Stress on Orthogonal Shear Stress
38. Photos of Mounted Brass Rolling Elements Before Tests
39. Sequence Photos of Rolling Track Grid Deformation in Blunting and Grooving
40. Summary of Eldredges Perfectly Plastic Grooving Analysis

TABLES

1. Summary of Material and Test Conditions for Pitting Endurance Data Presented in Figure 3	6
2. Pitting Endurance Tests	8
3. Description of Specimen Geometry and Material	14
4. Comparison of Essential and Critical Shear for Torsion using Styris Data for Hard 52100	17
5. Successive Adjustments of Pitting Endurance Data for Annapolis 52100 Steel Rolling Elements (Life in Millions)	19
6. Critically Stressed Volume for Annapolis Rolling Elements	20
7. Summary of Bearing Correlation with RC Rig Data	24
8. Octahedral Shear Stress for Initiation of Plastic Deformation of 52100 Steel in Tension, Compres- sion and Rolling Contact	29

This page is intentionally blank.

I. INTRODUCTION

From the initial use of rolling elements to support and transmit loads and provide alignment to present rigorous demands on bearing and gear performance, the failure of these rolling surfaces to function as designed has presented a wide variety of problems. Many scientific and engineering disciplines are involved in the study of these problems. Surface failures range from abrasive wear and surface-lubricant interaction phenomena through pitting, flaking, case crushing, excessive or variable torque and material dimensional instabilities, and depend on the particular environments, materials, types of loading and relative motions. Basic information has come from such fields as the physics and chemistry of surfaces and lubricants, metallurgy and mechanics.

High reliability and high temperature applications have placed greater emphasis on the whole class of problems, accentuating several and presenting new ones. Under this pressure, research (primarily in separate industries) has concentrated on materials evaluation and, in some instances, on the effect of metallurgical variables on one or more of the phenomena associated with a particular failure mode. The use of bench rigs or simulated testers, for reasons of speed and economy of evaluation, has increased in popularity.

Some features of this research may be criticized:

1. Much of the research is scattered, unorganized, and unreported in the technical literature. Industries themselves, recognizing the

state of affairs, have made an initial attempt to correct this by establishing an A.S.M.E. Research Committee on Contact Fatigue of Rolling Elements.^{(1)*}

2. Although the place of the bench rig in accumulating masses of data is important, not enough careful investigations have been conducted employing instruments capable of comprehensively studying the mechanics of the rolling process for a practical range of loads, speeds, and environments.

3. Because of a few discrepancies or lack of direct correlation with standard material tests, certain established principles of material behavior are often ignored.

4. The importance of fundamental research in the rolling contact phenomena is self-evident, but principles for its rational extension to technological application are lacking.

It is particularly in this last category that a contribution out of the discipline of mechanics of solids may be made. The engineering concept of material properties, together with geometric and dynamic principles familiar to the discipline, form a basis for the rational extension of fundamental data to various configurations, sizes, and conditions of material elements in particular applications.

In Appendix A, research limited to those phenomena or failures that are amenable to the field of mechanics are classified. In Appendix B

* Superscript numbers in parenthesis refer to entries in the References Cited section.

past research is critically reviewed according to this classification. The body of this publication is devoted to the investigation and analysis of two important modes of failure (pitting and cumulative deformation). Considerations necessary to extend or correlate bench rig data, and to establish the role of cumulative cycle-dependent plastic strain as an anticipated failure mode in critical high-

temperature applications, are emphasized. Research results from the literature and some unpublished original data collected in the course of this investigation are used in the analysis. The novice to the field of rolling contact is advised to study Appendices A and B before continuing, while the more knowledgeable reader will prefer to proceed, referring to the Appendices as the need arises.

DEFINITION OF TERMS

A	actual contact area	b	semi-minor axis of contact ellipse, otherwise indicates Weibull's slope
B	normal stress influence factor	c	material exponent appearing in Lundberg and Palmgren statistical analysis
B_{10}, B_{50}	lives at 0.10 and 0.50 probability of failure	d	normal force offset in rolling (Fig. 36)
C_e	quantity used to determine track width (Fig. 12)	e	material exponent appearing in Lundberg and Palmgren statistical analysis, otherwise indicates configuration index
D	diameter of a rolling element	h	material exponent appearing in Lundberg and Palmgren statistical analysis, otherwise indicates chord height relating radial deformation and track width
E	modulus of elasticity	k	factor relating Radzimovsky's surface endurance limit to other static strength properties
F	mean probability of failure	k_ϵ	function of bending and torsion fatigue strength
K	percentage increase in track width over theoretical width	ℓ	chord length relating radial deformation and track width
L	track length	u	radial deformation
M	quantity used to determine track length (Fig. 13)	u_E	theoretical approach of elastic bodies in contact
N	number of stress cycles	u_p/u_E	groove depth after 20 cycles - elastic approach of a ball and plate
P	load	w	track width
Q	range of maximum orthogonal shear stress \div maximum contact stress ($2\tau_o/\sigma_{max}$)	w_E	theoretical elastic track width
R	minor principle profile radius	Δ	quantity used to determine track width
R'	major principle profile radius	θ	characteristic life in Weibull cumulative distribution function
R_o	original profile radius	$\Sigma \frac{1}{R}$	sum of reciprocals of principle profile radii
R_p	deformed profile radius	α	size effect exponent
S	probability of survival	β	size effect exponent
T	torque		
V	volume of highly stressed material		
Z_o	depth to maximum orthogonal shear stress		
a	semi-major axis of contact ellipse		
a'	length of contact ellipse in rolling direction		

μ	Poisson's ratio	σ_y	yield strength
σ	normal stress	τ_C	critical shear strength in fatigue
σ_B	bending fatigue strength	τ_T	fatigue strength in torsion
σ_{\max}	maximum contact (Hertz) stress	τ_o	orthogonal shear stress
σ'_{\max}	corrected maximum contact stress	τ_{oct}	octahedral shear stress
σ_n	complimentary normal stress on critical shear plane	τ_{ϵ}	experimentally determined essential shear strength in fatigue
σ_o	normal stress on plane of maximum orthogonal shear stress	ω	angular velocity
σ_t	maximum surface tensile stress		

II. ANALYSIS OF THE PITTING MODE OF FAILURE

Synopsis: This section contains information from many sources that illustrates the effect of bench rig design and/or rolling element configuration on pitting endurance. Significant features are presented of the stress system created by the rolling action, and the mechanism of pitting is discussed with respect to both initiation and propagation. An analysis is given which includes the effect of size of the critically stressed region of material on endurance and the effect of stress level on statistical variability. The change in stress due to plastic deformation of the contacting bodies is also discussed.

The normal end of life for most rolling element mechanisms is by surface pitting or flaking. Such failures have been associated with the usual fatigue process discussed in Appendix B. However, the influence of many features peculiar to the rolling contact situation complicate this already complex process. The metallurgist is deeply involved in discerning what properties of materials are significant in resisting such failure and in developing better materials to prevent it. A wide variety of bench rig tests are used in this type of research (Figure 1).

The purpose here is to examine what valid statements can be made about pitting, apart from the discussion of specific materials, to help eliminate the confusion of specimen configuration and size effects in such research.

In addition to relative evaluation information sought in bench rig testing, there is interest in a more quantitative relation between bench rig data on pitting resistance of a material and its performance in an assembled commercial mechanism. In fact there has been hope expressed from time to time that a correlation between pitting resistance and standard material tests could

be established. It has been popular to refute this hope although as Sachs⁽²⁾ points out, no systematic or conclusive argument has been advanced against the principle of such a correlation.

Complete success in direct correlation, even when the testing conditions in the bench rig are as near to the bearing as possible, cannot be expected at present in the face of such problems as the lack of full dynamic comparison of the rig and bearing, or the effect of rolling element shape and motion on pressure distribution through the usual lubricant film. However, certain important considerations can be made on the basis of existing knowledge that will provide a more rational foundation for the correlation.

It is the purpose of this section to demonstrate the effect of rolling element configuration and size on pitting strength or life and to analyze some factors responsible for this effect. This necessarily involves a proposed mechanism for the initiation and propagation of the fatigue damage under normal rolling conditions. Although the usual inhomogeneities in material contribute to failure as in other fatigue phenomena with especially steep stress gradients, the variation of material properties with depth will not be considered in the following analysis. Thin cased steel presents further complications that will not be included here.

A. EFFECT OF ROLLING ELEMENT CONFIGURATION ON PITTING

A striking demonstration of the influence of rolling element configuration on pitting strength is provided by tests at the U.S. Naval Engineering

Experiment Station at Annapolis. An extensive series of tests of hardened 52100 steel rollers with a major radius of 1.5 inches and a profile radius of 0.25 inches mated with a cylinder of 1.562-inch radius were initially conducted. When in a later series of tests the toroid geometry was changed from 1/4-inch to 1/2-inch radius, unexpected results were obtained. Since this result is of particular significance, the original paper is quoted below:⁽³⁾

Rollers with increased radii in the longitudinal direction were operated in NaK at 250°F and in oil at 110°F. In these rollers, the longitudinal radius of the double curvature element was 0.500" as against 0.250" for standard rollers. Thus, under equivalent loads the stresses induced in these rollers were 80% of those of standard rollers while the theoretical area of contact was greater by 37%. Because of the reduced stress in rolling contact, it was considered that the life of these rollers would be increased considerably beyond that obtained for standard rollers. Increasing the longitudinal radius of the contact rollers did not result in increasing rolling fatigue life. In NaK at 250°F and, more surprising, in oil at 110°F, lower life or load carrying capacity was indicated for rollers with increased radii. In bearing studies, reduced load capacity has been found to result from increasing ball size. Recognition of this fact is incorporated in empirical rating formulae for bearings--. Such reductions are attributed to metallurgical factors associated with the depth of sections. In these rollers, however, section change resulting from the increased radius is slight; as the increase in roller mass was only 0.6%. Thus, it is not seen how metallurgical factors would account for these reductions. Further work on the effect of radius change on rolling fatigue of metallic materials is planned in future work.

Data collected from several sources, including cylindrical and "point" contact, are reported in Reference 4 and summarized graphically in Figure 2. With the exception of the specimens from the General Electric Rolling Contact Rig, all the specimens are 52100 steel of approximately the same hardness. The G. E. specimens are MV-1 tool steel of comparable hardness (Rockwell C 64). In terms of maximum theoretical Hertz stress the apparent fatigue strength for toroidal rollers is several times that for cylindrical rollers. The

theoretical contact area shape is also indicated in Figure 2. The orientation of the contact ellipses is for rolling in the horizontal direction.

Tests are usually conducted at one stress level in rolling contact fatigue programs to determine the effect of material variables. The data are often reported on Weibull probability paper. In this way both mean life and variability can be graphically represented by means of a straight line. Data collected from many sources for three popular steels are presented in Weibull fashion in Figure 3. The ordinate of these plots is

$$\log \log \frac{1}{1-F}$$

where F is the mean (50 percent) probability of failure (see Johnson⁽⁵⁾ for derivation). In order to compare these data on a fair basis, since the actual stress level of tests varied, they were adjusted in life (stress cycles) by the relation

$$N_{800,000 \text{ psi}} = \left(\frac{\sigma_{\text{max rep}}}{800,000} \right)^9 (N_{\text{reported}}) \quad (1)$$

Equation 1 employs the observation mentioned in Appendix B: for both ball bearings and many bench rigs most researchers agree that the life varies inversely as the ninth or tenth power of the maximum contact stress.

The conditions for the tests shown in Figure 3, in so far as they are known, are listed in Table 1. The Weibull lines are keyed to the particular rig and test conditions by the numbers 1 through 12. A discussion of the divergence of data from various bench rigs is given in Reference 6.

A convenient parameter of rolling element configuration is the ratio of the axis of contact ellipse in the rolling direction to the transverse axis, e . There are notable exceptions, particularly the Macks spin rig data, but in general those data with the largest e have the longest life (see the Annapolis data for three sets of toroid geometries, all tested in the same type of rig Figure 3, lines 1, 2 and 3).

TABLE 1

Summary of Material and Test Conditions for Pitting Endurance Data Presented in Figure 3

Key No.	Mat'l Type	Rig Type	Ref.	e	Material Modifications (Rockwell C Hardness)	Lubricant	Temp. °F	Speed (SCM)	Unadj. Max. Stress	No. Spec.
1	52100	Toroid and Cylinder	33	0.84	RC 61-63	Navy designation 2190T oil	90	1,780	840,000	26
2	52100	Toroid and Cylinder	33	1.00	RC 61-63	Navy designation 2190T oil	90	1,780	851,500	13
3	52100	Toroid and Cylinder	33	1.33	RC 61-63	Navy designation 2190T oil	90	1,780	826,000	21
4	52100	Flat Washer and Ball	43	1.00	Induction Vacuum	DTE Med. Heavy oil	room	2,625	731,000	24
5	52100	Macks Spin Rig	180	1.13	Commercial air melt SAE grade 1 balls	SAE 10 mineral oil	room	163,000	750,000	74 balls 27 fail
6	M-1	Nut-Cracker (G.E. RC Rig)	181	0.77	Commercial air melt RC 61	Mil-L-7808	room	30,000	725,000	4
7	M-1	Flat Washer and Ball	43	1.00	Vacuum Melt	DTE Med. Heavy Oil	room	2,625	731,000	22
8	M-1	Macks Spin Rig	42	1.13	Induction Vacuum 8-ASTM G.S. RC 62	Mil-L-7808	room	178,000	800,000	17
9	M-50	Nut-Cracker (G.E. RC Rig)	77	0.77	Commercial air melt 10.4 ASTM G.S. RC 62	Mil-L-7808	room	30,000	732,000	4
10	M-50	Nut-Cracker (G.E. RC Rig)	77	0.77	Commercial air melt 3.4 ASTM G.S. RC 62	Mil-L-7808	room	30,000	732,000	4
11	M-50	Flat Washer and Ball	43	1.00	SKF Designation "Ingot Bar 1A"	DTE Med. Heavy Oil	room	2,625	731,000	14
12	M-50	Macks Spin Rig	42	1.13	Induction Vacuum 8 ASTM G.S. RC 62	Mil-L-7808	room	178,000	800,000	12

1. Pitting Tests at Illinois

In order to further explore the effect of rolling element geometry on pitting endurance, a brief experimental program was initiated in 1958 at the University of Illinois using the apparatus shown in Figure 4. This apparatus was used in both the pitting endurance tests and the cumulative deformation experiments to be described later.

Lubrication was provided by dip-feed from a constant-level reservoir of non-detergent SAE 10-20 oil. For the pitting tests a 2-hp motor driving the load roller shaft at 200 rpm was used. The specimen spindle was supported in tapered roller bearings and the lower drive shaft was supported and held in axial position between spherical ball bearing pillow blocks.

The main feature differentiating this roller rig from many others of nearly the same design is the provision for the introduction of any desired angle of skew between the driver roller and the specimen roller in the upper level arm. This is accomplished by pivoting the "foot" supporting the lever arm directly below the point of contact (see Figure 4).

Toroid specimens of the two configurations shown in Figure 5 were used in the pitting endurance tests. When pressed against the load cylinder the ellipses of contact have the same eccentricity for both specimens; however, the rolling direction is reversed. The ratio of theoretical contact ellipse axis in the rolling direction to the transverse axis, e , is 1.44 for the specimen having a 0.36-in. profile radius and 0.695 in. for the specimen with a 1.08-in. profile radius.

The specimens were machined from SAE 4340 steel to within 1/32-in. of finish dimension and austenitized for one hour in a salt bath at 1525°F. After an oil quench (Rockwell hardness C 55) they were tempered at 600°F for 1-1/2 hours in cast iron chips. The final hardness was C 50. Finish machining of profile radius was accomplished with a sharp tool, using a high speed and

low feed. Final polishing was performed with fine emery and oil to remove all tool marks. Run-out on some of the specimens amounted to as much as 0.003 in. The load rollers for these tests were 4620 steel, case hardened to Rockwell C 60, with dimensions as shown in Figure 5.

Observations of the specimen tracks were made throughout many of the tests with a 40-power microscope. Radial deformation was determined on several of the specimens with a supermicrometer. Track widths were obtained by microscope and shadowgraph techniques. Most of the tests were audited by a tape recorder which was modified to sample the noise level every 12 minutes, to obtain the time and number of cycles to failure. The data are tabulated in Table 2 and typical failures are shown in Figure 6.

Since several modifications of the test rig evolved over a period of three years, three main machine adjustments have to be taken into account when considering the data. Specimens designated P-1, P-2 and P-3 were preliminary tests on the first setting, after which the machine was aligned as accurately as possible. However, later experiments on the brass toroids revealed a lack of parallelism and a third adjustment was made, after which specimens B-4 and A-6 were run.

Despite the brevity of the program and the unknown influence of skew adjustment, the results lend support to the view that even under identical environmental and test conditions there is an effect of rolling element geometry that is not accounted for simply in terms of maximum surface stress. It is clearly shown in Table 2 that the larger e is, the longer is the pitting life for the same maximum contact stress and conditions of testing. Before attempting to explain this it is appropriate to summarize the significant influence of the stress system in rolling contact on the fatigue life.

B. ANALYSIS OF CRITICAL STRESS IN PURE ROLLING

Almost without exception, all the stress calculations employed in the analysis of the rolling

TABLE 2
Pitting Endurance Tests

Specimen Designation	Configuration Index, e	Load (lbs)	Maximum Theoretical Contact Stress (Millions) σ_{\max} (psi)	Stress Cycles N	Measured Track Width w (in.)	Theoretical Track Width w_E (in.)	Radial Deformation u (in.)
P-1 ^a	1.440	688	532,000	1.00*	0.062	0.041	
P-2 ^b	1.440	562	496,000	0.15	0.043	0.035	
				1.28	0.050	0.035	
				15.13*	0.057	0.035	
P-3 ^c	0.695	688	365,000	0.12	0.081	0.072	
				6.71	0.092	0.072	
				7.74*		0.072	
A-2 ^d	0.695	1698	500,000	0.18*		0.097	
B-1 ^e	1.440	578	500,000	2.98*	0.065	0.039	
A-3 ^f	0.695	1698	500,000	0.005	0.109	0.097	
				0.22*	0.140	0.097	
B-2 ^g	1.440	578	500,000	2.05		0.039	
A-4	0.695	1698	500,000	0.77*	0.109	0.097	0.00047
B-3	1.440	578	500,000	8.70*	0.047	0.039	0.00038
A-5 ^h	0.695	1698	500,000	0.15*	0.124	0.097	0.00052
B-4 ⁱ	1.440	578	500,000	52	0.050	0.039	0.00027
A-6	0.695	1698	500,000	31	0.120	0.097	0.00062

Specimens presented in order of testing.

Last two specimens (B-4 and A-6) were tested at adjusted angle of skew (approximately $1/2^\circ$ change) so as to produce symmetrical blunting of brass toroid.

* Indicates failure by pitting.

a Two pits approximately 0.025-in. in diameter.

b At 14×10^6 cycles oil supply cut off temporarily. Some burnishing occurred. Large pit at failure.

c Several small pits (approximately 0.020 in.) began at 3.78×10^6 cycles and continued until test stopped.

d Abrasion due to accidental motion of load roller--repolished--large shallow pit and incipient flake.

e Two small pits (less than 0.015 in.).

f Period of burnishing and wear early in life.

g Vibration and chatter causing wear-repolished. Test stopped after appearance of small pits.

h Burnishing as load was increased at start of test.

i Radial deformation indicates change from first cycle.

contact problem are based on the elasto-static solution stemming from Hertz's approximation for the distribution of contact pressure between elastic bodies in contact. For pure rolling, it is customary to ignore any tangential traction or dynamic effects or even the influence of possible lubricant films. Many other features in which the ideal differs from the real could be listed, but important information can still be gleaned from the elasticity solution, including numerical values of engineering significance. The "pseudo-effect" of rolling is determined by solving for the stress at a point as a function of distance from the contact area on a plane parallel to the surface and passing through the point.

1. Maximum Range of Shear Stress

The greatest variation or range of shear stress on planes of fixed orientation occurs on planes perpendicular and parallel to the surface. The location or depth to the maximum range, as well as the magnitude of this range, is a function of the ellipticity and orientation of the contact ellipse with respect to the rolling direction. This may be described by the parameter e . The range ($2\tau_0$) of this orthogonal shear stress expressed as a fraction of the maximum contact stress is plotted against e in Figure 7. Other stress components may be plotted as a function of e but none vary as significantly as the orthogonal shear stress which decreases continuously with increase in e . For cylinders this range of shear stress which is created by the action of rolling is 60 per cent larger than the maximum range of shear stress under repeated normal loading. It is significant that tests conducted by Kennedy⁽⁷⁾ revealed no evidence of subsurface cracks when hard steel balls were repeatedly pressed together, indicating that rolling is required to cause cracking at these stress levels.

2. Surface Tensile Stress

It is interesting to examine the surface tensile stress at the leading (or trailing) edge of

the contact ellipse (ignoring any dynamic effect) as a function of e . Contrary to the trend with the orthogonal shear stress, the tensile stress increases for a significant initial range with increase in e as shown in Figure 8. Calculations for this figure were made on the basis of the solution given by Timoshenko.⁽⁸⁾ Additional analysis of stress as a function of e is given in Reference 4.

C. DISCUSSION OF THE MECHANISM OF PITTING

Both the stress-life dependence and the microexamination of failure sites verify that pitting is a result of metal fatigue. As such, pitting failure may be associated with the generally accepted body of knowledge in ordinary fatigue. It is convenient to consider the fatigue process in two stages, initiation and propagation, for purposes of the discussion which follows.

1. Initiation

In the past, a great deal of argument has been devoted to the location of the crack nucleation site, whether surface or subsurface. This will of course depend on both the type of surface traction or interaction and the material, if its strength properties are a significant function of depth. For nearly pure rolling it is generally accepted^(9, 10, 11, 12) that the origin is subsurface. These conclusions are based on many metallographic observations of longitudinal subsurface cracks of considerable length, the pronounced evidence of severe subsurface plastic flow, and the influence of element configuration on pitting. This last point is discussed more fully in Reference 4 but briefly may be summarized; there is a significant effect of configuration, with large e values having greatest strength for similar test conditions. The significant fatigue stress is the range of alternating shear stress due to rolling. The range of alternating shear stress decreases as e increases. This stress range occurs in the subsurface. The origin of fatigue is therefore subsurface. This argument is simple but direct and does not depend

on quantitative unknowns. In fact, the argument allows some rational connection of fatigue strength values from rolling contact and a more standard laboratory test like torsion fatigue.

The possibility of surface initiation under certain circumstances should not be overlooked, however. It is significant that the reports of surface initiation are usually in connection with gear research. Tests by Dawson⁽¹³⁾ with a bench rig having cylindrical rollers geared to produce various degrees of rolling and sliding and under various lubrication conditions demonstrate the existence of surface initiated pitting.

Many of the discussions of the mechanism of fatigue on the atomic or crystalline level have been concerned with the intrusion-extrusion phenomenon observed at free surfaces of pure crystals subjected to fatigue stresses.⁽¹⁴⁾ This method of crack initiation is similar in some respects to the scheme proposed by Shanley.⁽¹⁵⁾ However, the fact that most fatigue failures occur at the surface is probably only evidence that in most cases the severe stress or chemical conditions exist at the surface, and not proof that all fatigue failures are surface originated. Observation of blisters in the rolling track in pure copper by Eldridge⁽¹⁶⁾ is significant in this context.

There has been much emphasis placed on the role of inclusions in the initiation of fatigue cracks. The role of residual tensile micro stresses in crack initiation at inclusion sites has been extensively discussed by Almen.^(17 and 18) Part of the emphasis is due to the fact that it presents a possible means for manufacturers to do something about fatigue pitting. The other is the fundamental difficulty in imagining the opening of a fatigue crack against a macro-stress field with a significantly high hydrostatic compressive stress component. The role of inclusions, though important, is not peculiar to the rolling contact situation nor, for that matter, is fatigue under nominally high compressive stress fields. Crossland's⁽¹⁹⁾

torsion fatigue tests under hydrostatic fluid pressure indicate that the fatigue process is inhibited but not stopped. However, the mechanism of crack propagation in this unusual applied stress environment deserves consideration.

2. Propagation

The propagation of fissures or microcracks through the subsurface band of plastically worked and slip damaged metal is probably influenced by the macro-residual radial tensile stress, which acts when the applied stress is released after passage of the rolling load. The origin of this residual tensile stress is discussed by Johnson and Jefferis⁽²⁰⁾ and Stulen,⁽²¹⁾ although no accurate estimation of its magnitude for three dimensional contact has been made. In the advanced stages of propagation the stress due to the presence of the crack itself influences propagation, even to the extent of causing more severe tensile stress at the surface, as Barwell⁽²²⁾ has conjectured. It is of interest in this connection to consider an observation made in the pitting tests reported above. In Figure 9 a plan and section view of a flaked area and an incipient flake are shown. The orientation of the incipient flake is significant in that its "mouth" is directed away from the approach of the contact load, thus opposing the hydrodynamic theory of propagation of initial surface cracks. It is also of interest to consider a phenomenon reported in personal communication with Dr. Yoshiaki Masuko of Sumitomo Metal Industries, Osaka, Japan. Dr. Masuko investigated the nature of fatigue pitting on hollow steel rolls that had been press fitted to roll cores. Subsurface examination revealed a number of radial cracks near the surface but not reaching it. The circumferential residual tensile stresses near the surface due to press fit were about 25 percent of the fatigue limit of the metal in ordinary fatigue tests. A reasonable explanation of these observations of initiation and incomplete propagation on radial planes can be proposed. Initiation took

place in the subsurface region of high shear reversal (shear stress on radial plane = shear stress on circumferential plane), and under the influence of the circumferential tensile stress due to press fit, propagated radially out of this region, being arrested because of subcritical stress conditions or even opposing compressive stress due to plastic deformation.

D. STATISTICAL CONSIDERATIONS IN FATIGUE PITTING

Since fatigue and other fracture phenomena in real materials are inherently statistical in nature, interpretation of test results on the basis of limited samples cannot be made without recourse to statistical methods of analysis. In keeping with the popular Weibull presentation of bearing fatigue data, a discussion is given below of the influence of rolling element size and contact stress level on two significant parameters of the distribution function: characteristic life, θ , and statistical variability or slope, b .

1. Size Effect

The effect of specimen size on fatigue strength determined in laboratory testing has been a subject of wide concern and speculation. A review of much of the literature on size effect and a rational method for allowing for the apparent lowering of the fatigue limit due to increase in the effectively stressed volume of material is given by Kuguel.⁽²³⁾ Weibull's "weakest link" concept⁽²⁴⁾ and probability arguments have been adopted and extended to the rolling contact situation by Lundberg and Palmgren, who incorporated size effect (track width x depth to maximum shear x length) into a complex empirical equation for purposes of bearing rating. In view of the many varieties and sizes of bench rigs it is appropriate to present a simple analysis that may be applicable in comparing results from such test rigs and that illustrates the basic statistical formulation of such phenomena.

For simplicity assume that the volume of

significantly stressed material is represented by length of rolling track only. If contact situations having much different track width and depth to maximum shear stress are considered, the problem is theoretically more complex since the individual elements on a volume basis do not have independent survival probabilities.

Consider two rolling elements of different track lengths. The track length, L_1 , of one element can be thought of as an assemblage of tracks of length L_2 . Since the probability of survival of the assemblage, S_1 , is the product of the component probabilities, S_2 :

$$S_1 = S_2^{L_1/L_2} \quad (2)$$

Using the Weibull cumulative distribution function, $F(N)$, the probability of survival is

$$S = 1 - F(N) = e^{-(N/\theta)^b}$$

where b is the Weibull slope, θ is the characteristic life, and N is the number of cycles. Equation 2 becomes

$$\left(\frac{N}{\theta_1}\right)^{b_1} = \left(\frac{N}{\theta_2}\right)^{b_2} \frac{L_1}{L_2}$$

Since this relation must be valid for all N , if the Weibull life distribution is to describe the assemblage

$$b_1 = b_2 = b.$$

It then follows that

$$\theta_1 = \left(\frac{L_2}{L_1}\right)^{1/b} \theta_2 \quad (3)$$

A change in track length would therefore be expected to translate the Weibull line in accordance with Equation 3, the slope remaining constant.

2. Effect of Stress Level

The effect of stress level on life variability

(Weibull slope, b) in fatigue tests was treated by Sinclair and Dolan.⁽²⁵⁾ The general trend of a reduction in standard deviation in log of life with increase in stress level is stated to be a feature inherent to the phenomenon of fatigue fracture in polycrystalline metals.* It appears that some size effect may have entered in their analysis of bending fatigue strength of aluminum, since stress gradient (and therefore significantly stressed volume) increases with stress level. However, this should enter primarily in shifting mean life and not changing variability to the extent reported.

There is not enough data available at this time in the rolling contact situation to make a similar analysis. It should be pointed out that the analysis formulated by Lundberg and Palmgren⁽⁹⁾ does not include such an effect. They have represented the survival probability by a product in which the exponents of the factors are independent of stress.

E. CONSIDERATION OF PLASTIC DEFORMATION

The fatigue process is intimately related to the mechanism of plastic deformation for even nominally low stresses such as design stresses in the "elastic" range. This much is axiomatic. In the rolling contact case, plastic deformation also affects the magnitude of applied stress by changing the geometry of the contacting elements. In comparing contact fatigue results at high nominal stress with those at lower stress, some account of this stress reduction should be made since it is the purpose of an effective stress index to indicate the true severity of applied stress. In this connection, certainly, one definite statement can be made concerning the maximum contact pressure on the basis of equilibrium of the contacting bodies alone. That is: the maximum

contact stress is greater than or at least equal to the total load divided by the actual contact area

$$\sigma_{\max} \geq \frac{P}{A}$$

Although increase in area of contact may occur in cases of high loads, at least a lower bound to the maximum contact pressure can be given if the contact area can be measured. Loose statements concerning a reduction in stress may thus be avoided.

There is evidence that even in the presence of a plastic zone, the stress distribution is nearly the same as the elastic one. For a partial uniform load on an infinite strip, Mesmer's experiments⁽²⁶⁾ indicate that the elastic distribution remains valid through a considerable range of plastic strains. Since bearing steels have no pronounced yield points, the inhomogeneous yielding characteristics of low carbon mild steel is not expected or observed. Of course, it is questionable to extend the results of static tension tests directly to a discussion of the plastic properties of a relatively small volume of material immersed in a region of supporting elastic material.

Lundberg and Palmgren cope with the effect of local plastic flow and inclusions in the statement:

However, the microscopic alterations in the material do not affect the macroscopic stress distribution and thus need not be considered in the determination of the macroscopic stress magnitudes.

They recognized that when finally a microscopic crack becomes macroscopic in size, the stress distribution is changed. But this is only in the advanced fatigue stages where the continuation of the destructive process swiftly leads to rupture. A number of investigators have noted in this stage that the presence of a subsurface crack may make the surface stress condition much more severe. With such a crack present, the model of a plate with built in edges resting on a continuously elastic foundation is useful in imagining the stress situa-

* It is interesting to note that the standard deviation in fatigue strength is nearly a constant at all lives.

tion.

In summing up, certainly stresses computed on the basis of ideal elastic action are not strictly valid, especially for high loads. Yet, with auxiliary experimental observation of contact area, and consideration of the materials used, these elastic stresses may serve as useful indices for correlating the existing data.

On the basis of the data at high stress levels presented in the Annapolis reports, indicating the percentage increase in track width over the theoretical, and a lower limit of first measurable plastic deformation established by Timken (personal communication with H. R. Neifert), the relation between theoretical stress and percentage increase in track width, K , can be estimated. Figure 10 exhibits a plot of this estimated relation.

As the width of the contact ellipse increases $K\%$, the correction factor for contact stress becomes $\frac{1}{(1 + \frac{K}{100})^2}$. A demonstration of this follows:

In terms of the maximum contact stress, σ_{\max} , the total applied load P is given by

$$P = \frac{2}{3} \pi ab \sigma_{\max}$$

where

P is the total load

a is the semi-major axis of contact

b is the semi-minor axis of contact

Since the total load acting is not affected by plastic action at the contact, expressions for P in terms of corrected and uncorrected maximum contact stress can be equated.

$$\frac{2}{3} \pi ab \sigma_{\max} = \frac{2}{3} \pi (1 + \frac{K}{100}) a (1 + \frac{K}{100}) b \sigma'_{\max} \quad (4)$$

where K is the percentage increase in track width over theoretical, and σ'_{\max} is the corrected maximum contact stress.

It is assumed that the percentage increase

in width of contact ellipse is the same for both axes.

The ratio of σ'_{\max} to σ_{\max} is then, from Equation 4

$$\frac{\sigma'_{\max}}{\sigma_{\max}} = \frac{1}{(1 + \frac{K}{100})^2} \quad (5)$$

Hence, if K is determined, the uncorrected stress must be multiplied by this factor to obtain a "true" value.

If sufficient information is available concerning the deformed geometry, principally profile radii, corresponding stresses may be calculated elastically. This method was employed by Niemann and Kraupner⁽²⁷⁾ and Zaretsky et al.⁽²⁸⁾

Some standard procedure should be adopted since stress reduction is a function of the number of cycles because of cumulative plastic deformation. For convenience, the stress reduction at 10 percent of the mean life would be satisfactory. However, for comparing contact fatigue results at nearly the same nominal stress these considerations are not necessary.

III. CORRELATION OF PITTING FAILURES

Synopsis: As an illustration of some of the considerations necessary in accounting for rolling element configuration and size effects, the following examples of data correlation are presented. In the first example, rolling contact fatigue data from several bench rigs are correlated with torsion fatigue strength. The second example is a correlation of pitting life data for specimens of different geometry tested in the same rig. Finally, full scale bearing performance is predicted on the basis of minimal rolling contact rig data.

A. CORRELATION OF PITTING AND TORSION FATIGUE STRENGTH

It is possible to treat many rolling contact fatigue failures on the basis of mechanical considerations relating to the critical stress cycle and inherent material properties. A numerical de-

monstration of the relation of fatigue to pitting in rolling contact was presented in 1958. (4 and 29) Improvements in correlation technique and the addition of recent information are needed to develop a unified rolling contact fatigue theory. However, several of the topics treated in these early reports provide a basis for future development. To this end a summary of the correlation procedure as developed previously is provided here.

The rolling contact and torsion fatigue data selected for analysis have been collected from four sources and are described in Table 3. Geometric definitions are given in Figure 11.

Rolling contact tests were made under nor-

TABLE 3
Description of Specimen Geometry and Material

Source	Material	Rockwell Hardness C Scale	Geometry Description	
Navy (3 and 33)	52100 Steel	59-61	$R_1 = 0.25''$	$e = 1.35$
			$R_1' = 0.50''$	$e = 0.84$
			$R_1' = 1.500''$	$R_2 = 1.562''$
G.E. (181)	MV-1 Tool Steel	64	$R_1 = 0.25''$	$e = 0.77$
			$R_1' = 3.75''$	$R_2 = 0.187''$
Bacha (182)	52100 Steel	61	$R_1 = e = 0$	$w_E = 0.58''$
			$R_1' = 0.58''$	$R_2 = 2.57''$
Styri (32)	52100 Steel	62	Standard fatigue rotating beam and torsion specimens	

mal environmental conditions of temperature and non-corrosive light oil lubrication. The data are displayed in Figure 2, in which maximum theoretical contact stress is plotted against the log of the number of cycles to failure. Only two points are available for $e = 0.84$, but it is significant that these fall within the range of the data for similar geometry, $e = 0.77$. Despite the number of test points, the stress range for $e = 1.35$ is relatively small and therefore a characteristic point is selected in the data and assigned the same S-N slope as for the $e = 0.77$ data in subsequent operations. Before proceeding to the actual data correlation the following considerations are pertinent.

1. Plasticity

Plastic increase in contact area will cause a reduction in actual contact stress. A curve, using these data and a point of first measurable plastic deformation, obtained at the Timken Roller Bearing Company, is shown in Figure 10. In the absence of more complete data, the same stress deformation curve may be used for all geometries. If the plastic action is not so excessive as to cause a significant change in geometry, then from Equation 5, the reduced stress is

$$\sigma'_{\max} = \frac{\sigma_{\max}}{(1 + \frac{K}{100})^2} \quad (6)$$

This assumes only that the contact ellipse after plastic action has the same eccentricity as before.

2. Statistical Strength Concepts

Another consideration or correction of stress stems from the observations that the strength of a specimen increases with reduced dimensions.

Weibull's analysis is based on the multiplicative law of probabilities and the dispersion of material strength in the volume under consideration. It was developed only for conditions of uniform stress. Lundberg and Palmgren⁽⁹⁾ have modified a similar theory for application to rolling contact data. The life formula is given as:

$$\log \frac{1}{S} = V \cdot F(\tau_o, N, Z_o) \quad (7)$$

where: S is the probability that the material will endure N million stress cycles and V is a volume representative of the stressed region F is given as a power function, and Equation 7 becomes:

$$\log \frac{1}{S} \sim \frac{\tau_o^c N^e w L}{Z_o^{h-1}}$$

The constants c , e , and h are determined by bearing tests.

w is width, Z_o is the depth to the maximum orthogonal shear stress, and L is length of track (circumference of rolling body). If for two different geometries of rolling contact fatigue specimens, the same probability of survival (or failure) is desired for a given number of cycles, the ratio of orthogonal shear stress will be

$$\frac{(\tau_o)_1}{(\tau_o)_2} = \left[\left(\frac{Z_1}{Z_2} \right)^{h-1} \frac{w_2 L_2}{w_1 L_1} \right]^{1/c}$$

From this standpoint, cylindrical contact will be inherently the weakest case since it involves the largest volume subjected to stress. To eliminate the statistical size effect and judge the data on a common basis, the corresponding values for fatigue strength (in terms of τ_o) for elliptical contact are multiplied by a factor $(\tau_o)_c/(\tau_o)_t$. Using the values determined by Lundberg and Palmgren:*

$$\frac{(\tau_o)_c}{(\tau_o)_t} = \left(\frac{Z_c}{Z_t} \right)^{0.129} \left(\frac{w_t L_t}{w_c L_c} \right)^{0.097} \quad (8)$$

* These values were obtained for a particular type of hardened steel, but in the absence of more direct data they will be used for the 52100 steel data considered here.

where subscripts t and c refer to toroid and cylinder, respectively. This ratio may be expressed as a function of the respective maximum contact stresses with the use of the following identities from contact theory:

$$w_t = C_e \Delta_t \sigma_{\max t}$$

$$Z_t = 0.5 w_t M e$$

$$Z_c = 0.5 \Delta_c \sigma_{\max c}$$

where: C_e is determined from Figure 12

M is determined from Figure 13

and the geometry parameter Δ is:

$$\Delta = \frac{1}{\frac{1}{2R_1} + \frac{1}{2R_2} + \frac{1}{2R_1} + \frac{1}{2R_2}} \left(\frac{1-\mu_1^2}{E_1} + \frac{1-\mu_2^2}{E_2} \right)$$

where E and μ are elastic constants.

With these substitutions, Equation 8 becomes:

$$\frac{(\tau_o)_c}{(\tau_o)_t} \left[\left(\frac{\Delta_c}{M e} \right)^{0.129} \left(\frac{L_t}{w_c L_c} \right)^{0.097} \left(\frac{1}{C_e \Delta_t} \right)^{0.032} \right]$$

$$\frac{\sigma_{\max c}^{0.129}}{\sigma_{\max t}^{0.032}} \quad (9)$$

3. Fatigue Criterion

In developing a fatigue criterion for the stress condition arising from rolling contact, account must be taken of both the range of shear stress and the inhibiting influence on crack propagation of the normal compressive stress acting on these critical shear planes. Fatigue theory and test results involving multi-axial compressive stress are scarce but the few excursions into this area have accentuated the inhibiting influence of compressive stress fields.

Especially significant are the torsion fatigue tests under hydrostatic compression of Crossland.⁽¹⁹⁾ After the specimen surface was sealed from the direct action of the pressure fluid, there was a large increase in life and

fatigue strength.

Usual expressions for fatigue strength are a modification of onset of plasticity, distortion energy, or maximum shear theories. In these expressions the hydrostatic component or normal stress is neglected. The limitations of such theories become evident under certain stress states.

Crossland found that his test results did not support a simple maximum shear stress or Mises-Hencky theory of failure. A linear modification of the Mises function by the volumetric stress was proposed. Figure 14 is a plot of the semi-range of Mises stress endured against volumetric stress for several stress states.

In a paper by Stulen and Cummings⁽³⁰⁾ in 1954, a theory of fatigue failure under multi-axial stress was proposed. Failure was assumed to be caused by alternating slip on certain planes. On these planes, the critical shear, τ_C , is a linear function of the complimentary normal stress, σ_n . For simplicity, an expression of this fatigue criterion may be taken as

$$\tau_C = \tau_\epsilon + B \sigma_n \quad (10)$$

In this expression, τ_ϵ is an experimentally determined constant (at N cycles) that may be considered as the semi-range of shear stress necessary to cause failure when no normal stress is involved. For reference purposes and convenience, it will be called the semi-range of essential shear stress. The symbol B will be referred to as the normal stress influence factor. Both τ_ϵ and B are constants for a given number of cycles but may vary with the number of cycles throughout the test. It is shown in a more elaborate treatment by Findley⁽³¹⁾ that τ_ϵ is not necessarily the fatigue strength in pure torsion, but is given by:

$$\tau_\epsilon = \sqrt{1 + k_\epsilon^2} \tau_T$$

where τ_T is the fatigue strength in torsion and k_ϵ is related to the ratio of bending fatigue strength, σ_B , to τ_T at N cycles by

$$k_\epsilon = \frac{2 \frac{\tau_T}{\sigma_B} - 1}{\sqrt{1 - 2 \left[\frac{\tau_T}{\sigma_B} - 1 \right]^2}}$$

Since hard 52100 steel will be used in the analysis of this paper, it is necessary to examine whether or not the fatigue strength in torsion can be used as a close approximation to the semi-range of essential shear. The data of Styri⁽³²⁾ will be used. Typical S-N curves for bending and torsion are given in Figure 15.

By selecting fatigue strengths for bending and torsion at different numbers of cycles, the values of k_ϵ may be determined. The ratios of fatigue strengths are given in Table 4. Thus the difference in the critical and essential shear stress in torsion is negligible.

It is not possible to obtain the value of the normal stress influence factor, B , directly. However, some indication of the range of values involved may be inferred from examination of a particular case in which data are available. For this purpose, Crossland's data will be used. In these hydro-torsion tests, the so-called "volumetric tensile stress" has the same value as the normal stress acting on the critical shear planes

(longitudinal and transverse). In this case the semi-range of the Mises function reduces to the semi-range of applied (or critical) shear stress. Figure 14 may be considered as a plot of critical shear versus complimentary normal stress for torsion specimens. The slope gives the value of the influence factor as 0.3. Here, the complimentary normal stress is held constant at a maximum value. In the case of contact fatigue, the normal stress varies from zero to its maximum value during rolling. A value of B , somewhat less than 0.3, would be expected.

Therefore, the fatigue criterion will be taken as Equation 10 with B to be determined from available data on rolling contact fatigue.

4. Correlation Procedure

First the data are corrected for plastic increase in track width by use of Equation 6 and Figure 10. The data for cylinders are of course not corrected. In order to facilitate the remaining steps the corrected data are presented using log-log coordination (Figure 16). In this plot the S-N line for Styri's torsion data is also given.

Next, the data are corrected for geometry using the range of orthogonal shear stress. This is accomplished by multiplying the maximum contact stress by the ordinate of Figure 7, Q , which corresponds to the given geometry factor, e .

The correction for volume stressed is

TABLE 4
Comparison of Essential and Critical Shear for Torsion using Styri's Data for Hard 52100

No. of Cycles	τ_T , psi	σ_B , psi	$\frac{\tau_T}{\sigma_B}$	k_ϵ	$\sqrt{1 + k_\epsilon^2}$
10^5	115,000	200,000	0.57	0.14	1.01
10^6	90,000	170,000	0.53	0.06	1.00
10^7	70,000	140,000	0.50	0	1.00

made by use of the semi-range of orthogonal shear stress and Equation 9. A constant factor of 0.5 is applied for the semi-range transformation.

For $e = 1.35$, Equation 9 becomes:

$$\frac{(\tau_o)_c}{(\tau_o)_t} = 0.215 \frac{\sigma_{\max c}^{0.129}}{\sigma_{\max t}^{0.032}}$$

for $e = 0.77$, Equation 9 becomes:

$$\frac{(\tau_o)_c}{(\tau_o)_t} = 0.236 \frac{\sigma_{\max c}^{0.129}}{\sigma_{\max t}^{0.032}}$$

Typical values at $N = 3 \times 10^6$ cycles for these combined factors are:

$$\frac{1}{2} \frac{(\tau_o)_c}{(\tau_o)_t} = \begin{cases} 0.402 & \text{for } e = 1.35 \\ 0.368 & \text{for } e = 0.77 \end{cases}$$

There is a slight decrease in this factor with increasing N . After multiplying by the correction factor, the data for the two toroids are nearly coincident and the maximum percentage difference in fatigue strength between elliptical and line contact has been reduced from about 97 per cent to 5 per cent at 3×10^6 cycles.

The fatigue criterion may now be applied to the contact fatigue data in order to relate it to the standard torsion data. The close similarity in S-N slope is considered to be due to similarity in mechanism of fatigue. Essentially, this is the observation made by Styri.

A transformation of critical shear stress to essential shear stress by use of Equation 10 can be performed. Under this transformation, the torsion data will not be influenced since it is demonstrated above that in torsion, the critical shear stress is the essential shear stress. The normal stress influence factor B will be selected so as to cause coincidence of the contact fatigue data for cylinders and the torsion data. The essential shear stress for cylinders can be ex-

pressed as:

$$\begin{aligned} (\tau_\epsilon)_c &= (\tau_C)_c \left[1 - B \left(\frac{\sigma_n}{\tau_C} \right)_c \right] \\ &= (\tau_o)_c \left[1 - B \left(\frac{\sigma_o}{\tau_o} \right)_c \right] \end{aligned}$$

From Figure 17 the ratio of maximum normal stress to shear stress amplitude on the plane of maximum orthogonal shear stress is

$$\frac{\sigma_o}{\tau_o} = 3.5,$$

at 3×10^6 cycles:

$$(\tau_o)_c = 108,000 \text{ psi}$$

and $(\tau_C)_T = 80,000 \text{ psi}$

where the subscript T refers to torsion fatigue data. Since

$$(\tau_\epsilon)_c = (\tau_\epsilon)_T = (\tau_C)_T, \text{ then } B = 0.074$$

The above operations may be reversed and combined to provide a means of predicting the fatigue strength of a toroid of general e :

$$\sigma_{\max} = \left\{ \frac{2}{Q} \theta \left[1 + \frac{K}{100} \right]^2 \frac{\tau_T}{1 + B \frac{\sigma_o}{\tau_o}} \right\}^{0.968} \quad (11)$$

where:

$$\theta = \frac{\left(\frac{Me}{\Delta_c} \right)^{0.129} \left(\frac{w_c L_c}{L_t} \right)^{0.097} (C_e \Delta_t)^{0.032}}{(\sigma_{\max c})^{0.129}}$$

In Equation 11, K is a function of σ_{\max} given graphically by Figure 10. Hence, two simultaneous relationships must be solved. However, the desired value of σ_{\max} may be obtained by a simple iteration procedure.

For example, consider a hypothetical toroid similar to the Annapolis rollers except $R_1 = 1$ inch instead of $1/4$ inch or $1/2$ inch. This results in $e = 0.53$. Equation 11 and Figure 10 yield $\sigma_{\max} = 570,000 \text{ psi}$ at $N = 3 \times 10^6$ cycles.

The slope may be determined by calculating additional points.

More generally, if only torsion data on a new material are available, a minimum fatigue strength in rolling contact can be estimated by initially ignoring the correction for volume stressed and plastic increase in track width, thus obtaining:

$$\sigma'_{\max} = \frac{2}{Q} \frac{\tau_T}{(1 - B \frac{\sigma_o}{\tau_o})} \quad (12)$$

This result can be modified as information concerning the plastic behavior of the metal and fatigue behavior at one particular geometry is obtained.

B. CORRELATION OF BENCH RIG LIFE DATA

A less ambitious and more straightforward problem than the above illustration is the correlation of life data from the same test rig but with different rolling element geometries. For this purpose the apparent divergence in life for the Annapolis (33) data will be examined. The unadjusted data are presented in Figure 18. Comparison of these data after a series of adjustments is made in Table 5. The volume of significantly stressed material is taken as the product of theoretical track width, depth to maximum shear stress, and track length. The relative values, compared to the Annapolis elements of $e = 1.00$ as base, are also given in Table 6. It should be

noted that the value of B_{10} and B_{50} life (life at which 10 per cent and 50 per cent of specimens tested may be expected to have failed) in terms of maximum contact stress have all been adjusted to 800,000 psi in accordance with Equation 1. If the range of orthogonal shear is significant then further adjustment is needed. The orthogonal shear stress is obtained from Figure 7 and all the data are again adjusted in accordance with Equation 1 to the orthogonal shear stress level of the Annapolis element $e = 1.00$ for illustrative purposes. That is, the adjustment in life is made according to the equation

$$\frac{N_1}{N_2} = \left(\frac{(\tau_o)_2}{(\tau_o)_1} \right)^9$$

where τ_o is the amplitude of orthogonal shear from Figure 7. To account for the size effect, Equation 3 is used disregarding the theoretical limitations, and replacing length as follows:

$$N_1 = \left(\frac{V_2}{V_1} \right)^{1/b} N_2$$

A Weibull slope of two is used in this calculation, and the results are given in the final Column of Table 5. All of the adjustments, in keeping with the above considerations, tend to cause convergence of the data.

TABLE 5
Successive Adjustments of Pitting Endurance Data for Annapolis 52100
Steel Rolling Elements (Life in Millions)

e	800,000 psi		Same Critical Shear Range		Same Effective Size	
	B_{10}	B_{50}	B_{10}	B_{50}	B_{10}	B_{50}
0.84	0.74	1.70	0.92	2.2	1.10	2.61
1.00	1.72	4.50	1.72	4.50	1.72	4.50
1.33	3.10	16.50	1.60	8.60	1.16	6.24

TABLE 6
Critically Stressed Volume for Annapolis Rolling Elements

e	Theoretical Track Width	Depth to Maximum Shear	Critically Stressed Volume	Relative Volume
0.84	0.0446	0.0241	0.00107	0.53
1.00	0.0656	0.0308	0.00203	1.00
1.33	0.0812	0.0350	0.00284	1.40

C. CORRELATION OF BENCH RIG AND FULL SCALE BEARING DATA

In an effort to more easily obtain bearing design information without the expensive and time consuming testing of full scale assembled bearings, the General Electric Company has developed the rolling contact fatigue machine (RC Rig). Bamberger and Baughman⁽³⁴⁾ fully described the machine in 1957 and reported that on the basis of preliminary data, "The fatigue data indicates a correlation with actual bearing data may be possible." Since then Bamberger et al have reported a number of studies concerned with the rolling contact fatigue behavior of different materials, variations from heat to heat of the same material, effect of hardness, grain size, surface finish, lubricant, and temperature. In the summer of 1959 the second author of this bulletin worked with the General Electric group on the correlation of the RC Rig data with full scale bearing results.⁽³⁵⁾

The problem and approach taken may be stated as follows:

Given the dimensions, loading and operating conditions of a bearing, made of a particular material, determine the life of the bearing from minimal RC Rig data.*

Following is a partial list of the variables which are important in the life of bodies in rolling

* This analysis is only concerned with the type of bearing failure known as pitting. Excessive wear or deformation or other types of failure will not be treated here.

contact.

- a) Maximum alternating shear stress (function of load and radii of the contacting bodies)
- b) Plastic increase in track width
- c) Volume of material stressed (size effect)
- d) Material composition
- e) Material hardness
- f) Grain size
- g) Surface roughness
- h) Lubricant
- i) Temperature
- j) Frequency

It will be presumed that variables "d" through "j" are controlled in the RC Rig to be the same as in the bearing of interest. Some of these variables, such as frequency, only have a measurable effect when varied over a wide range. In these cases it is not necessary to exactly duplicate the service conditions for the bearing in the RC Rig.

Variables "a", "b" and "c" are usually not the same in the RC Rig as in bearings. Each of these will be discussed below in detail.

a) Maximum Alternating Shear Stress: The significant stress quantity is the orthogonal shear stress. For the same Hertz stress the orthogonal shear stress depends on e . The value of e depends on the geometry of the contacting bodies. For the RC Rig $e = 0.79$. For any practical ball bearing, e at the inner race is less than 0.79 approaching $e = 0$, the value for a roller bearing.

From Figure 7 it can be seen that the error in stress would be less than 10% if Hertz stress is used rather than the orthogonal shear. It will be shown later that this change in the magnitude of stress causes a change in the life of only about a factor of two. The error is always in the same direction. Other factors being equal, a bearing will have a slightly shorter life than the RC Rig for the same maximum Hertz stress. Such variation in life is well within the scatter normally found in fatigue life measurements, so the maximum Hertz stress may be used to compare results from the RC Rig with results from tests of full scale bearings.

There is still another factor concerned with the stresses present in rolling contact which is not reproduced in the RC Rig. This is the general level or magnitude of stress. The maximum Hertz stress in bearings normally is between 200,000 psi and 500,000 psi. The stresses in the RC Rig are normally set between 500,000 and 800,000 psi. The reason for this large difference in the stress levels is that the "idea" of the RC Rig is to perform a short time test whereas a bearing is expected to last a long time.

The difference in stress level is not such an impediment to correlation as it might first appear. It has been shown many times for both bearings and for short time tests such as the RC Rig that the following relation between the maximum Hertz stress and life is reasonably valid for a range of lives from 10^5 to 10^{10} cycles:

$$\frac{N_2}{N_1} = \left(\frac{\sigma_{\max 1}}{\sigma_{\max 2}} \right)^9 \quad (13)$$

Where N_1 and N_2 are the pitting fatigue lives of two identical rolling assemblages under the maximum Hertz stress $\sigma_{\max 1}$ and $\sigma_{\max 2}$.

Another way of stating Equation 13 is that the S-N curve for bodies in rolling contact is linear on a log-log plot and has a slope of -1/9 when log

σ_{\max} is plotted vertically and log N is plotted horizontally. Such a plot is shown in Figure 19 for M-50 tested on the RC Rig at room temperature. The line with a slope of -1/9, (Equation 13) appears to fit the RC Rig data reasonably well.

If there were no other differences between the RC Rig and bearings except stress level, the number of stress cycles a bearing could endure, N_b , at a particular Hertz stress, $\sigma_{\max b}$, would be

$$N_b = N_{RC} \left(\frac{\sigma_{\max RC}}{\sigma_{\max b}} \right)^9 \quad (14)$$

where N_{RC} is the life of the same material tested in the RC Rig at some convenient maximum Hertz stress of $\sigma_{\max RC}$.

b) Plastic Increase in Track Width: It is possible to estimate the effect of the plastic increase in track width, as follows: for $\sigma_{\max} = 650,000$ psi (which would be representative of the stresses in the RC Rig), the value of K (Figure 10) is about 5%. For $\sigma_{\max} = 300,000$ psi (which would be typical for a bearing), the value of K would be near to zero. Thus, if comparison of a bearing and the RC Rig is made on the basis of theoretical Hertz stress using Equation 14 there will be a small error introduced. The stress in the RC Rig will be less than computed by the Hertz method due to yielding at high stresses, whereas the stresses in the bearing will be close to the theoretical stress computed. An estimate of the error would be (Equation 5): $\sigma'_{\max} / (1.05)^2 = \sigma_{\max} / 1.10$.

Approximately the same magnitude of error is introduced by neglecting the plastic increase in track width that was introduced by using the maximum Hertz pressure rather than the more appropriate orthogonal shear.

c) Volume of Material Stressed (Size Effect): In general, the volume of material stressed in the RC Rig is only a small fraction of the volume of material stressed in a bearing.

From the analysis of Lundberg and Palmgren, it is possible to obtain the following equation:

$$\frac{(\tau_o)_1}{(\tau_o)_2} = \left(\frac{Z_1}{Z_2}\right)^\alpha \left(\frac{w_2 L_2}{w_1 L_1}\right)^\beta \quad (15)$$

where $(\tau_o)_1$ and $(\tau_o)_2$ are the orthogonal shear stresses in two bodies of different geometry for the same probability of surviving a given number of cycles. w_1 and w_2 are the widths and L_1 and L_2 are the lengths of track (circumference of rolling bodies) and Z_1 and Z_2 are the depths of the maximum orthogonal shear stress. The exponents α and β are experimentally determined constants.

For our present purpose of relating bearings and the RC Rig, the ratio of the orthogonal shear stresses of Equation 15 may be replaced by the ratio of the maximum Hertz stresses.

$$\frac{\sigma_{\max b}}{\sigma_{\max RC}} = \left(\frac{Z_b}{Z_{RC}}\right)^\alpha \left(\frac{w_{RC} L_{RC}}{w_b L_b}\right)^\beta \quad (16)$$

where the subscripts b and RC refer to bearing and RC Rig.

Lundberg and Palmgren determined from bearing tests $\alpha = 0.129$. Using this value it can be shown that the influence of the "Z" term in Equation 16 is small for practical bearings.

Dropping this factor has the opposite effect on the predicted life as using Hertz stress instead of orthogonal shear or as neglecting plastic increase in track width. Thus, this simplification partially compensates for the error introduced by the two earlier simplifications.

Equation 16 may be reduced to:

$$\frac{\sigma_{\max b}}{\sigma_{\max RC}} = \left(\frac{w_{RC} L_{RC}}{w_b L_b}\right)^\beta \quad (17)$$

In terms of life from Equation 14:

$$\frac{N_{RC}}{N_b} = \left(\frac{w_{RC} L_{RC}}{w_b L_b}\right)^{9\beta} \quad (17a)$$

But from the previous analysis of statistical size effect the exponent 9β is identical to the reciprocal of the Weibull slope, b. This is based on the assumption that size effect is effectively given as the product of track width and length as in the analysis of the Annapolis bench rig data. A Weibull slope of 2 is an approximate value from the RC Rig data.

In Reference 35 an alternative approach is explained whereby an estimate of β is obtained using a large number of the same size specimens of M-50. From this data it was possible to show that for the same Hertz stress and all other factors equal, the life depends approximately on the square root of the track length* or

$$\frac{N_1}{N_2} = \left(\frac{L_1}{L_2}\right)^{1/2} \quad (18)$$

Since life and stress are related by the ninth power as in Equation 14 the value of β in Equation 17 is approximately $\beta = 1/2 \times 1/9 = 0.056$.

It is now possible to make an estimate from minimal RC data of the number of stress cycles a bearing will endure. Equation 14 accounts for difference in maximum Hertz stress. Equation 17 accounts for difference in volume of material stressed. All other factors are presumed to have only minor influence or to be controlled the same in the RC test as in the bearing. Combining the effect of relative stress level (Equation 14) and size (Equation 17a);

$$N_b = N_{RC} \left(\frac{\sigma_{\max RC}}{\sigma_{\max b}}\right)^9 \left(\frac{w_{RC} L_{RC}}{w_b L_b}\right)^{1/2} \quad (19)$$

* Proportional to the stressed volume.

Where;

- N_b = Life of bearing, in stress cycles on critical element of bearing (usually inner race).
- $\sigma_{\max b}$ = Maximum Hertz stress on critical element in bearing.
- $w_b L_b$ = Width and length of wear track in bearing.
- N_{RC} = Measured life from RC Rig on same material, lubricant, etc. as bearing. N_{RC} should be determined statistically such as B_{10} or B_{50} life from a Weibull plot. N_b will then be for the same probability of failure as N_{RC} .
- $\sigma_{\max RC}$ = Maximum Hertz stress at which N_{RC} was obtained
- $w_{RC} L_{RC}$ = Width and length of wear track on RC specimen.

Equation 19 is intended only for use as an estimate of the life of M-50 bearings. It is possible that the "1/2" exponent will also apply to other materials. It is fairly certain that the exponent "9" is universal for hardened (RC 60) steels.

The next logical step is to apply Equation 19 to a number of bearings on which life data is available. Comparison between predicted and observed lives would suggest in what manner the concepts involved need to be refined.

Examples of the application of the correlation Equation 19 follow.

1. Analysis of a Large Thrust Ball Bearing

Life data for this bearing were furnished by Mr. C. C. Moore of the General Electric Co. The Weibull plot for the bearing with life in hours is shown in Figure 20 under a thrust load of 20,000 lbs. Some of the details of the tests are given in the legend. The bearing consists of 14 balls, 1.531 in. in diameter. It has an initial contact angle of about 30° . The length of the wear track, L_b , is about 6.20 in.

The maximum Hertz stress is 290,000 psi and the track width is 0.416 inches. One bearing revolution produces about eight stress cycles on any point of the inner race track, which is the assumed failure location.

Equation 19 is applied to establish the predicted Weibull plot shown as a dashed line on Figure 20. The close correlation which was obtained for this bearing cannot be expected in general. There are several factors in the analysis which admittedly could account for a factor of as much as 4 in life.

2. Analysis of GEL 202K Radially Loaded Bearing

Tests on full scale bearings of this size are reported in Reference 36. A Weibull plot of the data is shown in Figure 21. The bearings are rather small, having a ball diameter of $D = 0.250$ in. as compared to the ball diameter of the previous bearing, which was over 1 1/2 in. These are the same bearings which have been cited in earlier publications concerning the correlation of the RC Rig with bearings. The calculated maximum Hertz stress is 440,000 psi. The calculated value of track width is 0.113 inches. For simplicity it is assumed that the radial bearing experiences effectively one stress cycle per revolution.

The B_{10} and B_{50} life of these bearings was computed using RC Rig data from Reference 34. The material is M-50, the lubricant is 7808, and the tests were conducted at room temperature. The conditions of the RC and the bearing tests are nearly identical.

The predicted Weibull plot shown as a dashed line in Figure 21 gives lives about twice those actually measured. Even this is considered good correlation for a process as statistical as fatigue. Also, the presumption that the inner race experiences only one stress cycle per revolution of the bearing in a radially loaded bearing is open to question. As the race begins to come into the load region, it is sure to experience at least one load nearly as large as the maximum load used in the calculations. This would have the effect of reducing the life of the bearing, thus making correlation even better.

3. Analysis of 207S MRC Radial Bearing

The Weibull plot for these tests which in

TABLE 7
Summary of Bearing Correlation with RC Rig Data

Bearing and Ball Size	Temp. & Lubricant	Load-(lb.) Frequency	$\frac{B_{10}(\text{Test})}{B_{10}(\text{Calc})}$	$\frac{B_{50}(\text{Test})}{B_{50}(\text{Calc})}$
Thrust Ball Bearing D = 1.531"	400F 7808	T = 20,000 7800 rpm	$\frac{180 \text{ hrs}}{130 \text{ hrs}} = 1.4$	$\frac{480 \text{ hrs}}{460 \text{ hrs}} = 1.0$
202K D = 0.250"	R.T. 7808	R = 426 50,000 rpm	$\frac{15 \text{ hrs}}{40 \text{ hrs}} = 0.4$	$\frac{32 \text{ hrs}}{80 \text{ hrs}} = 0.4$
207S D = 0.437"	R.T. 6081	R = 1750 11,250 rpm	$\frac{120 \times 10^6 \text{ sc}}{120 \times 10^6 \text{ sc}} = 1.0^*$	$\frac{210 \times 10^6 \text{ sc}}{240 \times 10^6 \text{ sc}} = 1.0^*$

* Corrected for differences in lubricant.

Figure 22 is plotted in terms of stress cycles rather than hours, since that is the way it was reported in Reference 34. The general size of this bearing is between the two which have just been analysed. Ball diameter is 7/16 in.

The computed Hertz stress is 450,000 psi. The theoretical track width is 0.184 inches. Again, it is assumed that the inner race experiences one effective stress cycle per revolution.

There is no available RC Rig data for M-50 at room temperature using 6081 lubricant, which is the condition under which these bearings were tested. The closest set of data is that reported in Reference 34 using 7808 lubricant at room temperature. In a way this lack of complete data is fortunate because it provides an opportunity to indicate the manner in which other variables which are not included in the "correlation equation" may be taken into account. Other RC Rig studies using M-1 steel have indicated that about twice the life is obtained using 6081 as is obtained using 7808. This agreed qualitatively and quantitatively with independent results obtained on the Mack spin rig. To "correct" the predicted Weibull plot shown on Figure 22 using RC data with the 7808 as lubricant to predict behavior of a bearing which is lubricated by 6081, the lives should be approximately doubled.

The predicted Weibull plot "corrected" for difference in lubrication is shown in Figure 22. It correlates nicely with the 207S bearing tests.

A summary of these examples of bearing correlations with bench rig results is provided in Table 7.

It should be possible to use the method employed above to obtain "correlation equations" for other bench rigs. In addition, rigs can be designed which eliminate much of the guess work in correlation by matching the conditions of rolling contact as much as possible to that of the bearings of interest. Variables which cannot be completely matched can be accounted for as illustrated above.

IV. ANALYSIS OF CUMULATIVE DEFORMATION

Synopsis: Available data on hard steel and results on brass in rolling contact obtained as part of this research are analyzed with regard to both the initiation and accumulation of plastic deformation. The nature of track strains and the effect of preload is experimentally studied using annealed brass rolling elements. Supplementary tests on the brass subject to complex combined stress cycles were also performed. The results are analyzed in an effort to relate the observations to existing theory and to establish that the magnitude and rate of accumulation of deformation in rolling contact might reasonably be accounted for by accumulation of plastic strain due to cycles of complex combined stress.

A few observations of failure due to dimensional change of rolling elements have been made in full scale tests, and this mode is anticipated as the dominant cause of failure in unlubricated bearings at high temperatures. The possible sources or mechanisms of the dimensional change are not well defined or understood. The term "wear" is sometimes used, although it has not been established to what degree attrition of surfaces contributes to this failure. Density increase caused by metallurgical instability is a possible source in some metals, for instance transformation of martensite to troostite in some hard steels. But even in this particular case it is difficult to account either for the magnitude of the observed dimensional changes or the influence of speed.

Under the complex cyclic stress state present in rolling contact, pronounced accumulation of deformation can occur. It is necessary, then, to establish and explore cumulative plastic strain under complex combined stress cycles as a major

source of deformation in this mode of failure. Viscoelastic and anelastic strains will not be treated here, although these introduce important effects in cases such as instrument bearings. In addition, no consideration of speed or temperature effects will be made. In a particular case (steel at 1000°F) Bamberger⁽³⁷⁾ has explored this effect.

The consequences of cyclic accumulation of plastic strain are a permanent change in geometry of contacting surfaces, causing a simultaneous reduction of applied stress, and an intensification of residual stresses due to the high degree of elastic restraint. The phenomenon itself is due to the complex loading cycle induced by rolling contact as well as the inherent cyclic material properties. Some of these aspects will be explored and substantiated in the following sections.

A. PRELIMINARY CONSIDERATION OF EXTERNALS

Without concern, at the moment, for details of the internal mechanism responsible for cumulative deformation in rolling contact, certain external aspects may be examined. This will include a convenient classification as to the appearance of deformation on the basis of limited observations and range of variables, analysis of contact stress as a function of deformation for these ideal types, and establishment of simple relations between the parameters of the deformed profile (track width, radial deformation, and deformed profile radius).

1. Classification of Extreme Cases

In static indentation tests, which always involve severe localized plastic strains, there is a natural classification according to the two general types of imprints. One type exhibits a raised coronet of metal displaced locally from the impression (characteristic of cold worked and high strength metals), and the other is manifested by a "sinking in" impression, the plastic strain being distributed and accommodated throughout the specimen (characteristic of soft annealed specimen). Similar observations were made in rolling tests performed as part of this research when a few cold worked brass toroids (Rockwell B 70 on the surface) were blunted by rolling them against a hard steel roller. Compared to the majority of specimens which were annealed (Rockwell B 10), the track edge or shoulder build-up of the cold worked brass was noticeably sharper. It seems appropriate to make two extreme classifications with regard to severity of plastic deformation and its proximity to the elastic strain range. To this end, the two types will be designated hereafter as pronounced plastic deformation and elastically restrained plastic deformation.

In pronounced plastic deformation, the loads are so high with respect to the yield strength of the rolling bodies that extreme and immediate changes in contact geometry result. The boundaries of this deformation, whether of the "raised coronet" or "sinking-in" type, are sharp and well defined. Further plastic deformation during rolling pushes these frontiers aside. The primary single factor in determining the relations among the dimensions of the deformed track is the profile of the harder rolling body either grooving or blunting this surface. This is true, since such extreme cases are, in general, deliberately induced, whereas in more practical circumstances a combination of both blunting and grooving of profile rolling elements might be expected.

In the elastically restrained case the distortion of profile geometry that develops with

cycles of rolling is a continuous transition from the original profile radius, increasing in the case of blunting and decreasing in the grooving case. This transition is such that on any cycle the track width calculated on the basis of the deformed profile radii using the usual elastic theory closely approximates the measured track width. Niemann and Kraupner⁽²⁷⁾ have verified this approximation for the blunting of steel at room temperature, by direct measurements of the deformed profiles.

2. Relations Among Parameters of Deformation

For pronounced plastic deformation, relations among original and deformed track dimensions may be derived from simple trigonometric considerations. Consider first the blunting of a convex element by a cylindrical surface. Assuming local redistribution of plastically displaced material, the area of the original segment shown shaded in Figure 23 a must equal the strip above the chord of this segment, bounded by the flattened track. Mathematically,

$$R_o^2 \sin^{-1} \frac{w}{2R_o} - (R_o - h) \frac{w}{2} = (h - u) w$$

where R_o is the original profile radius, u is the radial deformation, w is the track width, and h is the chord height. The angle $\sin^{-1}(w/2R_o)$ is expressed in radians.

Radial deformation in terms of original profile radius and track width is

$$u = R_o - \frac{1}{2} \sqrt{R_o^2 - \left(\frac{w}{2}\right)^2} - \frac{R_o^2}{w} \sin^{-1} \frac{w}{2R_o} \quad (20)$$

For the redistribution shown in Figure 23 b, a similar result for grooving of an originally straight profile may be obtained. Here the area of a sector of radius equal to the deformed profile radius must be set equal to a triangle formed by these rays and the original surface. The result, expressing radial deformation as a function of deformed profile radius and track width is

$$u = R_p \left(1 - \sqrt{\frac{\sin^{-1} \frac{w}{2R_p}}{\tan \sin^{-1} \frac{w}{2R_p}}} \right) \quad (21)$$

Without further consideration the deformed profile radius (R_p) is not known. Indeed, even in the case of pronounced deformation there is a slight decrease in curvature with cycles.⁽¹⁶⁾ However, with simplicity consistent with these approximations this radius can be taken as slightly greater than the profile of the grooving body, say 10 per cent greater. This approximate degree of conformity was observed in tests reported here as well as in Eldredge's tests. The applicability of these expected relations between radial deformation and track width to tests performed as part of this research is shown in Figure 24.

In the blunting tests, annealed brass toroids of 2.5-in. major diameter and 5/8-in. profile were loaded and driven by a 2.5-in. steel cylinder. In the grooving tests annealed brass cylinders of 2.5-in. diameter were loaded and driven by a hard steel toroid with the same dimensions as the brass toroids.

Also shown in Figure 24 a is the relation to be expected if the change in dimension were due entirely to wear or complete accommodation of the displaced material throughout the specimen. The theoretical curves for blunting and grooving form a lower limit, predicting less radial deformation or greater track width than measured. The agreement is sufficiently close that the difference may be attributed primarily to the nature of annealed brass in increased accommodation of elastic strain as mentioned above. The relation expected if wear were the mechanism is considerably too high. This was confirmed by auxiliary weight loss determination.

For the elastically restrained case, essentially two equations are available for the determination of the relations among the three parameters: radial deformation u , track width w , and

profile radius R . This first equation, in keeping with the definition of this case, is the elastic relation between load, principal curvatures, and contact area dimension (track width):

$$w = \text{constant} \cdot \left(\frac{P}{\Sigma \frac{1}{R}} \right)^{1/3} \quad (22)$$

where P is the load and $\Sigma(1/R)$ is the sum of the reciprocals of the radii of curvature. The second is a trigonometric relation among the three dimensions that was derived ignoring plastic redistribution for initial simplicity. From the inset of Figure 25 this relation is

$$u = \sqrt{R_p^2 - \left(\frac{w}{2}\right)^2} - \sqrt{R_o^2 - \left(\frac{w}{2}\right)^2} - (R_p - R_o) \quad (23)$$

or approximately* for R_p , the deformed profile radius:

$$R_p = \frac{\left(\frac{w}{2}\right)^2}{2(R_o - u - \sqrt{R_o^2 - \left(\frac{w}{2}\right)^2})} \quad (24)$$

To examine the range of applicability of such a relation the data of Niemann and Kraupner on the blunting of hard steel toroids is examined. The reported values of track width for various loads at 30×10^6 stress cycles are used in Equation 22 to obtain the deformed profile radii. The trigonometric relation expressed in Equation 23 is used to determine u . Experimental and predicted values of u are plotted as a function of maximum contact stress in Figure 25. There is an increasing divergence of the two for high load values with the theoretical relation predicting greater deformation. This is to be expected in view of the simplified trigonometric relation if local redistribution of material at contact is significant, as it should be for the higher loads. If the profile crescent in Figure 25 were deformed into a plate of uniform thickness with the same curvature, the

* Ignoring $\left(\frac{w}{2R_p}\right)^4$ and higher order terms in the binomial expansion of the first radical.

theoretical relation would be approximately halved.

3. Contact Stress as a Function of Deformation

As deformation accumulates, the area of contact increases, and as a consequence the contact stress is reduced. A rational estimate of this stress as a function of track width may be obtained in pronounced blunting by assuming the toroid is simply deformed into a cylinder of length equal to the actual track width. For cylindrical contact,

$$\sigma_{\max} = \text{constant} \sqrt{\frac{P}{w}} \quad (25)$$

where σ_{\max} is the maximum contact stress. This situation is illustrated in Figure 26 where the result of typical calculation is presented graphically. It should be noticed that after an initial rapid drop in contact stress from some theoretical elastic value there is a flattening of the curve so that the contact stress drops only about 20 per cent for a 100 per cent increase in track width. The situation for pronounced grooving is more complex since no simple contact area is generated. In fact, for some initial period, perhaps 10^2 cycles, the contact area resembles an ellipse, truncated at the ends of its transverse axis. With soft tin and other materials Eldredge has concluded that a complete contact ellipse is eventually established. Without unwarranted detail, the two situations of blunting and grooving can be compared as regards contact stress. For the same track width a higher contact stress would be expected in the grooving situation.

The contact stress for the elastically restrained case may be determined by using the deformed geometry in calculations based on the elastic solution. Stress and strain indices are derived on this basis in Reference 38.

B. PLASTIC DEFORMATION IN ROLLING CONTACT

Analysis of the phenomena of cumulative

plastic deformation divides naturally into two categories: initiation and accumulation. Questions pertinent to this section are: How much plastic deformation is to be expected initially in rolling with a given load, material and element configuration? What is the effect of number of cycles on this amount? Can this increase in groove depth or radial reduction with cycles be rationally attributed to plastic deformation? While these questions cannot at this time be answered completely for a full range of variables and conditions because of scarcity of experimental data, the foundation for more comprehensive answers may be constructed.

1. Initiation

From experiments at one extreme (grooving of very soft metals like tin and lead), Eldredge's data may be interpreted as predicting the amount of plastic deformation on the basis of the static hardness (load divided by projected area). That is, the initial track width for any size ball grooving a flat surface may be estimated closely by calculating the impression diameter expected on the basis of the static hardness. For annealed copper, because of work hardening caused by the forward displacement due to the rolling motion, the track width is noticeably smaller than the static imprint diameter. The effect is much smaller for cold worked metals.

For hard 52100 steel with various amounts of retained austenite Drutowski⁽³⁹⁾ reported track depth as a function of nominal maximum contact stress for plate grooving with cemented carbide balls of two diameters (1/4 in. and 1/2 in.). This data may be presented all on one plot (Figure 27) over the full range of contact stress if the radial deformation is made dimensionless by dividing by the theoretical elastic approach of the ball and plate, u_E . These data actually represent the groove depth u after 20 cycles. This method of presenting data, i.e., normalizing the measured deformation by dividing by the corresponding theo-

retical elastic deformation, is a convenient way of taking into account the element size.

Often the high calculated values of maximum contact stress are defended by the statement that even though these numbers are much higher than ordinary yield stress values, such stresses are possible because of the high degree of constraint. As regards initiation of plastic flow, elastic constraint on gross plastic flow is significant in some situations where the plastic nucleus is small. However, a more rational examination of the situation reveals that the values of initiation stress predicted on the basis of uniaxial tests are not as divergent as has been supposed. For this purpose consider the uniaxial tension and compression results of Sachs et al ⁽²⁾ for reasonably similar 52100 steel, and the elastic limits in tension reported by Drutowski. ⁽³⁹⁾ The value of octahedral shear stress at these "elastic limits" and the maximum octahedral shear stress at the point of first measurable plastic deformation in rolling contact for the various hardnesses are presented in Table 8. There is variation to be

sure, especially with so ill-defined a property as elastic limit, but the tension and compression values tend to bracket the rolling contact values. As stress is increased, the deviation of actual contact stress from theoretical is probably in accord with the allowances proposed above. This is further evidence that the contact situation cannot be examined wholly on the basis of maximum contact stress but requires consideration of state of stress and, as will be established below, the effect of the rolling action. This is true whether the phenomenon considered is static indentation, initiation, or accumulation of plastic deformation in rolling or fatigue.

2. Accumulation

Tabor ⁽⁴⁰⁾ has reported that in static indentation tests there is no accumulation of plastic deformation with repetition of load after the first application. In addition Jones ⁽⁴¹⁾ reports that the flattening of the ball in the indentation test is several orders of magnitude smaller than the plate indentation. Both of these statements are invalid when plastic deformation due to rolling contact is

TABLE 8
Octahedral Shear Stress for Initiation of Plastic Deformation of
52100 Steel in Tension, Compression and Rolling Contact

	Drutowski				Sachs		
	Ret. Aust.	Hardness*	τ_{oct} **		Ret. Aust.	Hardness	τ_{oct}
Tension	0	58	58,000		0	58	84,500
	7.4%	62	27,500		Trace	62	66,000
	3.9%	64	60,000		Trace	64	47,000
Compression	---	--	---		0	58	153,000
	---	--	---		Trace	62	145,000
	---	--	---		Trace	64	127,000
Rolling Contact	0	58	115,000		---	--	---
	7.4%	62	90,000		---	--	---
	3.9%	64	114,000		---	--	---

* Rockwell C hardness

** Maximum octahedral shear stress at reported "elastic limit", psi.

involved. In addition to the experimental evidence to be presented here from cumulative blunting and grooving of brass, there is the published data of Neimann and Kraupner⁽²⁷⁾ and Zaretsky and Anderson⁽⁴²⁾ referred to in the review.

A qualitative verification that plastic deformation accumulates, even at room temperature in hard steels, is furnished by the superimposed profile traces of a grooved surface (originally flat) presented in Figure 28. The traces were made at SKF⁽⁴³⁾ on a hard steel surface (Rockwell C 61.3) after various numbers of stress cycles in rolling. The maximum nominal contact stress was 730,000 psi (500 lbs. on 1/2 in. -diameter ball). Clearly, not only does the depth of the groove increase but the shoulder of displaced materials grows with cycles. Similar traces are presented by Zaretsky and Anderson for blunting of a ball constrained to roll over the same path in the Macks spin rig. On the basis of the limited evidence from the SKF rig there appears to be considerably less wear than reported by Zaretsky and Anderson at 750,000 psi after 10,000 stress cycles in Figure 9 of their paper.⁽⁴²⁾ Wear is determined by comparing the area of the shoulder bulge to the groove area.

The data of Niemann and Kraupner for the effect of cycles on the blunting of hard steel may be condensed and presented as a single graphical relationship if the reported track width is made dimensionless by dividing by the nominal elastic track width. This plot is given in Figure 29 a and the closeness of fit to the reported data is illustrated in Figure 29 b. It must be concluded that the accumulation of plastic deformation into millions of cycles, even for moderate loads at room temperature, is appreciably greater than the initial values. While a careful separation of wear and plastic deformation for a range of conditions has been achieved, there is indication that at high temperatures plastic deformation is very pronounced (Bamberger⁽⁴⁴⁾).

In order to conduct a more complete investigation in a situation allowing simple measurements, tests were performed on specimens of annealed brass in both blunting and grooving situations. Radial deformation and track width were measured at logarithmic intervals of 1, 10, 10^2 , 10^3 and 10^4 cycles for five load levels using the apparatus shown in Figure 4. A 1-1/2 h.p. motor drove the load roller at 1000 rpm for the plastic deformation experiments.

Specimens were designed so that a circular contact area would theoretically develop when they were mated with a hard steel load roller (either cylindrical or toroidal depending on the specimen tested). The dimensions of these specimens are given in Figure 30. As received, the brass varied from Rockwell hardness B 80 near the surface to B 53 in the center. After machining, the specimens were annealed at 960°F for four hours and furnace cooled. The final hardness was Rockwell B 12. Several of these specimens, both toroids and cylinders, had grid lines spaced at 0.020 in. scribed at two locations on the surface. After annealing, the specimens were polished with fine emery and oil, then buffed. The bore of the specimens was machined so as to provide approximately 0.001-in. press fit with the spindle.

In both the experiments on blunting and grooving the brass specimen was placed on the spindle in the lever arm and driven by the steel load roller. Before the tests on the annealed specimen, the effect of skew on the nature of the plastic deformation was assessed by use of un-annealed brass toroids. Various amounts of skew were introduced by adjusting the angle of the lever foot. It was observed that a change in angle of skew of less than 30 minutes was sufficient to cause unsymmetrical deformation to transfer from one side to the other. The foot was locked in the position that produced symmetrical blunting.

The lubricant for all tests was a commercial SAE 10-20 motor oil. The first 100 cycles

were turned by hand at a rate of approximately 100 rpm. The load was removed and gradually re-applied to the lever arm when the motor was started.

The test was interrupted and measurements were made at logarithmic intervals. A super-micrometer was used in measuring diametrical deformation while the specimen was still mounted on the spindle. For the measurement of groove depth the micrometer was fitted with knife edge feelers. Track width was measured by use of a scale and low power magnification.

Results are plotted in Figures 31 and 32. A dimensionless summary of the track width data for both blunting and grooving after the manner of Figure 29a is given in Figure 31c. While the accumulation of deformation beyond 10^2 cycles is greater for grooving, the numerical results on the whole are comparable, the rate of accumulation being nearly a linear logarithmic increase for grooving.

Wear could not possibly account for the phenomena reported here. Weighing of the specimen before, after, and at intervals during the tests, confirmed that the amount accounted for by wear, either the total amount or the change between various intervals, is a small fraction of the total volume displaced.

The fact that plastic deformation does accumulate in blunting as well as grooving confirms that the growth in track width is not primarily an external configuration effect as proposed by Eldredge. It has been shown that there is a definite reduction in contact stress with increase in track width in the case of pronounced blunting. There is no density transformation in brass that would account for such a large deformation. Accepting that the phenomenon is indeed due to accumulation of plastic strain by applied cycles of rolling even though the contact stress is reduced by the deformation, it is natural to ask the question: how?

Two possible sources of this phenomenon

are:

1.) Interaction of bulk residual and applied stresses during the complex loading cycle to produce cyclic flow even though the material is basically cycle-independent. The mechanics analysis of plane strain rolling of an elastic-perfectly plastic half space by Merwin and Johnson ⁽⁴⁵⁾ is such a case.

2.) Inherent cycle-dependent material behavior even in the absence of macro-stress or strain gradients.

These possible sources were proposed in a discussion of papers presented at the General Motors Symposium on Rolling Contact Phenomena in Warren, Michigan, October 1960. ⁽⁴⁶⁾

The actual situation may involve both. The second possibility should be explored before extensive mechanics analysis is devoted to the first. This is the approach taken below.

The usual assumption of the identity of current loading and subsequent yielding surface in classical plasticity theory is reasonably well founded for simple radial (proportional) loading. However, there are important experimental qualifications even for repeated tensile loading at room temperature.

The observation of accumulation of plastic strain by means of repeated stress was made early in the investigation of behavior of metals under cyclic stressing. Bauschinger's "natural elastic limit" was a consequence of this observation. Bairstow ⁽⁴⁷⁾ also measured cumulative plastic strains for repetition of stress.

Yet these deviations from the theory do not appear sufficiently pronounced to account for such a large accumulation of plastic strain in rolling contact where the contact stress actually reduces. However, for the particular brass used in the toroid specimens, tensile tests under repeated load were made to explore this possibility. No accumulation of plastic strain of the magnitude observed in rolling contact could be measured for cyclic loading in tension.

The effect of the rolling action on the stress history of an element in the highly stressed volume of material in the contact region appears to be a significant feature in accounting for the observed accumulation of plastic deformation. A subsurface element in the track center is first sheared forward as the rolling load approaches and then backward after it passes. When the contact area is in the near proximity of the element the associated stress deviator has a significant tensile component transverse to the rolling direction or track. Subsurface elements at the track edge also experience a shear reversal, in addition to the orthogonal shear in the transverse direction which increases to a maximum and decreases as the load passed by. Thus, while the element is in the region of high distortion there is a shear reversal, flow being induced transverse to the track.

As an illustration of this history, the stress variations on a subsurface element for the elastic case of cylindrical contact is given in Figure 33.

Unlike one directional repeated stressing, reversal of the shear stress may cause large changes in the inherent deformation resistance of metals. Tuler and Morrow⁽⁴⁸⁾ have reviewed the cycle-dependent stress-strain behavior of metals and present data for OFHC copper demonstrating both hardening and softening in the cyclic state. Smith, Hirschberg, and Manson⁽⁴⁹⁾ report on the cyclic stress-strain behavior of several steels including 52100 at a hardness of Rockwell C 53. All of the heat treated steels softened as a result of being cyclically strained. For the 52100 steel a cyclic strain amplitude of 1% caused a drop in the stress amplitude from about 280,000 psi to 200,000 psi. Such a cycle-dependent softening would lead to a cycle-dependent increase in contact area. Thus, the geometric changes of elements during rolling contact may be partially due simply to an inherent cycle-dependent reduction of deformation resistance of the metal subjected to repeated reversals of shear stress.

To explore the possibilities of accumulation of plastic strain with cycles of complex stress under controlled conditions, combined tension-torsion tests were preformed on a double gage length solid specimen of annealed brass. The axial load was increased to a maximum value with a constant torque, unloaded, the torque reversed, and loaded again. This loading program caused an accumulation of axial plastic strain.

The nominal tensile stress-plastic strain path for a series of these cycles is shown in Figure 34. It should be noted that repetition of the load cycle without reversing the torque did not cause measurable plastic deformation to accumulate. The magnitude of the increments in plastic strain, the tensile yielding at a point well below the maximum load, and the cyclic work hardening are features which are qualitatively in agreement with the observed cyclic deformation in rolling tests.

Certain features of the phenomenon might be associated with incremental collapse or "shake-down" models familiar to structural analysis. However, it is probable that this cyclic instability is an inherent feature of metal behavior.

Because the specimens were solid the torque causes a macro-strain gradient. In order to eliminate this, steady tension and alternating shear stress tests were performed on thin wall copper tubing. Some of the results of these tests are presented in Figure 35. The shear stress-strain hysteresis loops are also shown. Therefore, it appears that cyclic strain accumulation is an "inherent" material response to such complex stress cycles, and may be expected to play a significant role in the cumulative deformation observed in rolling. A more complete exploration of this phenomenon is given in Reference 50.

Because of unexplored areas of cyclic deformation even in simple radial loading, lengthy speculation as to the fundamental mechanism is unwarranted. Nevertheless, it seems reasonable that after considerable dislocation generation due to initial plastic deformation, new routes of escape

from dislocation entanglement or other barriers to slip are provided by the complex stress cycles used in these tests. In addition, vacancy capture and mechanically induced climb mechanisms may be expected to operate under repeated load conditions. This process would be accelerated with increase in thermal energy provided in high temperature environments.

C. ASSOCIATED PHENOMENA

In addition to observations of the amount and rate of accumulation of external deformation, some associated phenomena were studied. The nature and intensification of distortion of orthogonal grids on the rolling tracks for both blunting and grooving, the effect of an initial cycle at high load on subsequent deformation at lower load, and some remarks about the nature of residual stress pattern to be expected as a result of plastic deformation in a simple case, complete the treatment of cumulative deformation in rolling presented here.

1. Influence of Rolling on Surface Grid Distortion

A phenomenon that has provoked a great deal of discussion is the surprising forward (direction of disk rotation) displacement of transverse surface lines and the associated subsurface displacement due to rolling that Crook⁽⁵¹⁾ and Welsh⁽⁵²⁾ observed in mild steel disks. The nominal maximum contact stress was 240,000 psi, and the frequency was 1500 rpm. The contact was lubricated with a jet of oil of about 50 centistokes viscosity. For pure rolling, originally straight lines parallel to the cylinder axis appeared to be "pulled" into the contact area. This occurred on both the driver and driven roller, thus opposing any tangential friction. As might be expected the plastic zone is confined to a subsurface band because of the depth to the maximum shear distortion in the contact situation. But this band is displaced forward in the rolling direction, causing a distortion of radial lines as shown schematically in Figure 36. Crook gives a

rather improbable explanation of this by stating that the forward shear is a result of the increase in velocity of material under the contact point, due to change in effective cross sectional area. Thus, it appears that this velocity increase must be due to increments of plastic deformation each cycle and not elastic compression, and further, that the intensity of the phenomenon must depend predominantly on speed of rotation. A number of more feasible alternative explanations based on the existence of a hydrodynamic film which modifies the static Hertzian contact pressure have been offered in the discussion which accompany Crook's paper. Milne and Lewicke⁽⁵¹⁾ proposed that the high local tangential lubricant shear stress in the outlet direction (because of short outlet area) produce the plastic tangential "creep."

Another suggested explanation is that proposed by Christopherson and Johnson. For simplicity, consider the identical disks shown in Figure 36 which are independently driven so that no resultant friction exists between them. Since plastic work is being done (as well as "elastic" hysteresis energy dissipation), there must be an offset of resultant normal force towards the leading edge of the contact area. Also, from hydrodynamic lubrication theory, there must be a displacement of resultant force from the point of nearest approach toward the leading edge, and more important, a gradual build-up of pressure at entrance and a sharp drop-off at exit.

As the subsurface element approaches the contact it is sheared backward and then forward as it passes under. The maximum shear stress will be expected in the forward direction due to the abrupt drop-off of contact pressure after the point of resultant force is reached. To examine the possible order of magnitude of this effect, a calculation for the orthogonal shear stress was carried out in Reference 38 for an extreme asymmetric pressure distribution. This shear stress is plotted in Figure 37 at a depth of one-half the contact length. The increase of forward

over backward shear stress is 18 per cent. Thus there is a small mean shear stress in the forward direction which could account for the preference for distortion in that direction. Benham,⁽⁵³⁾ for example, has shown that only a small bias in stress is required to cause a large accumulation of strain under cyclic loading. However, the small bias in stress proposed above depends on the presence of a lubricant. The validity of the above concept is clouded by the conflicting observation made by Hamilton⁽⁵⁴⁾ that forward displacement occurs even in the absence of a lubricant.

Perhaps the most probable explanation is that based on an analysis recently proposed by Merwin and Johnson.⁽⁴⁵⁾ By assuming the elastic strain cycle and integrating the Prandtl-Reuss plasticity relations by increments, they determine the corresponding stress cycle. This procedure gives residual values of orthogonal shear stress which because of final equilibrium considerations are relaxed at zero. This implies a residual shear strain that accounts for a "forward" shear displacement. Even though the analysis is approximate in that it violates equilibrium during the loading cycle and compatibility when the residual stresses are relaxed, many essential features of the phenomenon are dealt with logically.

Using brass toroids and cylinders a similar study for the three-dimensional situation are conducted as a part of this investigation. Several factors emerge: For severe grooving, differential slip had the predominant influence on distortion of transverse surface lines. In blunting, the original backward displacement of transverse lines is in accord with the fact that a bulge or hill of material is formed on the inlet side, as in plastic reduction in strip rolling. This pattern is not accentuated with cycles after the initial severe blunting. The tangential drag, or possible mechanisms mentioned in connection with Crook's phenomenon, tends to straighten the line after this. The specimens before test are shown in Figure 38, and photographs

of the tracks are displayed in Figure 39. The backward displacement of the side portion of the lines in grooving is not as pronounced as the forward displacement, possibly because of the net friction force required to drive the brass cylinder.

2. Effect of Preload

After large numbers of cycles Niemann and Kraupner⁽²⁷⁾ observed smaller total accumulation of deformation in rolling after an initial period of high load, compared to tests at the lower load during the same running time. The effect of previous cold work in reducing the rate of accumulation of deformation even at high temperatures has been observed by Bamberger.⁽³⁷⁾

This preload effect was also observed in the rolling tests with brass specimens. In both blunting and grooving only the initial cycle was at the high load. The results are presented graphically in Figures 31 and 32. When the cross over occurs in track width the contact stress on the preloaded specimen is actually higher than that in a companion toroid at the same load, yet the rate and total accumulation is slightly lower.

Two factors contribute to the increased resistance to deformation as a result of preloading. There is a set of residual stresses created by preloading which algebraically opposes the applied stresses at lower loads, and the metal in the contact region is cyclically hardened to a higher level than possible by continuous operation at the smaller rolling load.

3. Residual Stress

As a result of cumulative plastic deformation, residual stresses may be expected to intensify with cycles of rolling. Such observations in hard steel have been reported by Bush et al.⁽⁵⁵⁾ Analysis of the residual stress distribution in a perfectly plastic half space due to rolling has been made by Johnson.⁽⁵⁶⁾ Unlike the half space problem a tensile residual stress normal to the surface can be developed in a disc or roller. Consider a solid cylinder subdivided into three

regions: an outer ring, an inner concentric ring, and a solid core. If the inner ring is plastically expanded and the assembly is fitted back together, residual tension between the plastically deformed inner ring and the elastic core, as well as tangential compression, develops. Typical calculations are illustrated in Reference 38.

In the three dimensional situation the elastic constraint is even higher because of the adjacent elastic material at the side of the track. Hence, a more severe residual stress pattern might be expected.

For more complete information on residual stresses induced by rolling and the influence of residual stresses on fatigue, the reader is referred to a recent book by Almen and Black. ⁽¹⁸⁾

V. SUMMARY AND CONCLUSIONS

This bulletin has two main parts. The Appendices deal with a review and classification of research concerning aspects of the failure of surfaces in rolling contact. The text contains analyses of certain features of two modes of failure (pitting and cumulative deformation) involving original experiments and interpretation of appropriate experiments from the literature and examples of correlation of pitting data. A brief summary and statement of conclusions follows.

A. REVIEW

Research has been classified and identified according to two indices: mode of failure and phase of research. Representative research from areas defined or located by these indices have been critically reviewed.

1. Pitting

A great deal of research over the years has been conducted in all phases of pitting failure, centering heavily in the area of controlled experimentation (material and lubricant evaluation) with the bench rig tester playing an important role. Theory and interpretation have not been so well explored. Effort exists not only to screen and evaluate, but to extend minimum material data and fundamental properties to actual component performance. Principles for this extension or correlation of data are not well established, the possibility and extent of the correlation being debated in the literature. Some fundamental research into the nature of lubricant films involved in rolling contact has been started for the two-dimensional situation.

2. Cumulative Deformation

Observation of excessive run-out developing in bearings in the relatively few high-temperature investigations has alerted researchers to a new failure mode, but the primary cause has not been established even in the first efforts at controlled experimentation. Cycle-dependent cumulative plastic deformation has been advanced as a cause. However, no comprehensive theory or interpretation is available even from fields of pure material research concerning the accumulation of plastic strain under repeated stress. A three-dimensional plasticity solution for one rolling cycle might at least serve as a rational basis for eliminating size and configuration effect and estimating plastic strain associated with a given external deformation. But the complications existing in the present static indentation approaches are compounded, and a comprehensive solution even for simple stress-strain idealizations appears beyond present expectations. Some analyses of the two-dimensional case for perfect plasticity have been developed. As a result of this sparse research there are yet no well-established fundamentals to serve as the basis for prediction or design.

3. Excessive Rolling Resistance

The phenomena associated with this mode of failure have been subjects of research interest for perhaps the longest time. Yet the least controlled experimentation of fundamental significance in the range of practical interest has been conducted in this area. This is especially dis-

concerting since such information is important to a rational mechanics analysis of the two other failure modes. Rejection or failure of instrument bearings in service due to excessive or variable torque has led researchers to consider both surface interaction energy losses and internal dissipation losses. Data for experimental separation of these phenomena are not available.

B. ANALYSIS

Features of two modes of failure (pitting and cumulative deformation) have been analyzed with regard to primary material cause and configuration and size effects.

The significance of the action of rolling in both of these modes is emphasized. The influence of rolling element configuration on pitting fatigue life is directly related to the effect of rolling in contrast to repeated contact. The rolling action reverses a subsurface shear, which is a function of configuration, producing a critical range of stress. Regarding cumulative deformation, the complex stress cycling involving shear reversal in highly distorted regions is responsible for the continuance of cyclic plastic flow, despite the resulting contact stress reduction.

1. Pitting

The effect of geometry or rolling element configuration on pitting fatigue life in bench rig experiments was established on the basis of the presentation of data collected from several sources. The effect of configuration on the magnitude of maximum reversed subsurface shear stress is such as to suggest it to be the critical stress, and an appropriate strength index for comparing widely divergent configurations of rolling elements. It is assumed that comparison is made in otherwise equivalent circumstances. Subsurface origin of fatigue cracks responsible for pitting is indicated, propagation parallel to the surface being enhanced by the residual radial tensile stress due to plastic deformation. A few observations of subsurface structure in pitting

tests conducted here tend to confirm this view.

A simple size effect analysis based on the usual Weibull distribution function and length of rolling track is the basis of an expression that permits extension of pitting life data to various sizes of rolling elements.

These considerations are applied in the correlation of

- a) torsion fatigue and rolling contact bench rig data
- b) rolling contact bench rig data and full scale bearing tests.

2. Cumulative Deformation

In an effort to identify the primary cause of this failure in a pronounced and easily measured situation, rolling experiments on brass elements mated with hard rollers, and tests in combined tension and torsion were conducted. The intensification in external deformation with cycles of rolling was attributed primarily to a material phenomenon of cumulative plastic strain via complex stress cycles for the following reasons:

1. The progressive reduction in diameter is not due to wear, since the weight reduction of the specimens account for only a small percentage of it.
2. The success of the relation among the parameters of deformation, which assumes redistribution of material at contact, in approximating the actual correlation of track width and radial deformation, as well as the relatively large volume involved, rule out simple density transformation in brass.
3. The cyclic intensification of plastic flow in the track indicated by the forward displacement of orthogonal grid lines scribed on the specimen attests to the accumulation of plastic strain.
4. Combined stress tests for complex loading cycles with the same material resulted in a cycle-dependent accumulation of plastic strain, indicating that the rolling contact mode is a mani-

festation of the same phenomenon.

Analysis of available data on hard steel was made in terms of a convenient deformation index. The index expresses plastic-deformation (radial or track width) as a fraction of its elastic counterpart, and its utility was indicated in condensing the data of Drutowski and Niemann and Kraupner.

Three salient features associated with this mode of failure are accumulation of plastic strain, reduction in applied stress, and cyclic intensification of residual stress.

VI. RECOMMENDATIONS

From the above review and analysis a number of recommendations for both research aims and technical application follow:

A. PITTING

The effect of alignment of rolling elements on surface failure, notably pitting, should be investigated. Skew of less than $1/2$ degree has been found to be sufficient to cause unsymmetrical deformation in blunting. There was also some indication of a marked decrease in pitting life for skew of that order of magnitude.

The effect of stress level on pitting life variability or Weibull slope should be investigated. This effect cannot be included in the form of the equation developed by Lundberg and Palmgren. The investigation will require collection and statistical analysis of sufficient contact fatigue data for a large stress range.

A fundamental correlation equation based on these findings and the most recent engineering descriptions of fatigue should be developed. The influence of lubricant, relative surface motions and interaction, and transient temperatures on the two major categories of mechanics analysis, critical loading cycle and inherent material property, must be evaluated.

B. CUMULATIVE DEFORMATION

The extent and intensity of plastic strain due to three dimensional rolling, even in pronounced cases, needs further experimental investigation. It is obvious that more controlled investigations will have to be conducted into effect of rate, temperature, and material on magnitude

of deformation accumulated. However, as a corollary to this, further investigation into the effect of configuration and size is needed for the extension of these data to practical designs.

The effect of preload or mechanical working, apart from or in conjunction with heat treating procedures, should be considered in developing more cyclically stable materials with a slower rate of accumulation of plastic deformation in high temperature applications. Such possibilities have been pointed out by Niemann and Kraupner (preload) and by Bamberger (previous cold work). It is possible that a short running period of high preload together with close fitting reassembly of pre-run component parts may increase life to excessive run-out. At any rate, material suitability in high temperature application is not determined by constant load creep or hot hardness tests but by stability under complex cyclic loading.

The basic material phenomenon must be investigated as it will most certainly become an important failure mode as higher temperatures and complex cyclic loading in structures are encountered. In this respect the rolling contact problem is only a single manifestation or forerunner of a broad class of problems. Gross dimensional instability of structures or frames subject to variable and repeated combined loading cycles is expected to be due in large part to this mechanism. The usual shakedown analysis based on ideal plastic action of frame components will not be directly applicable. Further laboratory tests of metals under complex stress cycles, extending

the combined tension-torsion tests reported here, are needed. Thin walled tubular specimens should be used to obtain macroscopically uniform stress states, thus eliminating compatibility or plastic strain gradient effects which give rise to shakedown phenomena in continuous media.

C. EXCESSIVE ROLLING RESISTANCE

A complete dynamic investigation is needed of the rolling phenomenon, including measurement of normal and tangential forces, as well as normal force offset or coefficient of rolling for a practical range of loads and speeds. This will necessitate independently driven surfaces--the torque on the system will have to be determined in a manner that eliminates the effect of support bearing friction. Only in this way can friction and internal hysteresis losses be separated for a range of controlled conditions.

D. GENERAL

In closing, the authors would like to criticize the current direction of research on rolling elements. It is our opinion that a disproportionate amount of effort is spent on uncontrolled and uncorrelated routine bench testing and on the lubricant and "metallurgical aspects" of the problem while the "mechanics" of rolling contact is slighted. We would encourage researcher and sponsors of research to reassess the obstacles to understanding the rolling contact problem and see if more effort could not be wisely spent in studying the forces, displacements, stresses and strains for bodies in rolling and sliding contact.

FIGURES

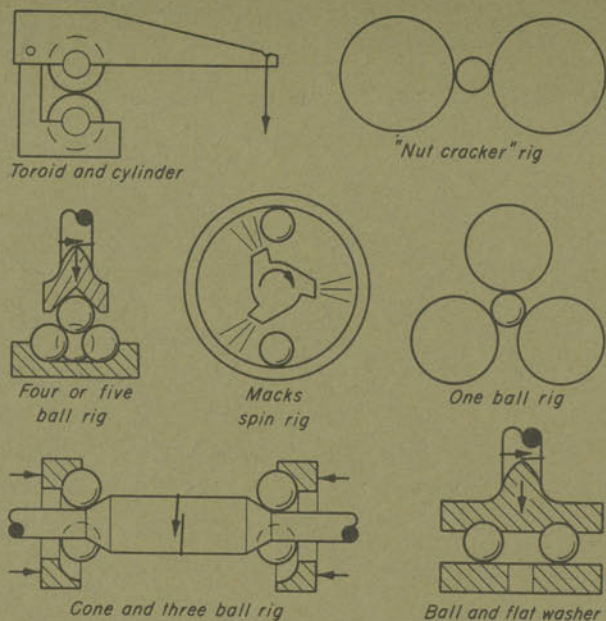
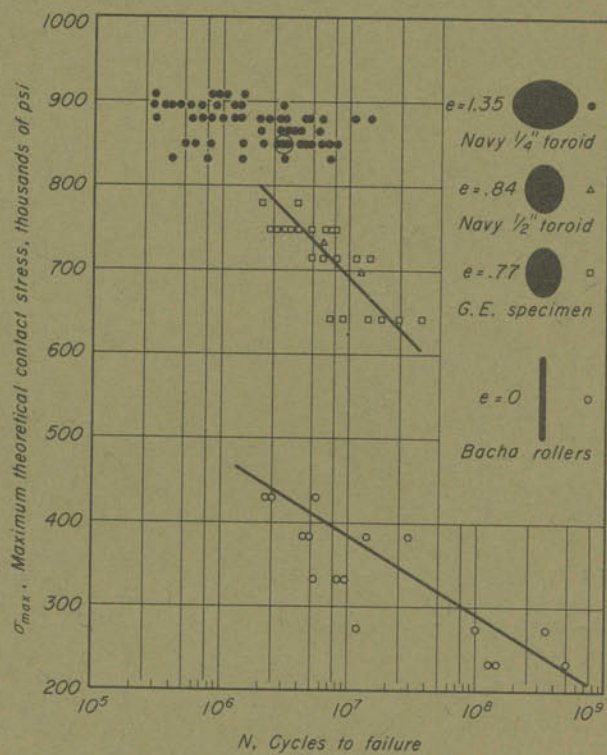


FIGURE 1. SCHEMATIC ILLUSTRATION OF VARIOUS ROLLING CONTACT RIG TYPES

FIGURE 2. CONTACT FATIGUE DATA FOR SEVERAL GEOMETRIES



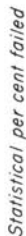


FIGURE 3. EFFECT OF RIG TYPES AND ROLLING ELEMENT CONFIGURATION ON PITTING ENDURANCE FOR THREE STEELS

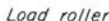


FIGURE 5. ROLLING ELEMENTS USED IN
PITTING ENDURANCE TEST

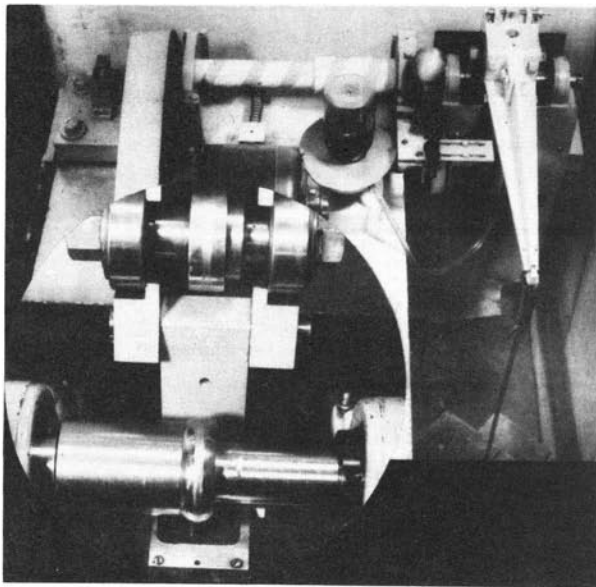
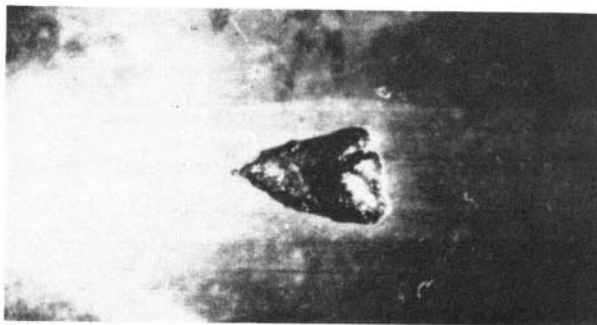
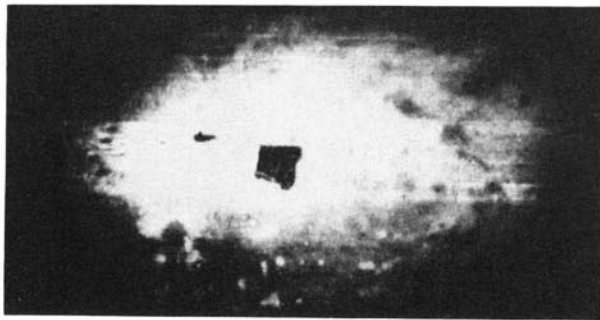


FIGURE 4. ROLLING CONTACT RIG
USED IN CUMULATIVE DEFORMATION
AND PITTING EXPERIMENTS



(a) Pit on specimen A-4 after $.77 \times 10^6$ cycles



(b) Pit on specimen B-3 after 8.7×10^6 cycles

FIGURE 6. TYPICAL PITTING FAILURES

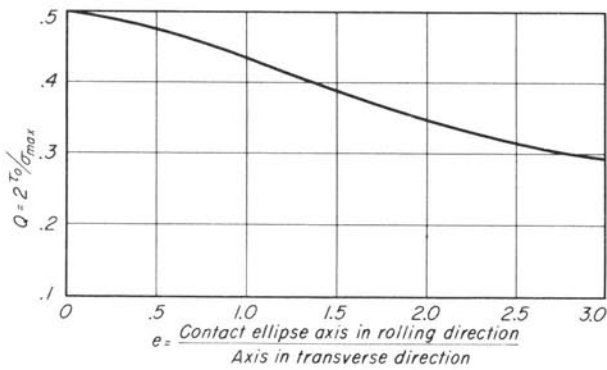


FIGURE 7. RANGE OF ORTHOGONAL SHEAR STRESS AS A FUNCTION OF ROLLING ELEMENT CONFIGURATION, e

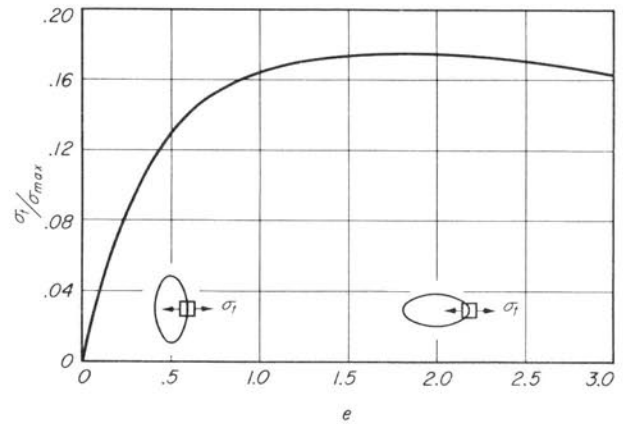
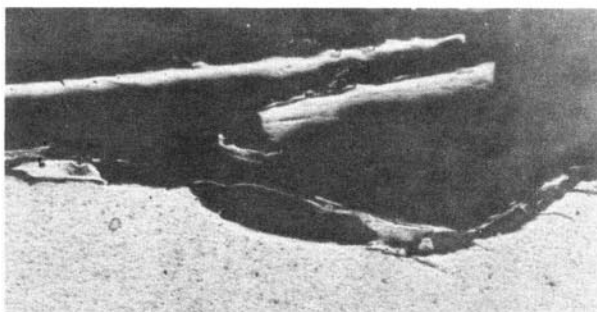
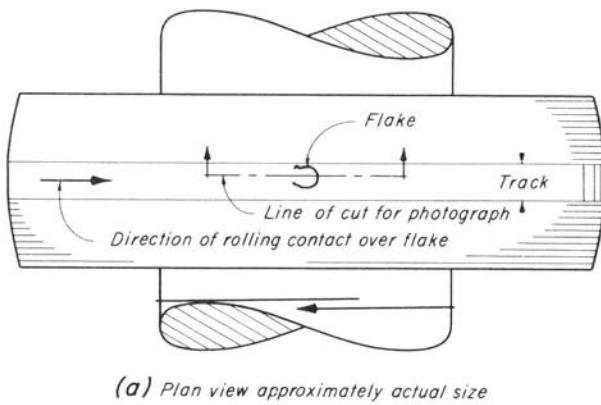


FIGURE 8. SURFACE TENSILE STRESS AT LEADING EDGE OF CONTACT ELLIPSE AS A FUNCTION OF ROLLING ELEMENT CONFIGURATION, e



(b) Enlarged photograph of sectioned specimen showing flake fragments lifted during grinding, approx 25x

FIGURE 9. INCIPIENT FLAKE ON TOROID SPECIMEN A-2

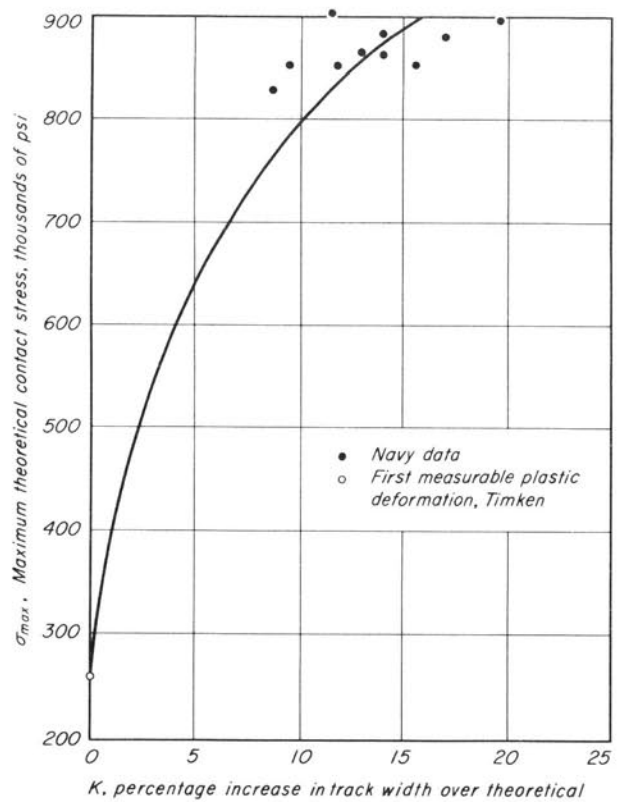


FIGURE 10. INCREASE IN TRACK WIDTH

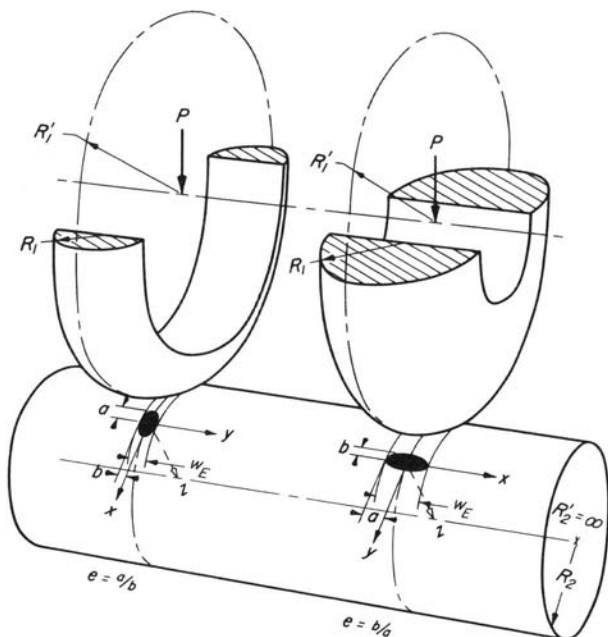


FIGURE 11. GEOMETRIC DEFINITIONS

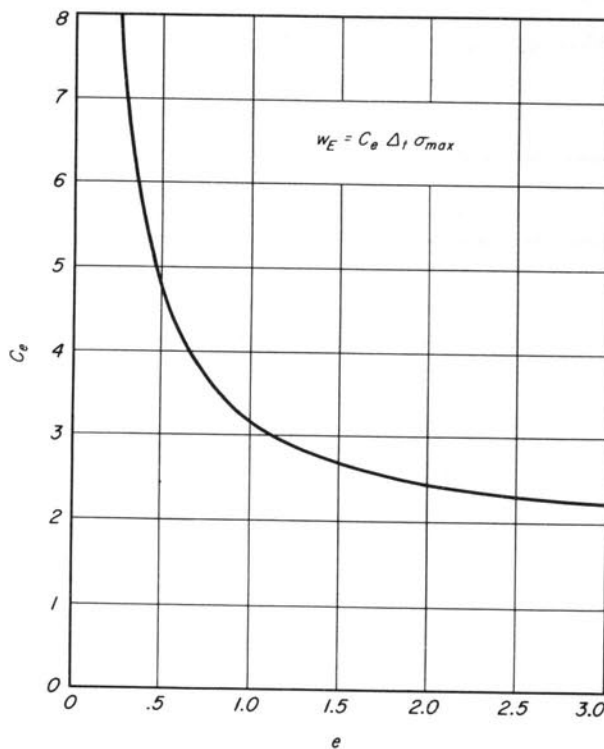


FIGURE 12. FACTOR FOR TRACK WIDTH CALCULATION

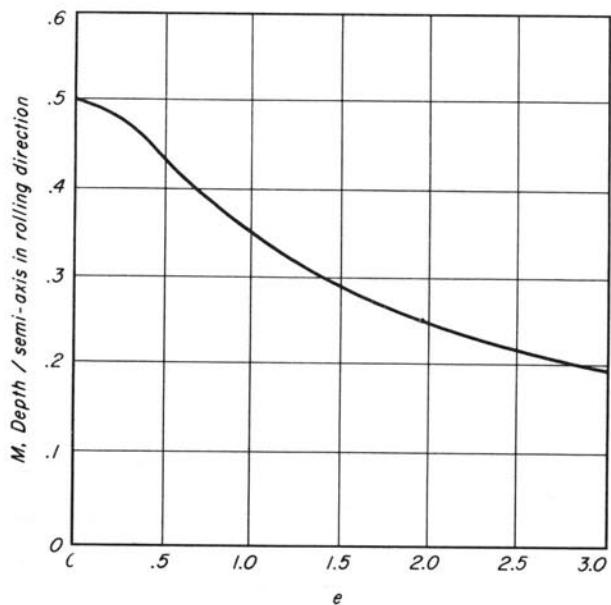


FIGURE 13. DEPTH OF MAXIMUM ORTHOGONAL SHEAR STRESS

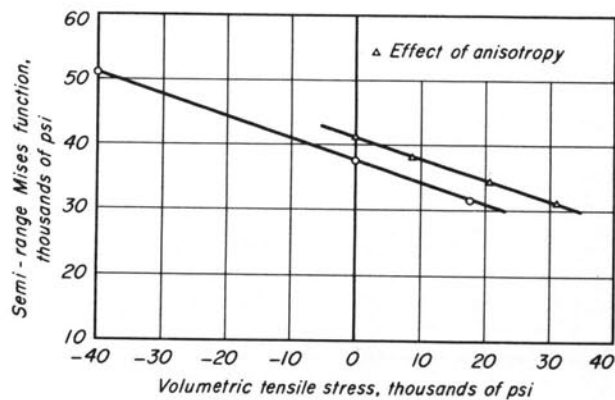


FIGURE 14. EFFECT OF HYDROSTATIC PRESSURE ON FATIGUE (CROSSLAND)

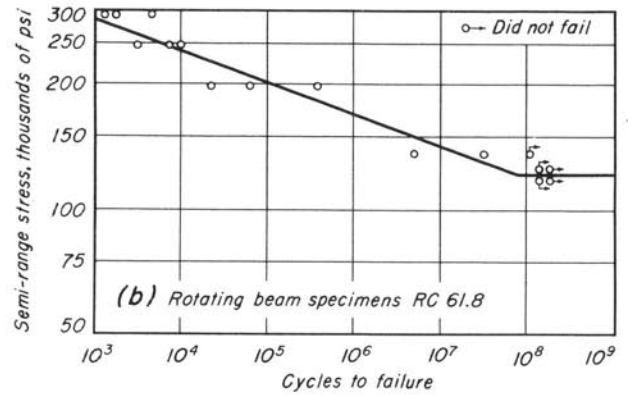
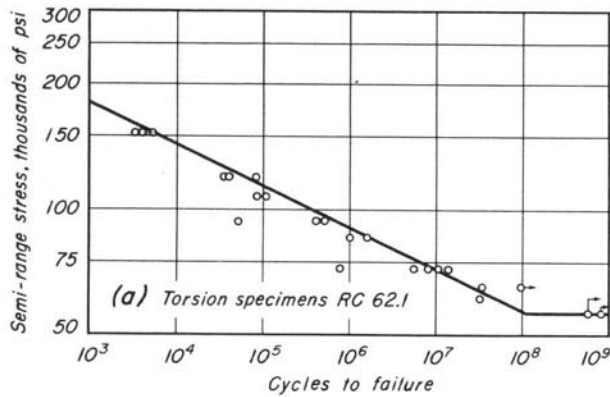


FIGURE 15. S-N CURVES FOR TORSION AND ROTATING BEAM TESTS OF HARD 52100 STEEL (STYRI)

- I Maximum contact stress corrected for plastic increase in track width
- II Range of orthogonal shear stress, geometry effect
- III Semi-range of orthogonal shear stress corrected for volume stressed
- IV Torsional fatigue strength or essential shear stress for contact fatigue, effect of state of stress

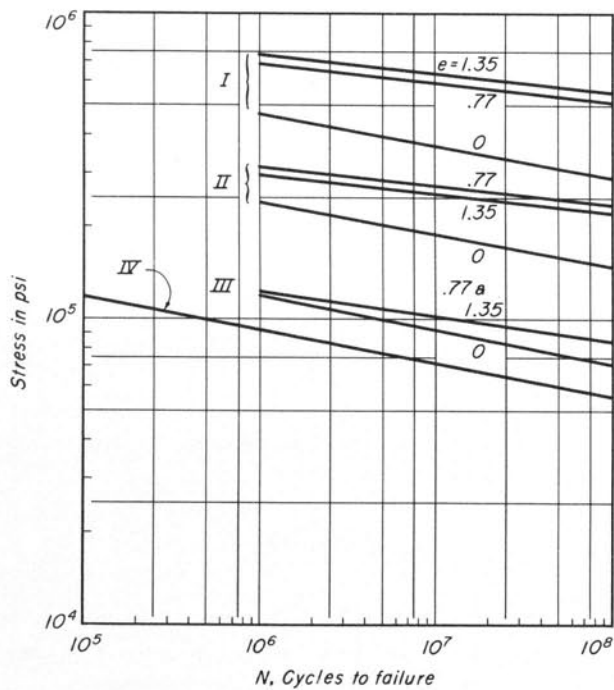


FIGURE 16. SUCCESSIVE STEPS IN CORRELATION OF DATA

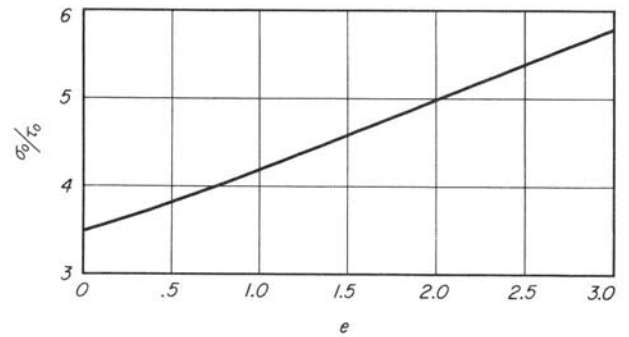


FIGURE 17. RATIO OF NORMAL TO SHEAR STRESS ON PLANE OF MAXIMUM ORTHOGONAL SHEAR STRESS

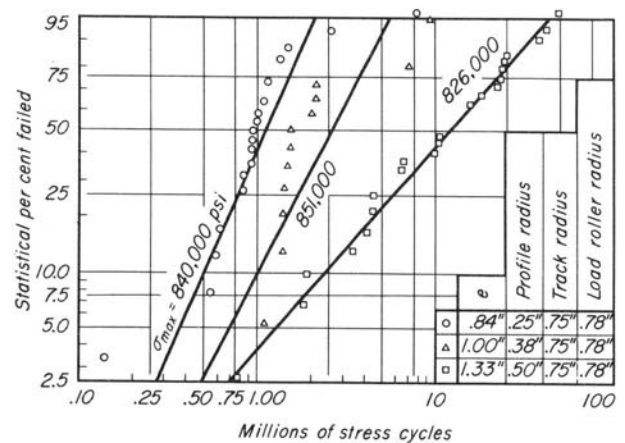


FIGURE 18. WEIBULL PLOT OF UNADJUSTED ANNAPOLIS DATA

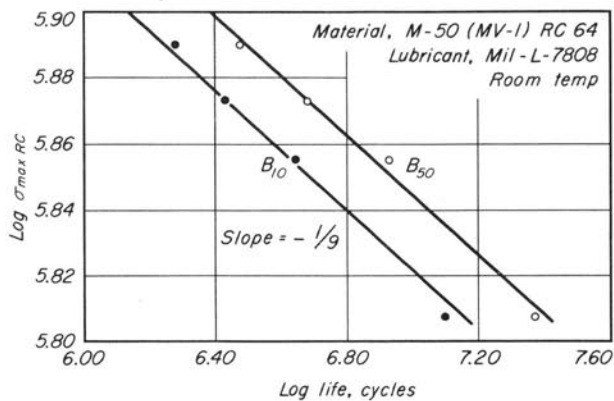


FIGURE 19. LOG-LOG PLOT OF RC DATA
SHOWING SLOPE TO BE $1/9$ TH

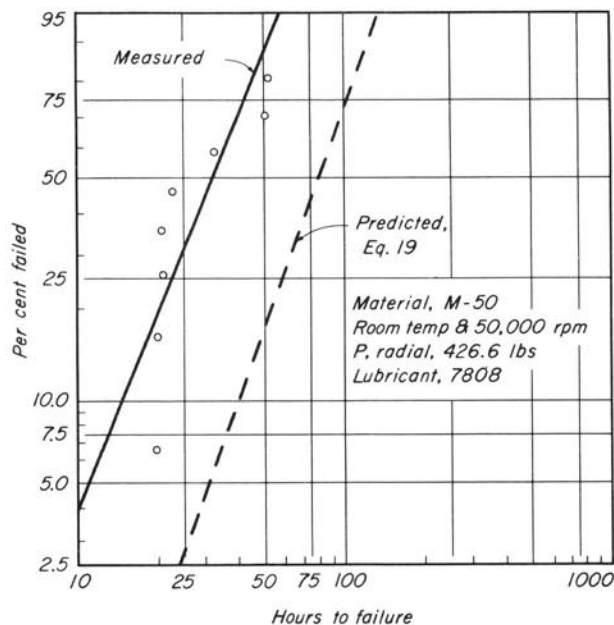


FIGURE 21. GEL 202K RADIAL BEARING DATA

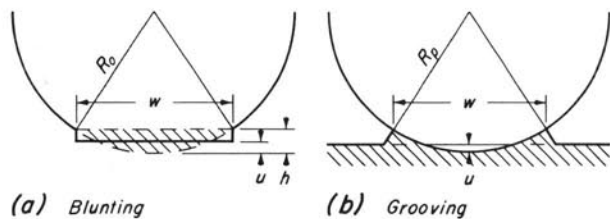


FIGURE 23. IDEAL PRONOUNCED PLASTIC
DEFORMATION

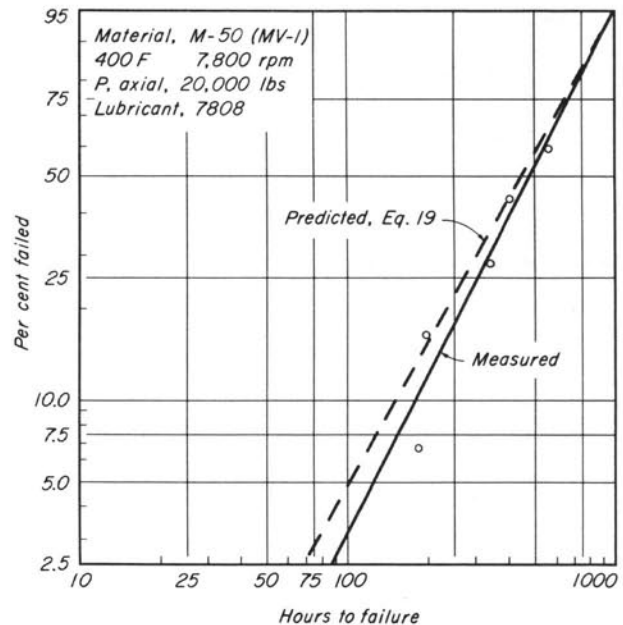


FIGURE 20. THRUST BALL BEARING DATA

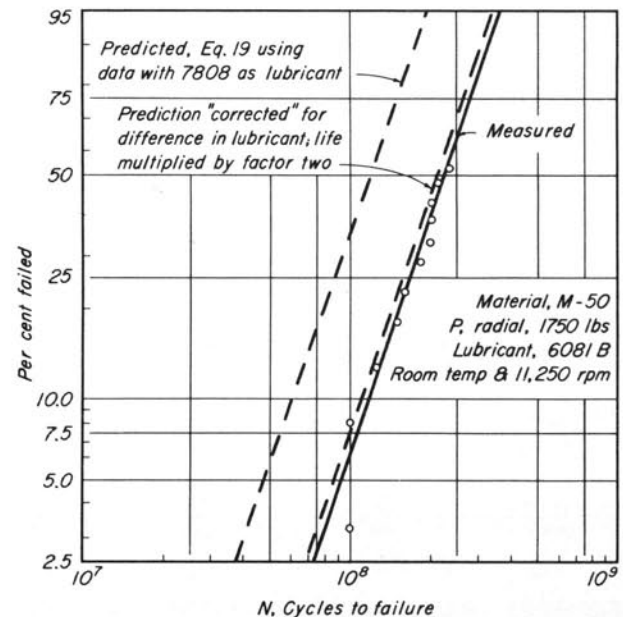


FIGURE 22. 202S MRC RADIAL BEARING DATA

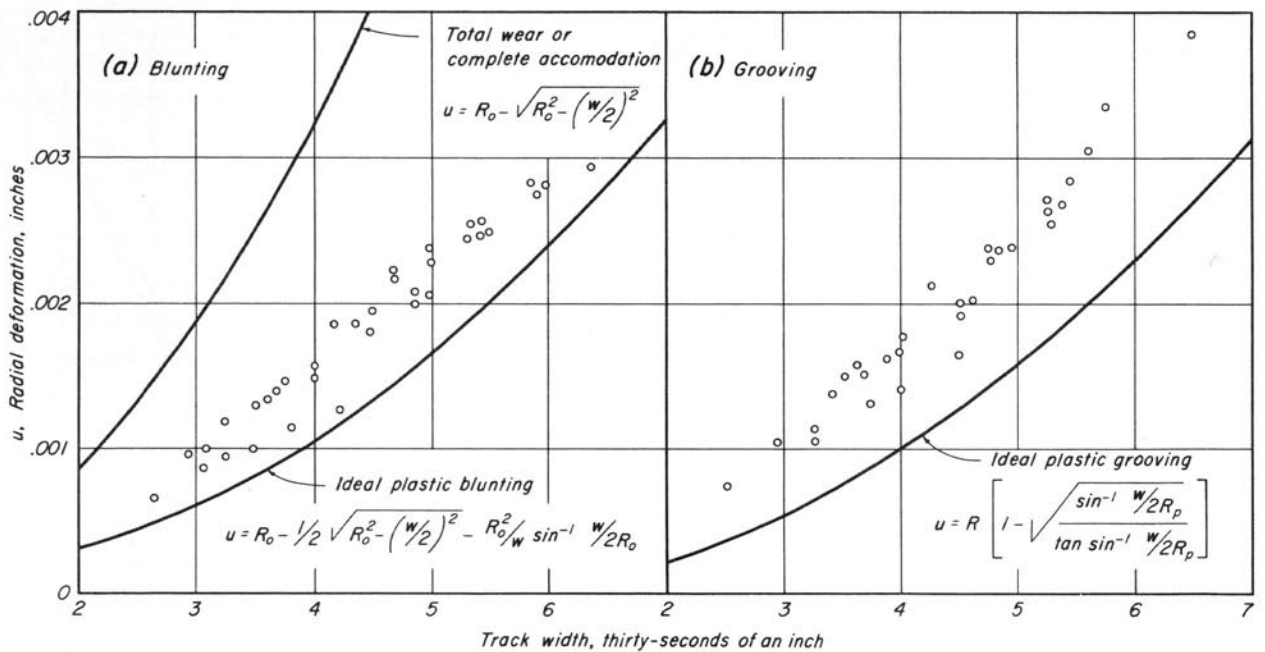


FIGURE 24. COMPARISON OF THEORY AND EXPERIMENT FOR PRONOUNCED PLASTIC DEFORMATION

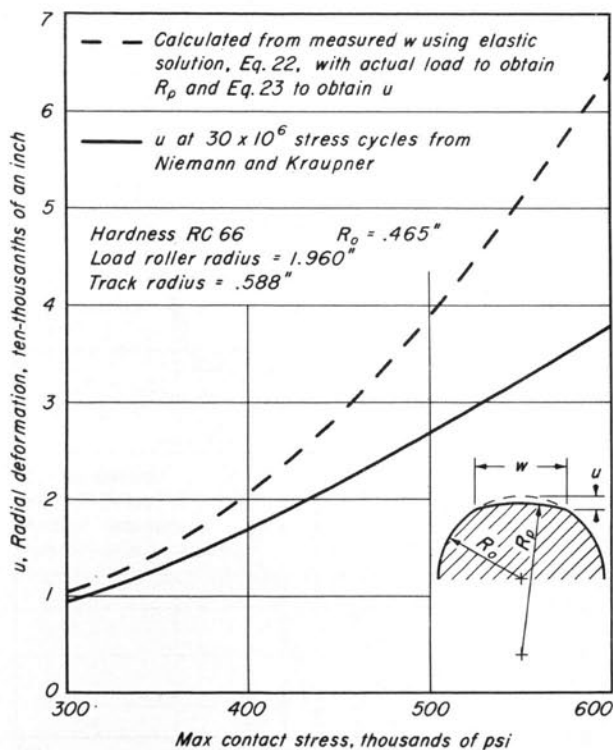


FIGURE 25. RADIAL DEFORMATION FOR ELASTICALLY RESTRAINED PLASTIC BLUNTING

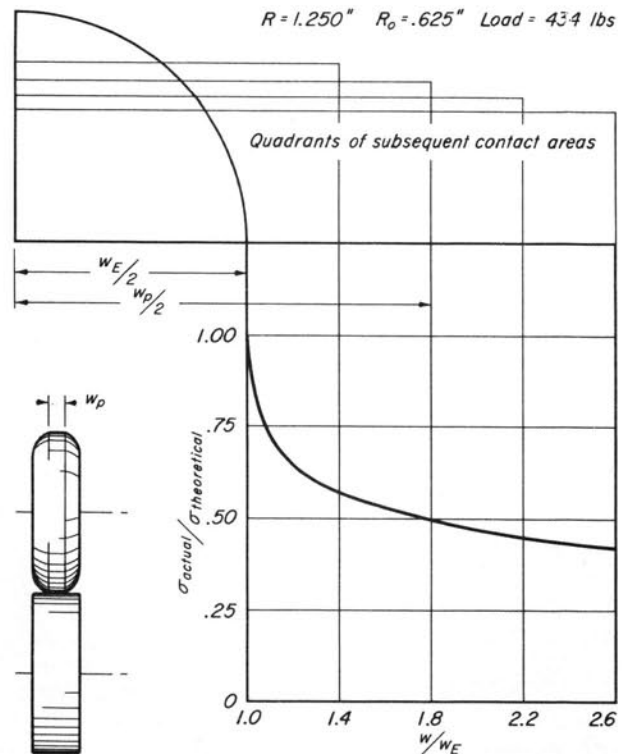


FIGURE 26. REDUCTION OF CONTACT STRESS IN PRONOUNCED PLASTIC BLUNTING

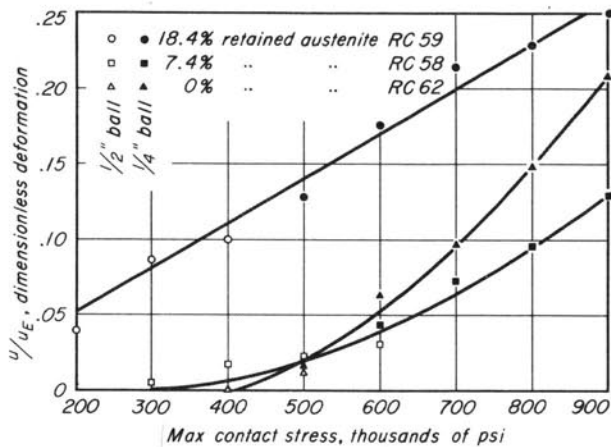


FIGURE 27. DIMENSIONLESS PRESENTATION OF DRUTOWSKI'S GROOVING DATA

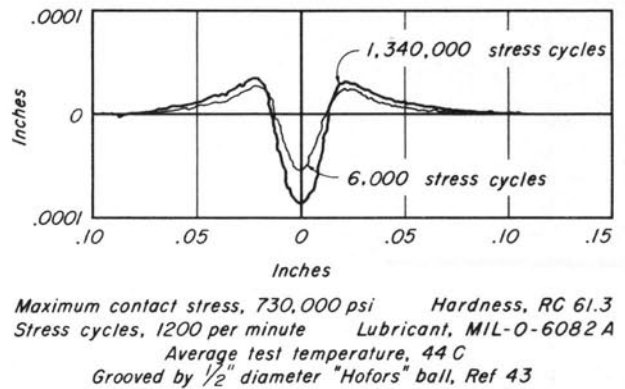


FIGURE 28. SUPERIMPOSED TRACES OF FLAT PLATE GROOVED BY ROLLING BALL

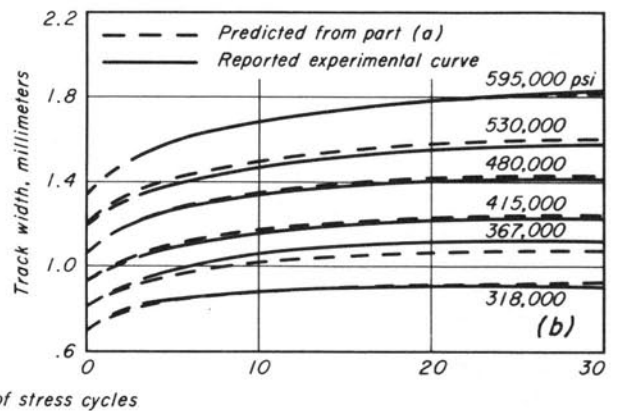
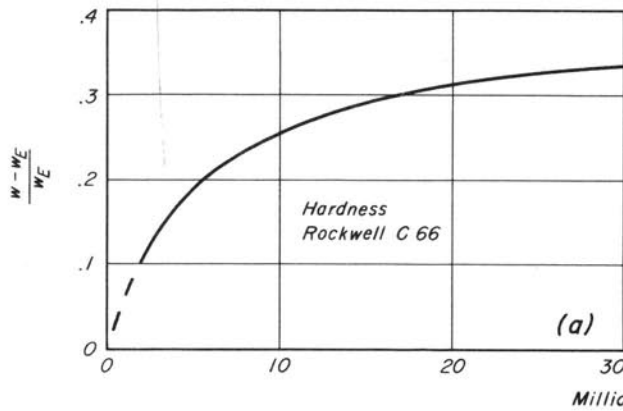
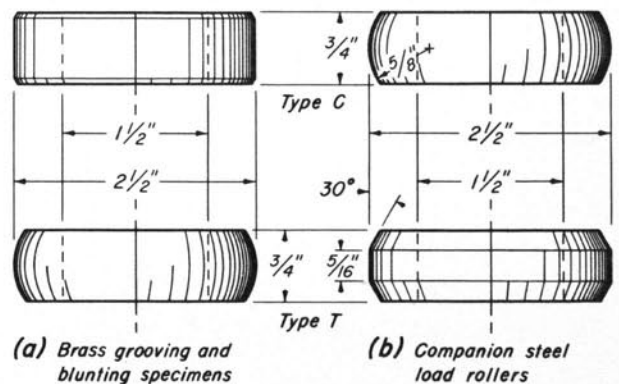


FIGURE 29. DIMENSIONLESS SUMMARY OF KRAUPNER AND NIEMANN'S BLUNTING DATA AND COMPARISON TO ACTUAL EXPERIMENTAL RESULTS

FIGURE 30. ROLLING ELEMENTS USED IN CUMULATIVE DEFORMATION TESTS



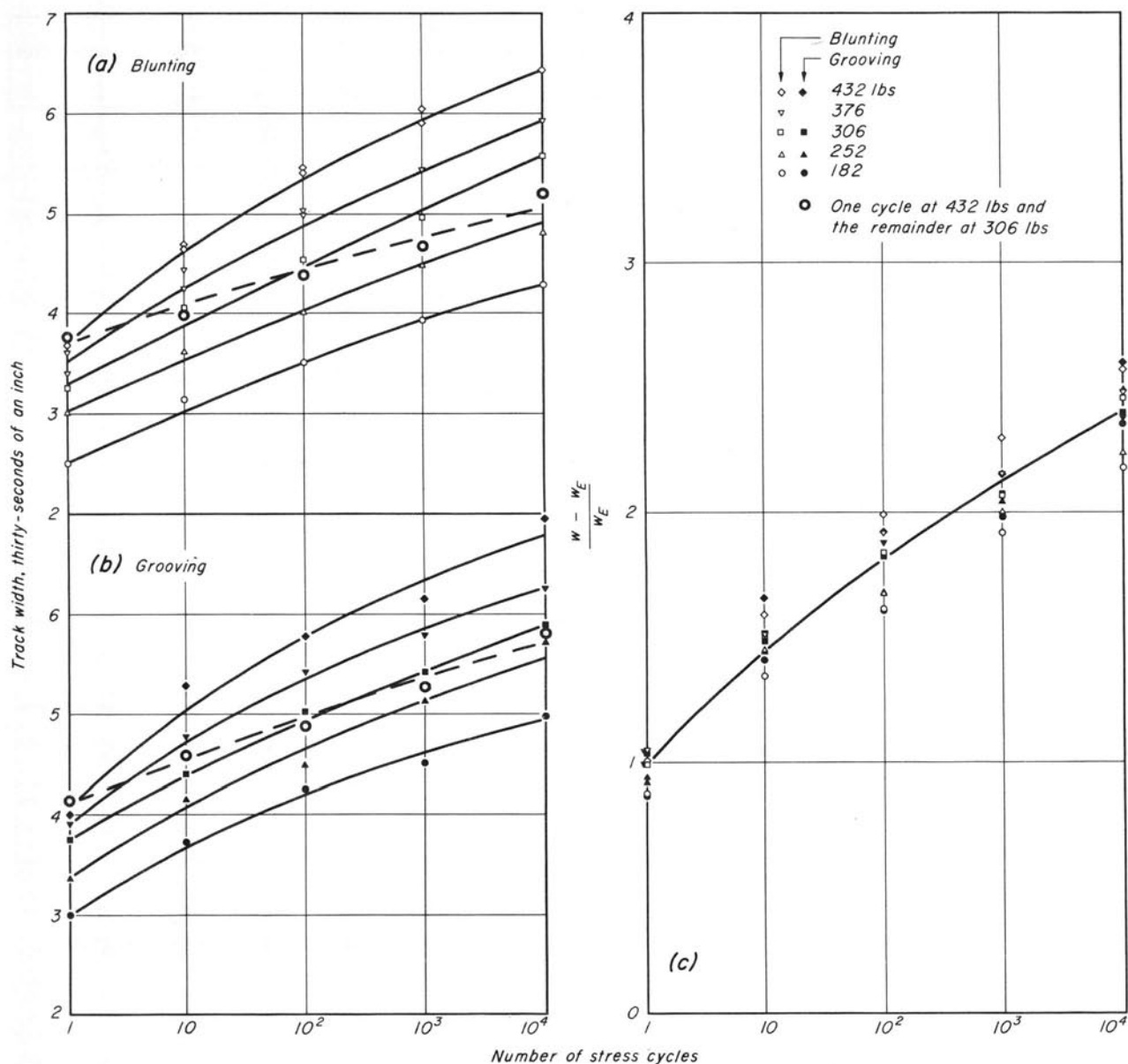


FIGURE 31. CYCLIC GROWTH OF TRACK WIDTH FOR PRONOUNCED PLASTIC DEFORMATION OF BRASS

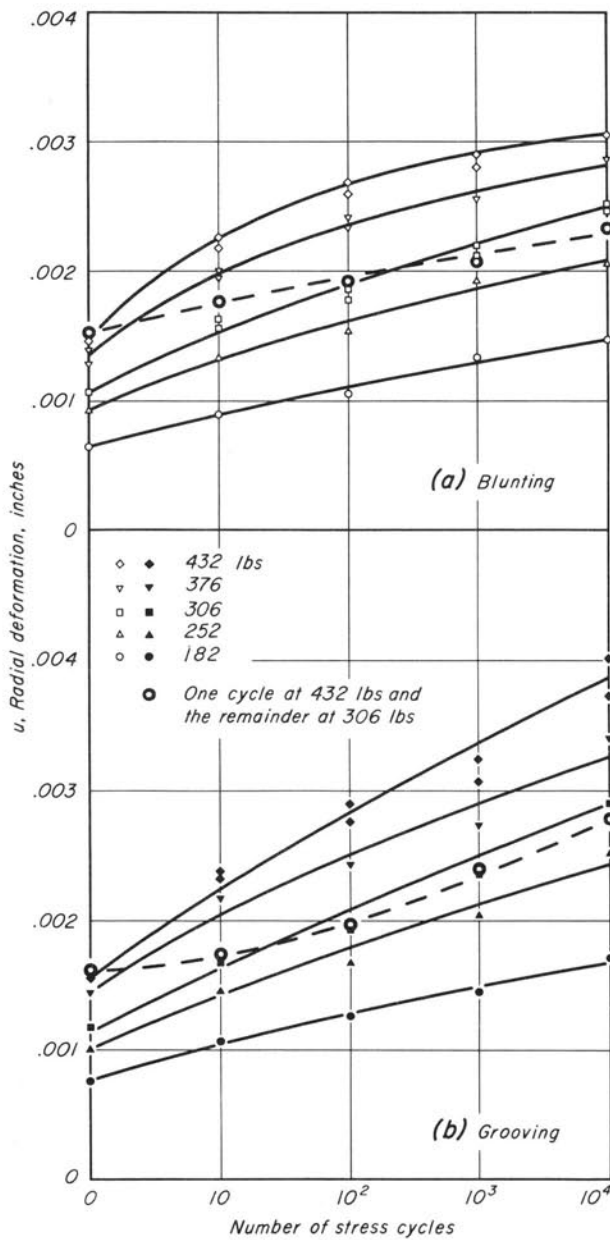


FIGURE 32. CYCLIC INCREASE OF RADIAL DEFORMATION FOR PRONOUNCED PLASTIC DEFORMATION OF BRASS

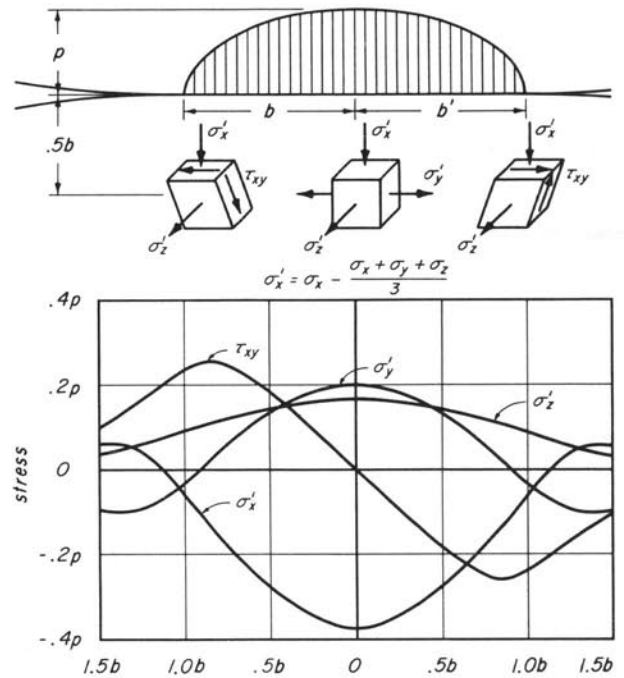


FIGURE 33. VARIATION OF DEVIATOR STRESSES AT DEPTH OF MAXIMUM REVERSING SHEAR STRESS

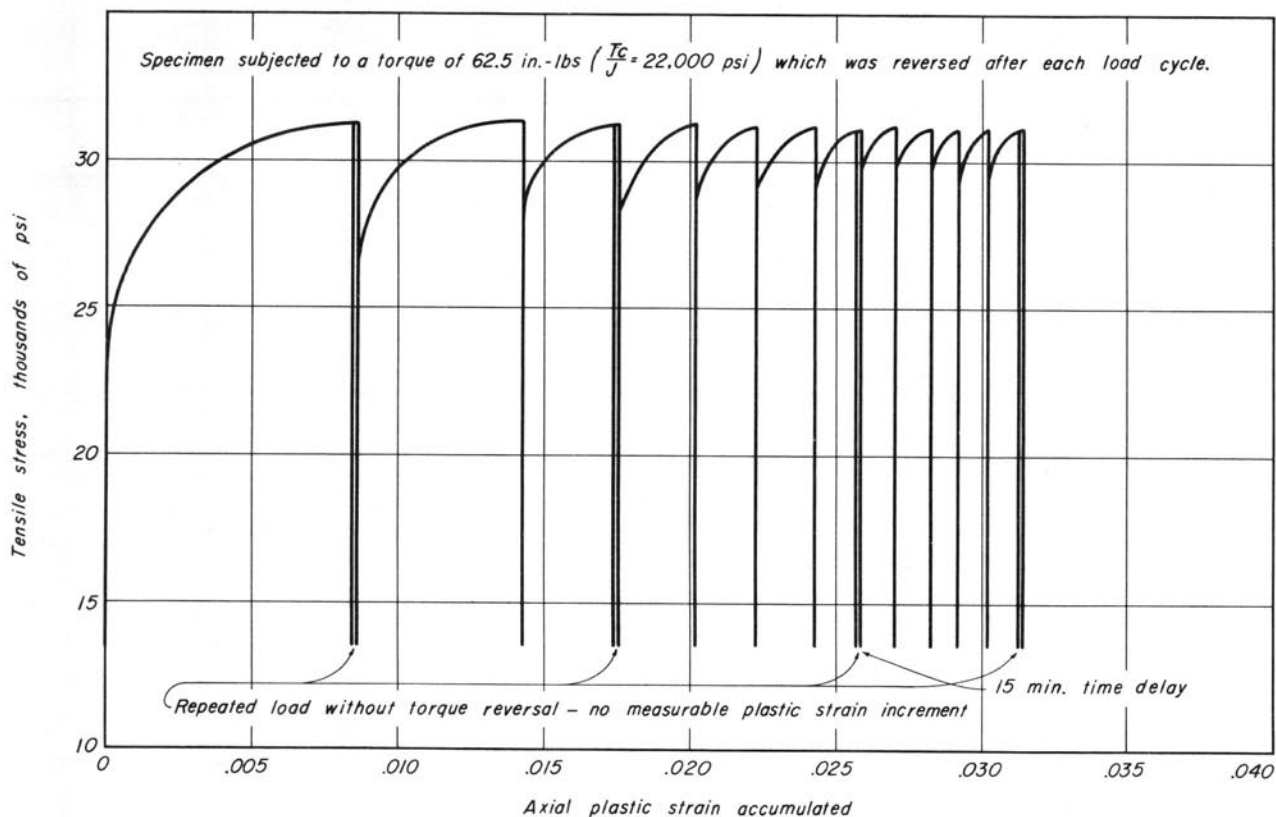


FIGURE 34. AXIAL STRESS - PLASTIC STRAIN LOCUS FOR COMBINED TENSION TESTS WITH ANNEALED BRASS

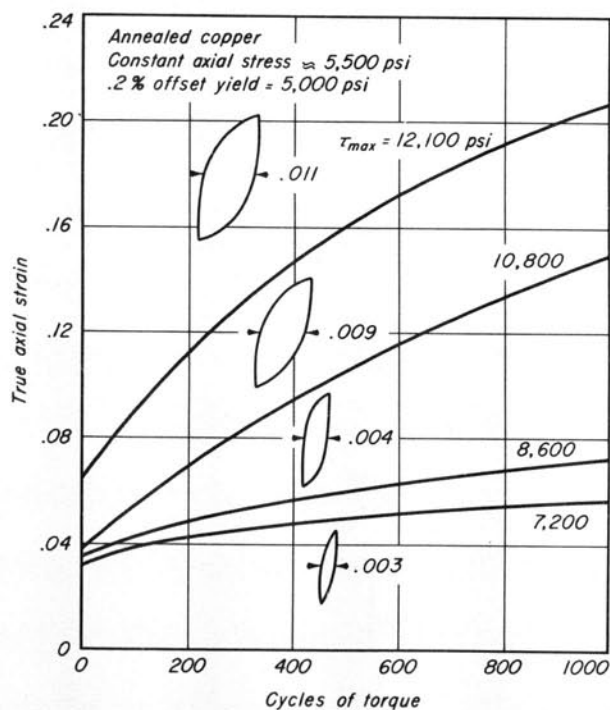


FIGURE 35. THIN WALL TUBE DATA

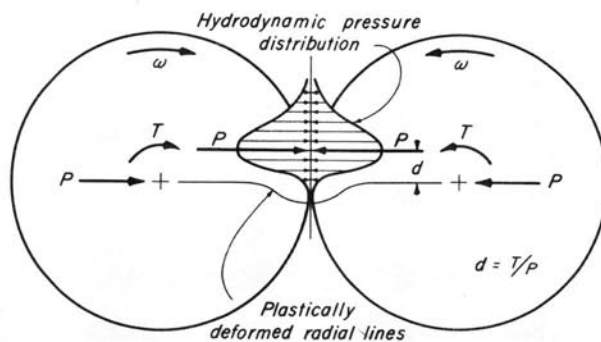


FIGURE 36. KINETICS OF LUBRICATED ROLLING DISKS

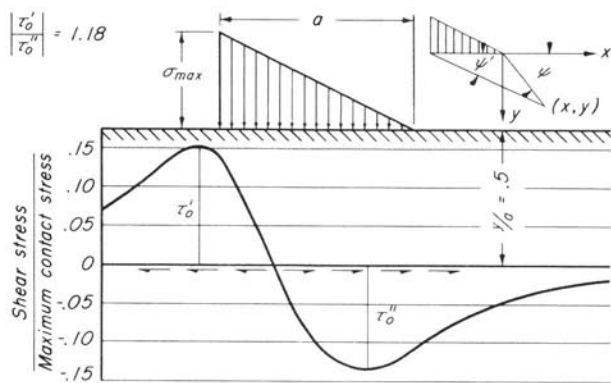
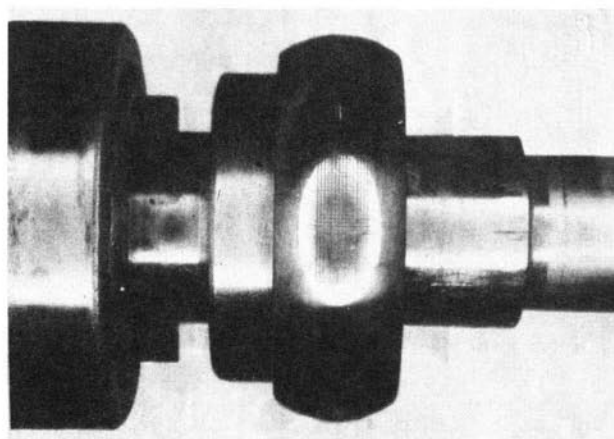
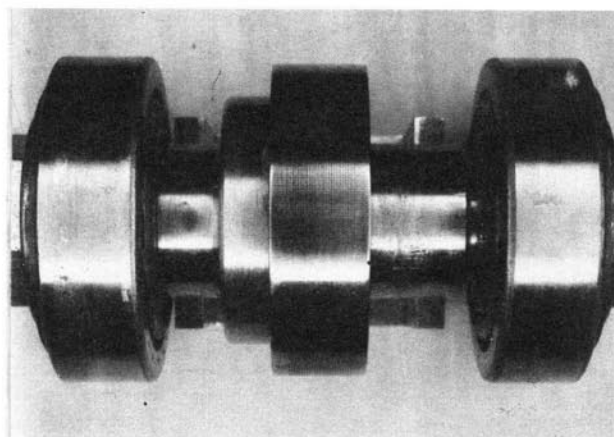


FIGURE 37. EFFECT OF ASYMMETRIC CONTACT STRESS ON ORTHOGONAL SHEAR STRESS



(a) Specimen T-5



(b) Specimen C-9

FIGURE 38. PHOTOS OF MOUNTED BRASS ROLLING ELEMENTS BEFORE TESTS

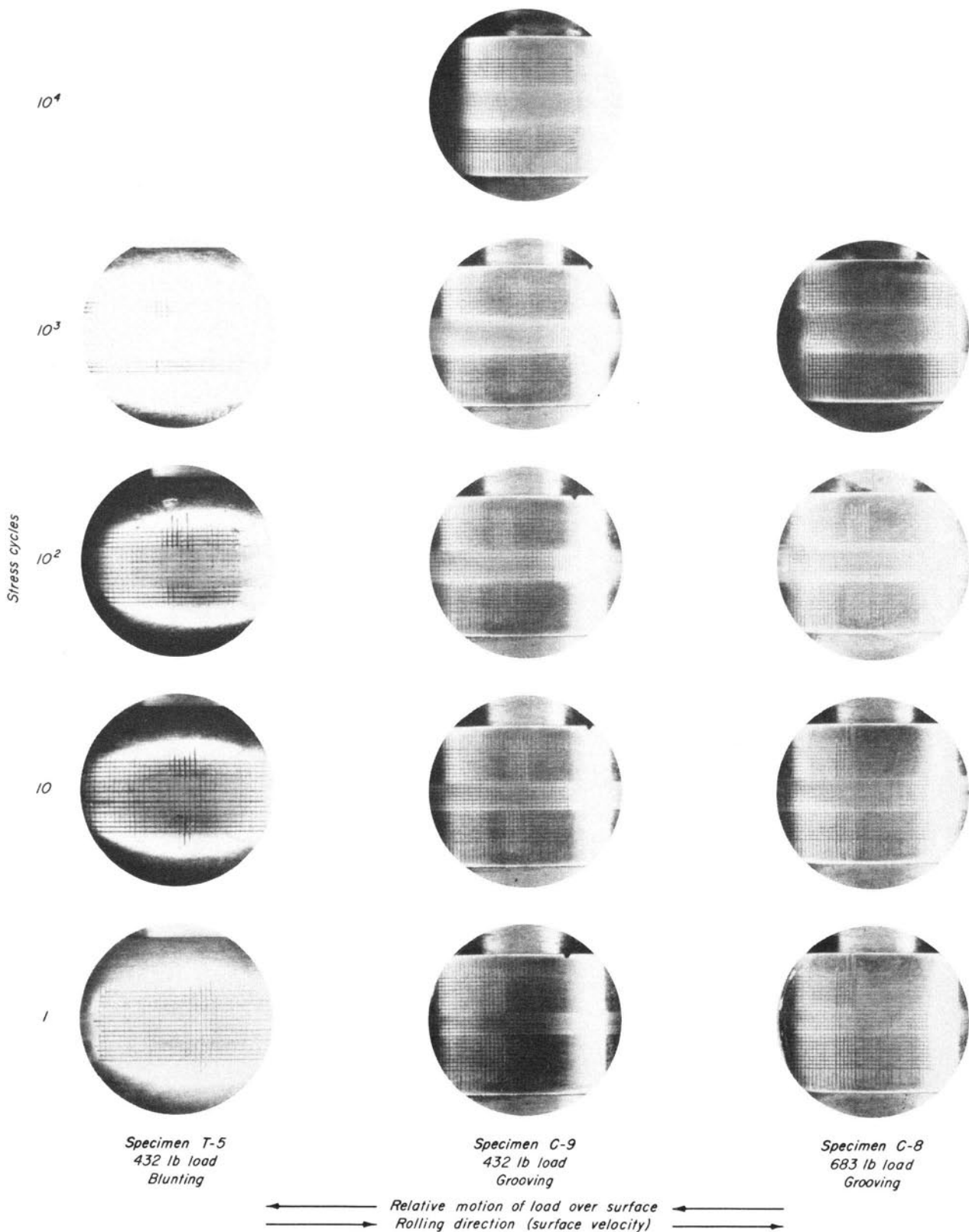


FIGURE 39. SEQUENCE PHOTOS OF ROLLING TRACK GRID DEFORMATION IN BLUNTING AND GROOVING

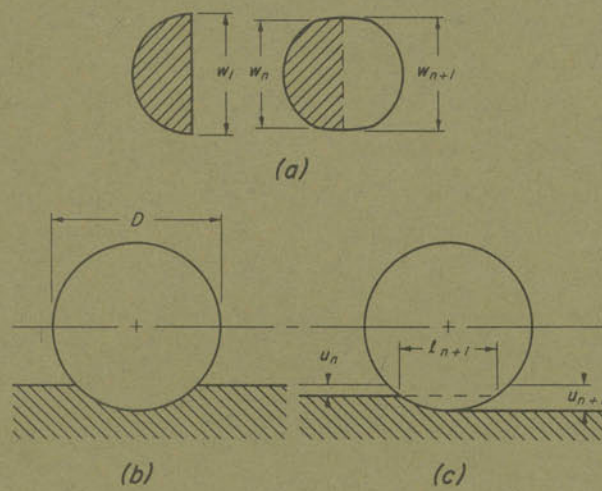


FIGURE 40. SUMMARY OF ELDREDGE'S PERFECTLY PLASTIC GROOVING ANALYSIS

VII. APPENDIX A. RESEARCH CLASSIFICATION

Research on the failure of surfaces in rolling contact has dealt with a wide class of phenomena under a multitude of particular conditions. The purpose of this classification is to establish a logical framework for future reference and to provide the basis for an organized review.

The major areas of research will be designated by two principal indices: mode of failure and phase of research. The research phases under each mode are drawn from Tykociner's classification of recurrent characteristics of any research problem.⁽⁵⁷⁾ Each of the areas located by the two principal indices may be expanded by the problematology principles enumerated by Tykociner, thus providing specific topics for research.

A. MODES OF FAILURE

Here failure means an action of the surface resulting from, or developing with, rolling under load in a particular environment that leads to unsatisfactory functioning of the mechanism. Not included in this definition are failures due to vibration and noise resulting from original imperfections in, or misapplication of the mechanism,⁽⁵⁸⁾ severe lubricant deterioration and fouling,⁽⁵⁹⁾ or abrasive wear.⁽⁶⁰⁾ Surface-lubricant

interaction phenomena are not excluded, but are subjugated to contributory roles in the modes treated. Surface includes the body material at or near the surface and corresponding films and lubricants involved in the contact. Thus, gross body failure via fracture or elastic deformation is excluded. Rolling contact is intended to include cycle-dependent phenomena, but excludes those failure mechanisms associated with gross relative sliding. Thus, no extensive consideration of gear failures will be made.

Three modes of failure have been selected for review: 1) pitting or flaking, 2) cumulative deformation of rolling elements, and 3) excessive or variable rolling resistance. Although these modes are more fully defined in the review, a few words to justify their treatment are appropriate.

1. Failure by pitting is a long established and recognized mode; in fact, pitting failure is the basis of life rating in bearing design.
2. Cumulative deformation leading to rejection of a mechanism due to dimensional instability of the rolling elements (in the case of rolling bearings--excessive run-out) is not a well-established or well-explored mode. However, its importance in future application will depend upon research at high temperature.

3. Rolling resistance has been the subject of curiosity and research for perhaps the longest time, and its minimization is a consideration in most design. It is included here as a failure mode, not as an external manifestation of other causes (for instance increased friction torque due to lubricant deterioration or excessive bearing preload, etc.), but as an inherent phenomenon of real deformable bodies in rolling contact. Concern generated because of required predictability of instrument bearings has placed new emphasis on this mode.

Additional modes of failure could be added and treated within a similar framework.

B. PHASES OF RESEARCH

The four phases of research⁽⁵⁷⁾ are:

- A. Phenomenological exploration: observation and classification. As applied to this research subject it has two subdivisions:
 1. Description of mode, place, and range of occurrence of failure.
 2. Primary observations and purely empirical relations among recognized variables.
- B. Controlled experimentation: measurement and collection of data. The best way to catalogue this area is by type of test. The following are considered here
 1. Full scale tests of associated mechanisms in which failure occurs, with appropriate instrumentation.
 2. Bench rig or simulated testers in which certain essential features of the rolling contact conditions are isolated and explored.

3. Pertinent material tests which explore material behavior associated with the failure mode under simpler conditions ranging from tension tests to lubricant pressure viscosity tests.

Each of these items may be further modified by a statement of:

- a) Variables treated
 - b) Measured quantities
 - c) Factual relations
- C. Hypothesis or theory: interpretation of experimental results. The analysis implied in this phase of research can be grouped into three sections:
1. Mechanics analysis. This section involves contributions from elasticity, plasticity, fluid mechanics, thermodynamics, etc., on the basis of idealizations pertinent to the above research findings.
 2. Material analysis. From fundamentals established by pertinent material tests, mathematical relations among "purified" variables are formulated.
 3. Synthesis. The findings of material analysis are extended by means of the mechanics of the particular situation to form a "solution" (correlation of facts).

Research in these sections can be modified by:

- a) Idealization or conditions treated
 - b) Nature of solution or variables interrelated
- D. General review and prediction. This area should include:

1. A summary of fundamental results and predictable features.
2. A critical review in preparation for further research effort.

A diagrammatic representation of this classification is given below. It should be pointed out that some published research papers may be placed with validity in more than one area as defined above.

CLASSIFICATION OF RESEARCH

Mode of Failure			<u>Phase of Research</u>
Pitting	Cumulative Deformation	Excessive Rolling Resistance	
I	II	III	
1	1	1	A Observation & Classification
2	2	2	
1	1	1	B Controlled Experimentation
2	2	2	
3	3	3	
1	1	1	C Theory & Interpretation
2	2	2	
3	3	3	
1	1	1	D Fundamentals, Prediction and Review
2	2	2	

- A — 1. Description of mode, place and range of occurrence.
 2. Primary phenomenological observation.
- B — 1. Full scale tests — a) Variables treated
 2. Bench rig tests — b) Measured quantities
 3. Pertinent material tests — c) Factual relations
- C — 1. Mechanics analysis — a) Idealizations of conditions treated
 2. Materials analysis — b) Nature of solution or variables interrelated
 3. Synthesis (correlation of facts)
- D — 1. Results, fundamentals, predictable features
 2. Critical review

VIII. APPENDIX B. REVIEW OF RESEARCH ACCORDING TO CLASSIFICATION OUTLINE

A review of research conducted under the three modes of failure selected earlier is given below according to the classification outline. The review of the literature is by no means comprehensive* but the references selected are representative of research in the particular phase. However, research in certain phases is sparse or nonexistent. These areas are indicated.

A. PITTING

Description of Mode I-A-1: Eventually the contacting surfaces of rolling elements experience a failure that is characterized by a flaking of metal fragments from the surface, leaving pits of such size as to interfere with normal operation.

The mode represents the end of useful life of all ball and roller bearings in the normal range of load and temperature, and for that reason it has been the basis of life and capacity rating. The same name has been extended to a similar class of failures found on gear teeth, valve tappets, etc.

* This review is limited primarily to English language publications. A review of contact fatigue treating many European references is provided by Schreiber and Ulsenheimer (61)

Primary Phenomenological Observations I-A-2 : In his experiments at the turn of the century, Stribeck⁽⁶²⁾ noticed this type of failure but did not consider it of fundamental importance in determining ball bearing capacity. This mode of failure was noted earlier by Crandell and Marston⁽⁶³⁾ in the study of the endurance of bridge rollers to repeated rolling. Load and cycles to failure are tabulated for 36 tests although no attempt is made to establish a life formula on the basis of the limited data. It remained for Palmgren some thirty years later⁽⁶⁴⁾ to produce an empirical endurance formula, based on pitting failure, relating life in bearing revolutions inversely to the cube of the load. Since that time, many full scale tests have been conducted for purposes of load rating, the kinship of the phenomenon to fatigue being manifest further in the dispersion in life exhibited in typical bearings. Perhaps the most far-reaching determination of dynamic capacity based on ordinary fatigue pitting, as it came to be called, is the work of Lundberg and Palmgren reported in 1947.⁽⁹⁾

A case study of many gear failures in service is given by Hoshino.⁽⁶⁵⁾ The failure is classified into two groups according to appearance: small pitch line pitting (position

of pure rolling) and flaking of other regions of the tooth face experiencing approach and recess sliding action. The directional flow of metal in the subsurface region of relative sliding and the orientation of the "oyster shell" flake indicates the influence of sliding on the nature of the failure.

Primary design data and service conditions, including numerous microphotographs of pitting failure sites in ball and roller bearings and gears for aircraft service, are summarized by Davies and Day.⁽⁶⁶⁾ The authors demonstrate that on the basis of a constant design life for all examples, except the gear, the stress frequency is inversely proportional to the ninth power of the stress. Observation of a "white phase" structural change in highly loaded zones and sometimes in association with subsurface fatigue cracks are reported.

"Spalling" is a failure mode of some concern in steel mill work rolls and backup rolls. A description of these failures and an analysis of roll deflections, pressure distribution, and critical subsurface stresses is given by Keller.⁽⁶⁷⁾ Here "pits" of 20-square-inch surface area are not uncommon in large (two-foot diameter or more) rolls.

From full scale tests conducted on rear axle assemblies, Almen⁽⁶⁸⁾ presents S-N plots of pitting fatigue failures for through hardened and carburized gears. Based on nominal maximum contact stress at the pitch line, the fatigue strength is noticeably less than for roller bearings of comparable steel.

Full Scale Tests I-B-1: In addition to testing for basis of load rating and relative material evaluation, some research of basic importance has been conducted with full scale

bearings. Jones⁽⁶⁹⁾ undertook an extensive investigation of the metallographic transformations induced in the subsurface of specially designed ball bearing races at a nominal contact stress of 800,000 psi for room temperature conditions, and in standard races for loads closer to design values. The material was a fully hardened 52100 steel. Interruption at various running times, together with metallographic observation, revealed subsurface transformation identified as troostite and slip lines. These regions intensified with running time. Hardness surveys indicated the material near the surface to be at a hardness equivalent to Rockwell C 63 or C 64 while in the center of these transformed and fatigued zones a few thousandths of an inch below the surface the hardness was Rockwell C 59. Sections were exhibited showing fatigue pits that corresponded to the depth of these transformed zones.

Endurance tests of groups of deep groove ball bearings with inner races (failed component) made of steel from various air and vacuum steel making processes were analyzed by Morrison et al.⁽⁷⁰⁾ They report that average L_{10} life for all vacuum melted steels is 1.7 times the corresponding average life for all air melt steels and that additional vacuum remelting continues the improvement to some extent. Data from bearing groups showing significant differences in trace elements are examined and evidence of a significant negative correlation between aluminum, copper and vanadium is cited.

A number of investigations have been conducted on full scale bearings to determine the effect of lubricants or lubricant properties

on pitting. From a series of tests with typical gear box aircraft roller bearings and lubricants of various viscosity and composition, Otterbein⁽⁷¹⁾ concluded that, in general, lubricants with low bulk viscosity have a detrimental effect on pitting life. He established a linear relation between viscosity and an index of bearing life. However, other results with bench rig apparatus have indicated that bulk viscosity alone is not a sufficient index and there has been more attention directed toward pressure viscosity and other lubricant properties.

In an effort to study the effect of local contact temperature without significantly changing lubricant properties, Sternlicht et al.⁽⁷²⁾ conducted ball bearing tests at two outer race temperatures (100° F and 125° F) with two lubricants of the same bulk viscosity at the respective test temperatures. The mean life of the lower temperature test series was eight times longer than the high temperature series. Taken by themselves, however, these tests do not establish maximum contact zone temperature as a criterion for fatigue.

The nature of rolling bearing lubrication and its possible influence on pitting failure has been investigated by attempts to measure lubricant film thickness in an angular contact ball bearing while running under load. A technique involving dielectric oilfilm breakdown voltage measurements was employed by Sibley et al.⁽⁷³⁾ to indicate significant lubricant films under various operating conditions of speed, load, and temperature for a number of lubricants. It is difficult to obtain more than qualitative results from their research at

this time. Assuming a pitch circle of 85 mm and osculation of ball and inner race equal 0.96, the thrust loads reported would produce nominal maximum contact stresses on the inner race of 185,000 psi and 266,000 psi, respectively, under static conditions. By way of illustration of results, the maximum dielectric breakdown voltage was reached at a shaft speed of 8,000 rpm for the higher load (150° with Mil-L-7808 lubricant), having increased steadily from a shaft speed of 2,000 rpm. While boundary lubrication is undoubtedly important, there is indication that contact stress is modified significantly in transmission through hydrodynamic films of some nature, particularly in light load and high speed applications.

Bench Rig Test I-B-2: A great many experiments with bench rig or simulated tester have been conducted since the early work of Way⁽⁷⁴⁾ and Buckingham.⁽⁷⁵⁾ These have increased both in number and diversity of design in recent years. The purpose of this research has been primarily to determine the influence of material and lubricant variables on pitting life. These variables may be grouped as follows:

1. Material types; metallurgical, surface finish and other material variables.
2. Elevated temperature.
3. Lubricant and lubrication variables.
4. Relative sliding of surfaces.
5. Rolling element hardness compatibility or pairing, and geometry or configuration effects.

Perhaps the greatest utility of the bench rig is in selecting or screening materials and their corresponding treatments. Carter⁽⁷⁶⁾

has reported Weibull lines determined from pitting tests in the Macks spin rig for ten promising high temperature steels and the standard 52100 steel. Apart from ranking of air melt steels as to B_{10} and B_{50} life at a reported nominal maximum contact stress of 725,000 psi, he found evidence that vacuum melting improved fatigue life for AISI M-1 tool steel, although no correlation of rolling contact fatigue life with cleanliness was obtained.

Baughman⁽⁷⁷⁾ has given a statistical analysis of the effect of various combinations of material variables on M-50 steel pitting life in the General Electric rolling contact rig. Although certain optimum values of significant variables like surface finish and grain size are determined, not enough tests were performed at each combination (four tests) to justify such elaborate statistical analysis. Zaretsky and Anderson⁽⁴²⁾ have examined the influence of hardness on pitting life of four steels that range in hardness from Rockwell C 55 to C 68, finding that the B_{10} life increased continuously with increasing hardness in all cases. It should be noted that only the B_{10} life was taken as a characteristic of life. Some inversions occurred at the B_{50} life.

Bear and Butler⁽¹⁰⁾ examined 52100 and AISI M-1 tool steels metallographically after testing in the Macks spin rig first at room temperature, then at 200° and 250° F. They found that metallurgical structure was stable at room temperature but was unstable at 200° F or 250° F, the decomposition product being troostite. Fiber direction, inclusions, and chemical segregation were said to contribute

to fatigue failures.

Various metallurgical factors, particularly nonmetallic inclusions, are studied in contact fatigue specimens from different steel making processes by Johnson et al.⁽⁷⁸⁾⁽⁷⁹⁾ The rig resembles a simple thrust bearing and maximum contact pressures of 563,000 psi are developed. The most detrimental inclusions are the brittle types like alumina and silicates even in small size ranges, especially if occurring in "cloud" distributions as observed in some vacuum induction-melted steels. Non-uniformity of carbide particles and retained austenite, associated with chromium segregation, are also held to be detrimental. It is interesting to note that some general correlation (ranking) between rolling contact and rotary bending fatigue tests is established in the earlier paper.⁽⁷⁹⁾

Tests performed in the G. E. rolling contact rig⁽⁸⁰⁾ on thirty-two heats of M-50 steels (hardness ranged from Rockwell C 62-C 65) at 500°F may be summarized as regards temperature effect on life by averaging all reported B_{10} and B_{50} lives. These values are respectively 2.54×10^6 stress cycles and 7.90×10^6 stress cycles. However, if room temperature data reported on essentially the same material⁽⁷⁷⁾ is examined it is noticed that the change in life is relatively small. In fact the difference in life is less than the variations due to metallurgical variables at room temperature. In the same rig under identical test conditions (700,000 maximum contact stress, Mil-L-7808 lubricant), except room temperature, the B_{10} and B_{50} lives for the best test were 3.4×10^6 and 10×10^6 respectively (the steel hardness was Rockwell

C 62.2). Other tests at the same hardness and higher (Rockwell C 64) gave lives shorter than the reported 500^oF results. At elevated temperatures the contact stress may have been reduced by the occurrence of plastic deformation if the mechanical load cell was not monitored and adjusted frequently.

As regards lubricant research, apart from ranking of various oils and synthetic fluids, the most significant findings are that bulk lubricant viscosity does not seem to be a dominant factor in determining pitting life. However, the test results of several lubricants (including mineral oils) show that with the same type of lubricant, pitting life is increased with increasing viscosity. Barwell and Scott⁽⁸¹⁾ state that compressibility and variation of viscosity with pressure may be most significant. Barwell⁽²²⁾ states that transverse cracks originate in the surface, being influenced by the chemical action of the lubricant. He suggests that these cracks associate with subsurface cracks developed in metallurgically altered subsurface regions to produce pits. Loads were usually exceedingly high in these four-ball tests. Nominal maximum contact stress as high as 1,000,000 psi was employed.

Anderson and Zaretsky⁽⁸²⁾ give results of tests from the fatigue spin rig with lubricants of five different base stock lubricants that have approximately the same atmospheric pressure viscosity. A relation of L_{10} life with pressure coefficient of viscosity is indicated. On the other hand Rounds⁽⁸³⁾ tends to discount the significance of pressure viscosity coefficient or viscosity index when lubricants of different chemical class are involved, and

emphasizes other lubricant properties like molecular shape, reactivity or polarity and antiwear characteristics. From short time tests with the four-ball rig at extreme contact pressures he reports longest lives with the diesters and polyphenyl ethers and shortest lives with the fatty acids and halogenated hydrocarbons. In general, ring structures or molecular branching usually gave longer lives, but reactive or polar groups were detrimental. The pertinence of such short time tests to the study of time-dependent phenomena and actual service failure is questioned in a discussion by Dolan.⁽⁸⁴⁾ Rounds suggests that the basis for observed correlation between full scale and four-ball tests may be that the resulting high surface temperatures accelerate the chemical reactions.

An extensive summary of research at the National Engineering Laboratory with the four-ball tester is provided by Scott.⁽⁸⁵⁾ In this context the results of tests with various lubricant additives and water contamination are of interest. Increased concentration of the more active extreme pressure additives resulted in life reduction. Even small amounts of dissolved water in lubricants are harmful except in conjunction with stainless steel balls. This effect of water contamination in mineral oil lubricants is attributed to hydrogen embrittlement.

The influence of viscosity of mineral oil lubricant on pitting fatigue limit and fatigue life of lower strength steels (96,000 psi tensile strength) is explored by Martin and Cameron⁽⁸⁶⁾ with the same test rig used by Niemann and Kraupner in their cumulative deformation experiments. Although it is possible to rank

pitting fatigue limit with viscosity (fatigue limit varies from 50,000 psi maximum contact pressure to 120,000 psi for variation of viscosity from 3 to 530 cS) some other property is apparently significant in determining life or the slope of the S-N curve.

Buckingham and Talbourdet⁽⁸⁷⁾ give S-N curves for pitting of steel rollers with various percentages of sliding showing the decrease in life with introduction of sliding. Nishihara and Kobayaski⁽⁸⁸⁾ have found that 20 per cent relative sliding produces the greatest tendency to cause pits in contacting cylinder. At higher values "the growth of pits can scarcely be observed." For relatively low strength steels (80,000 psi tensile strength) Dawson⁽¹³⁾ reports pitting life nearly independent of sliding for smaller slide/sweep ratios (surface velocity of disc - surface velocity of mating disc/surface velocity of disc) in the range -0.0005 to -0.04. He also reports that pitting is confined to the disc with the smaller peripheral velocity. Many of Way's experiments, indicating surface origin of pitting, are reproduced.

Further experiments⁽⁸⁹⁾ at two slide/sweep ratios (-0.046 and -0.0046) and with two test conditions giving calculated film thicknesses at first less than, and secondly much greater than, the total surface roughness of the discs, indicate that pitting life is almost independent of load above the fatigue limit. It should be noted that rather small pits a few thousandths of an inch across are the basis of these curves. The authors contrast these "inert" pits to the "continuously" propagating type observed at much higher stresses. The possibility arises that these

pits may be "premature pin hole" pits.⁽⁹⁰⁾

By increasing the contact angle, and thereby increasing the spin velocity or relative sliding, in the NASA five-ball tester at constant maximum contact pressure, Zaretsky et al.⁽²⁸⁾ were able to study the resulting decrease in fatigue life for hard ball bearing steels. As an example, a change in relative spin velocity of a factor of two corresponds to a change in life of a factor of two. Although the maximum contact pressures are high (800,000 psi), the results are in keeping with results at lower stress in full scale ball bearing tests but are not predicted by standard capacity formulae. Surface temperature at the highest contact angle (40°) is 60° F higher than at the lowest (10°).

Investigations of the influence of combined roll and spin on fatigue strength of hard steels are reviewed by Wernitz.⁽⁹¹⁾ These are tests conducted by Maass in Germany that indicate a relatively rapid drop in strength with slip until a value of about 4% slip is reached, whereupon a threshold fatigue limit appears to be established.

In the pitting fatigue research on 52100 steel conducted at the U. S. Naval Engineering Experiment Station⁽³³⁾ three geometries of toroidal test specimens were used. The profile radii were 0.250 in., 0.383 in., and 0.500 in. The toroid diameter was 1.500 in. and the cylindrical driving load roller was 1.562 in. in diameter. Tests were conducted at nearly the same maximum nominal contact stress for all geometries; however, mean life increased with decrease in profile radius. Other tests performed at the Station were in liquid sodium environments.

The effect of profile radius change or "crown" of toroids of large radius (near cylinder) on fatigue strength of case hardened roller bearing steels is studied in detail by McKelvey and Moyer.⁽⁹²⁾ In this case, except for the smallest profile radii (100 inch) used, a complete elliptical contact area is not formed, as in Greenert's tests. A correlation of S-N data on the basis of maximum contact stress is possible, taking into account stress concentration at the end of roller contact. End failures are shown to predominate except for the smallest profile radii, where the maximum stress occurs at the roller center.

Relative hardness or material combination is shown to be an important factor in pitting tests by Chesters.⁽⁹⁰⁾ The test rig consisted of a roller driving a pair of specimen discs similar to the Niemann and Kraupner rig. With the exception of case hardened rollers, the effect of increasing the hardness or tensile strength of the driving roller was to reduce the fatigue resistance of the driven disc materials. For a given roller material the fatigue strength of the disc material increases directly with tensile strength. Four different steels were used in the driven discs and six steels were used in the rollers, representing materials often employed in pinion/wheel gear combinations.

Tests with hard (958 D. P. H.) and soft (800 D. P. H.) balls in the four-ball rig (1 rotating -- 3 rolling balls) yielded results that indicate a marked influence of intrinsic hardness and relative position (rotating or rolling). Milne and Nally⁽⁹³⁾ also associated the physical appearance of the pitting failure with kinematic conditions of the rolling ele-

ments (whether rotating ball in four-ball rig, or cone in cone and three-ball rig). Greater tangential drag or traction on the balls is said to cause initiation of surface cracks whereas the cone failures are subsurface.

Rigs other than those involving rolling contact have been employed to obtain some insight into the pitting phenomenon. Burton et al.⁽⁹⁴⁾ have developed a rig for repeated contact loading of 52100 steel balls and have reported possible early indications of fatigue in the observed discontinuity in the specimen temperature vs. time plots. In addition to surface damage they report some indications of subsurface cracks, which Kennedy⁽⁷⁾ was unable to observe in a similar test arrangement.

Pertinent Material Tests I-B-3: Material tests, apart from the rolling contact situation, have been conducted on both steels and lubricants primarily for the purposes of screening or ranking for use in rolling element designs, evaluating heat treatment methods and determining the effect of environmental variables on purified material variables thought significant to the pitting fatigue strength.

Styri⁽³²⁾ made an attempt to develop a simple fatigue test which would allow study of the effect of a single factor pertinent to contact fatigue. The stress-life relations from various fatigue tests on hard bearing 52100 steel were compared to the usual contact stress-life relation determined from bearing tests. Torsion fatigue tests gave the closest correlation. He also noted the wide life scatter of the specimens of vacuum-melted steel which is relatively free of inclusions.

Because of the scarcity of reliable data

for extremely hard steels such as used in rolling element bearings, Sachs, Sell, and Brown⁽²⁾ undertook an investigation to determine the relation of tension, compression, and fatigue properties to steel hardness. The materials were conventional melt 52100 steel and three tool steels (Halmo, M-1 and MV-1) ranging in hardness from Rockwell C 50 to C 65. Tension and compression test results indicate an optimum in hardness at about Rockwell C 60. However, the fatigue strength determined in rotating beam tests did not decrease at high hardnesses. Induction vacuum melted 52100 steel appeared to have a higher fatigue strength at 10^8 cycles than the conventional melt. Fatigue strength (at 10^8 cycles) values ranked the materials (all Rockwell C 62) in this order:

1. Halmo (130,000 psi)
2. M-1 alloy and vacuum melt 52100 (120,000 psi)
3. MV-1 alloy (110,000 psi)
4. Conventional 52100 (100,000 psi)

In an appendix the results of full scale bearing tests with three of the same materials used in the investigation were presented in Weibull plots. The same ranking was given here as in the rotating beam tests.

Hersey and Hopkins⁽⁹⁵⁾ have given an extensive historical review and source of condensed technical data on the effect of pressure and temperature on lubricant properties such as pressure coefficient (defined as the rate of change of viscosity with respect to the pressure at constant temperature divided by viscosity). Experiments with a falling body viscometer illustrate the variation of pressure coefficient with pressure. Non-Newtonian

characteristics such as plasticity and time effects are said to be conspicuous in solidified oils at low shear rates. Non-Newtonian behavior such as the approach to limiting shear stress with high rates of shear has been observed more recently.

Sibley et al.⁽⁷³⁾ have reviewed the experiments of Charron, which involved impacts against a small piston which then forced the lubricant through a capillary tube. The measured viscosities were significantly smaller than would be expected from the magnitude of the pressures. Further experiments indicated a decreasing viscosity presumably caused by lubricant heating due to shearing action.

A falling needle viscometer with external electromagnetic indication suitable for pressures up to 20,300 psi was used by Boelhouwer and Toneman⁽⁹⁶⁾ in investigating the variation of pressure coefficient with pressure. The established pressure-viscosity relation is only satisfied for one of the fluids examined.

The fundamentals of boundary lubrication are treated by Bowden and Tabor.⁽⁹⁷⁾ Many experiments concerning the lubricating properties of films of various chemical composition and the associated surfaces are reviewed.

Mechanics Analysis I-C-1: Mechanics analysis of idealization pertinent to the rolling contact pitting failure have been directed toward determination of stress induced in contacting elastic bodies due to normal and combined traction, lubricant films, or thermal gradients caused by friction. The assumption made is that stress is a quantity significant to rational life determination. Some work has included inertial or dynamic effects in

the elastic bodies (moving concentrated load), but in general all analysis is elasto-static. Recent analysis has extended into the plastic range of strain caused by rolling contact.

The classical solution for the pressure distribution between elastic bodies in contact is due to Hertz.⁽⁹⁸⁾ A solution for the subsurface stresses on a vertical line through the center of the contact area in a half-space loaded with a Hertzian ellipsoidal pressure was given by Thomas and Hoersch.⁽⁹⁹⁾ The maximum shear stress was discovered to occur below the surface. Lundberg and Palmgren⁽⁹⁾ and Fessler and Ollerton⁽¹⁰⁰⁾ solved for the subsurface stresses on orthogonal planes, including the axis of the contact ellipse. Here the maximum orthogonal shear stress occurring in the subsurface is accentuated. For the two-dimensional case Poritsky⁽¹⁰¹⁾ and Smith and Liu⁽¹⁰²⁾ have solved for the stresses due to a combination of Hertzian normal and tangential surface stresses. The maximum shearing stress moves toward the surface with increased tangential traction and the maximum tensile stress is at the "trailing" edge of the contact area. A solution for the compliance (displacement divided by load) for combined surface traction in the more general elliptic contact is given by Mindlin.⁽¹⁰³⁾ The combined influence of tangential friction and twist or spin on surface displacement, strains, and ball motion has been analyzed by Hetenyi and McDonald⁽¹⁰⁴⁾ and Johnson.⁽¹⁰⁵⁾ The effect of curvature and finite size in the Hertz theory for cylindrical contact is studied by Loo⁽¹⁰⁶⁾ and discussed by Lubkin. Moyer and Neifert⁽¹⁰⁷⁾ present a method of calculating stress concentration at the edge of a

finite length roller in contact with an elastic half space.

A start on the plastic problem has been made. For the elastic contact pressure distribution, and the assumption that subsurface total strain cycle is essentially the elastic strain cycle, Merwin and Johnson⁽⁴⁵⁾ integrate the Prandtl-Reuss plasticity relation to obtain the plastic stress cycle and residual stresses. The influence of tangential force is also treated.⁽²⁰⁾

A solution for the viscoelastic problem has been proposed by Lee and Radok.⁽¹⁰⁸⁾ The problem treated is that of a rigid sphere and viscoelastic half space (linear viscoelastic operators in the time variable replace the elastic constants) and the cases of prescribed uniform indentation rate and load history are illustrated. There is a marked deviation from the Hertzian distribution, the distribution being flattened at indentation times equal to the relaxation time of the material. The solutions approach each other for very short indentation times.

Morland⁽¹⁰⁹⁾ solves the viscoelastic problem for the rigid cylinder rolling with constant velocity over a linear viscoelastic half space. The basic integral equations are solved by series expansion. A numerical example is presented for the case of contact time equal to the retardation time of the standard viscoelastic body.

It is apparent from the analysis of Cole and Huth⁽¹¹⁰⁾ that only for speeds near the sonic velocity of the material is the stress distribution due to a moving concentrated load significantly different from the corresponding static solution.

Based on the elasticity analysis of Smith and Liu and the thermal analysis for flash temperature of H. Blok, Kelley⁽¹¹¹⁾ has solved for the stress distribution due to the sliding action of bodies in contact. The combination of thermal and contact stresses are particularly severe on the disc with negative sliding (slower surface speed).

Photoelastic tests have supported analytical results in this phase. A dynamic photoelastic technique was applied by Sternlicht et al.⁽⁷²⁾ to compare the stress distribution under dry and lubricated rolling. They conclude: "For all practical purposes - the dry and lubricated pressure patterns are the same, and are not affected by load or speed." Greatest emphasis is placed on film temperature on the basis of their elasto-hydrodynamic analysis of lubricants with different pressure and temperature characteristics.

Since considerable attention has recently been directed to the role of the lubricant in pitting failure, analyses of the mechanics of rolling contact lubrication and related experiments have multiplied in number over the last few years. Some of these will now be reviewed.

Sibley et al.⁽⁷³⁾ have given a short but excellent survey of fluid mechanics and elasto-hydrodynamics analyses of film thickness and pressure distribution pertinent to gear and roller bearing lubrication. This has included Martin's isoviscous hydro-dynamic theory of 1916, its modifications for variable viscosity by Gatcombe, Bell, Cameron, etc., and the modification for elastically deformable surfaces by Lewicki and Dorr. Recent analyses such as Poritsky's have attempted to take

into account the effect of pressure on both viscosity and surface deformations. One incentive for these modifications is the good performance of roller bearings and gears at load values above those predicted as critical by the theories. The subsurface stress distributions corresponding to pressure distributions predicted from such two-dimensional elasto-hydrodynamic analyses are presented by Dowson et al.⁽¹¹²⁾ in terms of three defining parameters for speed, load, and pressure viscosity coefficient. In general they find that the pressure distribution and resulting subsurface stresses are near-Hertzian except at very high speed. The authors consider rise in temperature and consequent viscosity reduction to be insignificant in pure rolling, although deviation from linearity between shear stress and shear rate (non-Newtonian behavior) is thought to be significant in some lubricants.

Direct measurement of lubricant film thickness by use of columnated X-ray beams has indicated thinner films than predicted by the elasto-hydrodynamic theories mentioned. Sibley et al.⁽¹¹³⁾ attribute this to non-Newtonian behavior which leads to a "spreading" of the pressure distribution and thinner films. In these tests maximum contact pressures in the range of 100,000 psi to 180,000 psi are employed, and film thicknesses in the range of four to fifty micro-inches are reported. An empirical correlation of film thickness data on the basis of dimensionless forms obtained from examination of Grubin's theory is presented graphically. In a discussion to the paper Sternlicht criticizes the neglect of temperature rise in the film, especially since

the authors show that film thickness is sensitive to temperature and viscosity. Sibley in turn criticizes Sternlicht's analysis (which includes the energy equation) for assuming constant temperature across the oil and no conduction into the steel. He argues, as does Crook,⁽¹¹⁴⁾ that steel temperature or inlet oil temperature controls film thickness.

The effects of temperature rise and high rates of shear in the lubricant at the contact area on lubricant viscosity have not been considered extensively in analyses. However, some data of fundamental significance with regard to rate of shear and ambient temperature was obtained by Smith⁽¹¹⁵⁾ with a crossed axis ball and cylinder machine. In general a limiting shear stress or coefficient of friction is approached at high rates of shear for several fluids. Results are interpreted in terms of a shear plane model of flow where frictional force represents the shearing of a thick plastic film of lubricant. Smith remarks that his findings that the coefficient of friction decreases with temperature is contrary to the data of Misharin for somewhat similar experimental conditions. He suggests that a complete lubricant film was not established in Misharin's tests.

Other possible idealizations are the time-dependent Maxwell body, and even plasticity idealizations for semi-solid films. Many rheological behaviors and effects are discussed by Smith.⁽¹¹⁶⁾ He illustrates the effect of high rates of shear on two lubricants. In the crossed-axis ball and cylinder rig at a maximum contact pressure of 155,000 psi an ester-based lubricant behaves as a liquid of great viscosity below film shear stresses of

1,450 psi, but at higher rates of shear the ester behaves as a plastic solid. A silicone fluid, on the other hand, begins to lose viscosity and undergo plastic shearing at much lower shear stresses.

A theory of roller lubrication with the Bingham rheological idealization is proposed by Sasaki et al.⁽¹¹⁷⁾ At high speeds the distinction between this plastic-viscous model and the Newtonian ideal diminishes. Criticisms of certain assumptions regarding the boundary conditions of the solution and accuracy of some calculations are made in a discussion by Osterle. The form of fundamental equations for a visco-elastic body is given by Burton.⁽¹¹⁸⁾ He demonstrates that the influence of shear elasticity on the pressure distribution is one of magnitude and not of kind. With a Maxwell fluid the elastic component becomes increasingly significant at higher rates of loading.

It is interesting to note that the concept of full hydrodynamic lubrication with slip-free rolling is challenged by Blok.⁽¹¹⁹⁾ Evidence of complete fluid films concurrent with what they consider to be negligible slipping is presented in a discussion by Sibley and Whitney. Blok concedes that slip may be small but cannot vanish on the basis of equilibrium considerations.

Material Analysis I-C-2: Material analyses have been performed on both the solid rolling element parent metal, the lubricant, and their associated films. Apart from the many fundamental studies of the atomic mechanism of fatigue such as those reviewed by Mott,⁽¹²⁰⁾ analysis of the effect of state of stress on fatigue has been most applicable to

rolling contact conditions. In addition, research into the origin and nature of lubricant and film properties has contributed to the sum of knowledge pertinent to this failure mode. In connection with a discussion of fatigue in rolling contact, it is appropriate to mention that observations of subsurface-originated cracks have been made in basic fatigue studies, even in pure metals, despite the concentration on intrusion-extrusion models of fatigue. Bendler and Wood⁽¹²¹⁾ report subsurface fatigue fissures in OFHC copper specimens subjected to steady tension and alternating torsion.

From analysis of data compiled from many fatigue tests under conditions of combined stress, Stulen and Cummings⁽³⁰⁾ have presented a fatigue criterion expressed in equation form that modifies the critical damaging effect of the maximum reversed shear stress for the inhibiting effect on propagation of the compressive stress normal to the critical shear plane. Findley⁽³¹⁾ has also proposed a criterion based on essentially the same grounds.

As regards variation of pressure viscosity in many polymer lubricants, Boelhouwer and Toneman⁽⁹⁶⁾ suggest that it is related to the "flexibility" of the molecular chains.

Burton⁽¹²²⁾ gives a brief analysis of the molecular mechanism of deformation of simple liquids involving the kinetics of slip and "activation energy of hole formation." The mechanisms would explain viscosity increase with pressure and viscosity decrease with temperature. It is stated that these two effects are quite important and may account for more than a thousandfold variation in viscosity in typical

rolling contact situations.

The nature of surface films composed of parent metal and environmental contaminants, like lubricants and their compounds that form under pressure and temperature extremes, has been the subject of wide research. Some of this research is, of course, pertinent to the comprehensive understanding of rolling contact failure. Some indication of the nature of this research is given by Deryaguin et al.,⁽¹²³⁾ Davy and Edwards,⁽¹²⁴⁾ and Loeser and Twiss.⁽¹²⁵⁾

The importance of these films, acting both as lubricants modifying the friction and stress systems and their chemical effect on macroscopic crack initiation and propagation, emphasizes the need for more pertinent research.

Synthesis I-C-3: Synthesis of the results of both mechanics and material analyses in application to the mode of failure in actual rolling contact situations is still in the primitive stage, but some representative attempts have been made.

From an analysis of the effect of rolling on the range of subsurface shear stress in cylinders, Radzimovsky⁽¹²⁶⁾ took the orthogonal (occurring on planes parallel and normal to the surface) shear stress as the most critical. The strength condition is based on a modified Huber-Mises condition where the alternating stresses are reduced to statical form according to Goodman's linear relation. To account for the effect of ranges of compressive stress, the endurance limit due to completely compressive stress is used in the strength condition rather than the endurance limit caused by reversed stress. In this way an expression is developed for the "surface endurance limit,"

$$\sigma_{\max} = k \sigma_y$$

where σ_y is the uniaxial yield stress of the material and k depends on static material properties as well as the endurance limit in torsion. The equation compares favorably with results of Way and Buckingham for relatively soft steel rollers.

Moyar⁽⁴⁾ attempted to explain the effect of rolling element configuration on contact fatigue strength for hard steels and showed a rational numerical relation between torsion fatigue strength and contact fatigue strength. The stress analysis was based on the solution of Fessler and Ollerton.⁽¹⁰⁰⁾ The strength criterion modified the critical reversed shear stress in a manner similar to the criterion of Stulen and Cummings⁽³⁰⁾ for combined stress. Account was also taken of the volume of material subject to critical stress (statistical size effect) after the method of Lundberg and Palmgren.⁽⁹⁾ An application of this approach was made recently by Ollerton and Morey⁽¹²⁷⁾ to relatively soft rail steels with water lubrication.

The possibility of applying low cycle fatigue data to rolling contact situations involving appreciable cyclic plastic flow is opened by the analysis of Johnson and Jefferis.⁽²⁰⁾ They illustrate a possible relation between total strain accumulation and fatigue life.

Although a synthesis of facts to predict the effect of lubricant on pitting has not been conducted, application of theory to actual rolling element mechanisms has been made related to lubricant film thickness, pressure, and friction torque. Hopkins and St. John,⁽¹²⁸⁾ under the simplest assumptions of constant

viscosity, density, and negligible surface deformation, made an analysis of the motion of bearing elements in a typical roller bearing, accounting for both hydrodynamic conditions and metal-to-metal friction. V. Hackewitz⁽¹²⁹⁾ applied hydrodynamic theory based on the work of Dorr and Kapitsa to a particular roller bearing as an example of obtaining "accurate numerical results" for peak lubricant pressure and film thickness. Temperature and pressure viscosity effects are excluded. However, in general, oil film thickness between roller and raceways varies more with speed than with load. The dynamic peak pressure in the rotating bearing may be considerably less than the peak pressure (or maximum Hertz stress) in the stationary bearing.

Because the statistical method is a powerful tool for the correlation of experimental data, some research dealing particularly with this method as it applies to the fatigue phenomenon will be briefly reviewed in this section.

Weibull⁽¹³⁰⁾ has reviewed some of his early work in this area and has examined several methods for efficiently estimating the three parameters (location, scale, and shape) of his widely used distribution function. He makes an illustrative comparison of full scale bearing data and data from the Mack's spin rig. Assuming the location parameter to be identically zero, he demonstrates the close coincidence of the remaining parameters for both sets of data, although material loading and test conditions are not presented in his paper. He recognizes that the scale parameter depends on load and hence the close correlation

is described as "accidental." However, he implies that shape parameter (an indication of "scatter") is not load dependent.

An extensive summary of ball bearing data was standardized by Tallian⁽¹³¹⁾ for examination of the closeness of fit to the usual Weibull distribution with zero lower bound. He examines the deviations from theory at the lower and higher ends of the cumulative failure probability region of usual interest which result in longer lives than expected. Special regard is given to the postulates for the existence of the distribution and to the basic sequence of events in fatigue. The apparent minimum standardized life is associated with the short but finite macro-crack propagation time period. Tallian proposes that the variable excess experimental life observed up to about 6% failure probability is due to the variation of the period of this phase of the fatigue process with the concurrent development of "beneficial structural changes." The deviations from theory at the higher failure probabilities is attributed to the insufficient number of independent potential failure sites in the longer-lived specimens.

Results I-D-1: As a result of the intensified research effort, particularly with the rolling contact bench rig, much data has accumulated that allows relative ranking of materials and lubricants with regard to influence on pitting life. The observed relation between life and load is perhaps the only direct correlation between the bench rig and the bearing, with the exception of the correlation of rolling contact rig data and the results of full scale bearing tests in a particular circumstance made by Morrow.⁽³⁵⁾

Certain aspects of this research may be summarized. It appears that increase in lubricant pressure viscosity and material hardness increase pitting life. For normal conditions approaching pure rolling, the origin of the fatigue crack is subsurface in the transformed or damaged region, subject to maximum range of reversed shear stress due to the rolling action. The particular location may depend on local stress raisers or variation of material properties with depth. With increasing tangential traction due to relative sliding or mutual surface interaction due to severe environmental conditions, the origin of the fatigue crack may be in the surface, thus being directly influenced by the chemical attack of surface-lubricant films. Both of these mechanisms may occur simultaneously. The influence of lubricant film as chemical agent, heat conductor, and pressure and shear transmitter are all of significance in this respect.

Several complementary avenues of research are indicated. Among these would be a photoelastic study of the influence of inclusion shape, hardness, and location on distribution of contact stress. To make this feasible experimentally, the area of contact would have to be exaggerated. Also subsurface stress calculation can and should be made from boundary stress conditions other than Hertzian (for example see Dowson et al.⁽¹¹²⁾). Experimentally, the nature of chemical attack or stress corrosion on pitting failure in various controlled kinematic and thermal conditions is not well explored.

Critical Review I-D-2: Because of the emphasis on speedy collection of masses of data with the diverse bench rig types, there

is no comprehensive kinematic or dynamic information as to the conditions of tests. This prohibits anything like a standardization of rolling contact fatigue as a property, limiting comparison of data from various rigs or complete rational extension to various design configurations. While it is recognized that idealizations for the purposes of mechanics analysis must by definition differ from all the complexities of the real situation, results of useful engineering significance can be obtained if a more realistic knowledge of even the mechanical forces involved is established experimentally.

B. CUMULATIVE DEFORMATION

Description of Mode II-A-1: The term "cumulative deformation" is used to designate failures of rolling element bearings caused by decrease in diameter of the rolling elements and grooving of raceways which accumulates with stress cycles, leading to excessive "run-out." The result may be unacceptable vibration, noise, friction, torque, or the precipitation of a more catastrophic failure. It is anticipated as a dominant mode of failure in elevated temperature applications and may be observed as a phenomenon and perhaps a basis of failure at room temperatures in certain high-precision situations such as machine tool applications.

Primary Phenomenological Observations

II-A-2: From their tests with bridge rollers in the 1890's, Crandall and Marston⁽⁶³⁾ reported observation of "a flow of metal at the ends of the rollers and around the edge of the contact portion of the plate" after repeated rolling. Such cumulative deformation is

particularly pronounced in heavily loaded rail heads in association with "shelly" failures.⁽¹³²⁾ Glaeser et al.⁽¹³³⁾ have examined the failure modes of many air frame oscillating roller bearings tested in a temperature range between 300°F and 600°F, and conclude that the predominate failure mode is due to plastic deformation. In these oscillating bearings not only is the spherical inner race blunted, but the "hourglass" rollers are reduced in diameter. This reduction becomes so pronounced that in some cases the roller separator is allowed to ride on the inner race. Also, there is evidence of "mounding" at periodic locations along the inner race caused by the oscillating action. This leads to more catastrophic failure due to stress concentration and localized material work hardening. The results of subsurface micro-hardness surveys are reported on three steels (52100, M-2, and type 440C stainless) showing evidence of considerable subsurface plastic flow. From these tests load-life diagrams are reported.

In another exploratory high-temperature rolling contact investigation,⁽¹³⁴⁾ unlubricated needle bearings (0.051-in. roller diameter, 0.540-in. inner race diameter) with various aging treatments were tested at 1200°F. Constant loads were employed which resulted in nominal contact stresses of 234,000, 281,000, and 456,000 psi. The approach of inner and outer race under load as a function of running time was recorded, 0.001 in. being defined as failure. This phenomenon was termed "wear," but no determination of the amount of abrasive wear was made, although evidence of plastic deformation of the rollers and race impressions

were cited. It should be noted that rolling contact rig tests at the same company⁽⁴⁴⁾ have led to the statement that the mode of failure in high-temperature bearings is predominately due to plastic deformation.

Full Scale Tests II-B-1: Apart from a few exploratory tests such as those mentioned above, no controlled experiments with full scale bearings to investigate a range of variables such as temperature, speed, bearing design, and material variables have been found in the literature.

Detailed observations of associated phenomena -- subsurface microplastic deformation and the development of residual stress -- in full scale bearings have been reported, however. Bush et al.⁽⁵⁵⁾ identified from electron micrographs the "gray lines" observed previously by Jones⁽⁶⁹⁾ as alternating fine slip. A threshold maximum contact stress in the range of 422,000 to 480,000 psi for the hardened SAE 52100 steel ball bearings was indicated on the basis of the initiation of an altered microstructure. As contact stress is increased beyond this range, this microstructure and the residual stress pattern develop to a saturation value more rapidly.

Bench Rig Tests II-B-2: Research efforts utilizing rolling contact bench rigs apparently have centered about two purposes. The first type of research measures the amount of plastic deformation after some number of cycles as a method of ranking materials and treatments, reminiscent of indentation tests performed for static load capacity determination. The second recognizes the cumulative nature of the phenomenon

and its significance as a possible failure mode in itself. The first type is represented by the work of Drutowski,⁽³⁹⁾ Zaretsky and Anderson,⁽⁴²⁾ and Akaoka;⁽¹³⁵⁾ the second by the research of Niemann and Kraupner⁽²⁷⁾ and Bamberger.⁽³⁷⁾

Rolling cemented carbide balls between steel plates with various percentages of retained austenite, Drutowski measured groove depth after 20 cycles. The nominal contact stress ranged from 150,000 psi to over 900,000 psi. He determined that for low stresses (below 500,000 psi), steels with the lowest amount of retained austenite exhibit the smallest plastic deformation and highest initiation stress for measurable plastic deformation. At higher stress levels they were ranked roughly by hardness.

The first measurable plastic deformation depended on percentage of retained austenite, but was in the range 160,000 to 377,000 psi maximum contact stress.

Incidental to a series of fatigue pitting tests on both the Macks spin rig and a five-ball tester, Zaretsky made traces of ball track profiles to determine the amount of plastic deformation and wear as a function of hardness for five steels. No explicit numerical results are reported, but a relative scale indicates continuous decrease in deformation with increased hardness. Plastic deformation was from 12 per cent to 90 per cent greater than wear for various steels and hardnesses at 10,000 stress cycles and 750,000 psi in the spin rig. The data reported from the five-ball rig on M-1 steel after 1.7×10^9 cycles at 800,000 psi indicates wear 40 per cent to 60 per cent greater than plastic deformation. Emphasis is placed on hardness,

closely controlled at the highest value consistent with other metallurgical factors, despite the inverse effect at lower stress reported by Drutowski and the lower operating stress in many practical bearings.

Akaoka⁽¹³⁵⁾ replaced the inner race of standard radial ball bearings with hardened steel cylinders equivalent to SAE 52100 with various forging ratios and melt compositions and tested them in a dynamic rotating unbalance machine at high stress levels. From dimensions and load given in the paper a theoretical maximum contact stress of 1,210,000 psi may be calculated. He reports plastic deformation (grooving) at the end of fatigue life, and correlates long lives with those specimens exhibiting greatest plastic deformation. This correlation is not a simple consequence of accumulation of plastic deformation with longer running time, he argues, because almost all the deformation occurs very early in life -- as might be expected at these high stresses from the findings of Bush et al. Although the four materials had nearly equivalent chemical composition, macro and microstructure, and mechanical properties, the materials with the higher forging ratio had the greater plastic deformation (groove depth and width) and longer lives. Many subjects are treated in this paper, and some important questions raised.

The rig used by Niemann and Kraupner⁽²⁷⁾ consisted of a test bar with various profile radii, driven and loaded between cylindrical rollers. The variables were hardness, profile radius, and load (maximum contact stress range from 31,800 psi to 596,000 psi), and the quantities measured were radial deforma-

tion, track width, and deformed profile radius. A major part of the deformation occurred between 2 million and 30 million stress cycles. The "initiation stress" was determined by extension of the relation between deformed radius and nominal contact stress to the value of original profile radius. This stress value was expressed empirically as a function of hardness. Specific plastic deformation determined in static tests was much smaller than that determined on the basis of permanent approach at 30×10^6 cycles. For hardness equivalent to Rockwell C 61 the initiation stress is 164,000 psi.

Bamberger⁽³⁷⁾ explored the effect of speed, temperature, and previous cold work on cumulative deformation of a cobalt base alloy using a rolling contact rig consisting of a 3/8-in. -diameter test bar driven between two toroid load rollers. Radial deformation was given as a function of running time for a nominal contact stress of 500,000 psi at 1200° F and 25,000 stress cycles per min. The rate of accumulation of radial deformation is roughly constant under these conditions, the most severely cold worked steel having the smallest rate. It was stated that the process is akin to creep. However, in high temperature creep tests there is usually an increase in creep rate for material with the most extensive grain boundaries such as highly cold worked materials. Although the process may resemble creep, important differences in the nature of the plastic slip process are indicated. Life (N, number of cycles) to some prescribed deformation was in accord with the equation $N = C \sigma_{\max}^m$, where C is a constant that depends on amount of deformation defined, σ_{\max} is the stress level,

and m is an empirical constant with a value of 0.7 for these conditions.

In an investigation treated more completely elsewhere in this publication, Moyar and Sinclair⁽¹³⁶⁾ studied the cumulative blunting and grooving of annealed brass rollers at room temperature.

Other manifestations of cumulative plastic deformation have been studied by Hamilton.⁽⁵⁴⁾ The forward (into the leading contact edge) shear displacement of a subsurface layer of material due to rolling (first observed in mild steel discs by Crook in 1957) is examined in cold worked copper by Hamilton. The shear displacement per cycle is nearly constant for fixed test conditions and is not dependent on the presence of a lubricant or strongly influenced by speed. Corrugation of the surface, another interesting mode of deformation, was observed at slow speeds and high loads in the driven disc specimens.

Pertinent Material Tests II-B-3: Material tests have been conducted with a view toward selecting materials suitable for high temperature rolling bearing applications. These have included hot hardness, dimensional stability, and yield strength determination. Dimensional stability tests involve measurements of expansion (retained austenite transformation) or contraction (martensite tempering) of alloy steels held for specified periods of time at elevated temperatures. For example, a typical heat treated 52100 steel contracts 0.001030 in./in./at 800°F for 1000 hours while M-50 steel expands 0.000027 in. under the same conditions.⁽¹³⁷⁾

These determinations of material prop-

erties are convenient and probably serve a purpose in qualitative ranking, but regarding more explicit design information related to failure due to cumulative deformation they offer no help. Indeed, even pure research into the cyclic plastic strain behavior of materials subject to simple repeated loads and range of temperature is relatively unexplored. Under conditions of controlled strain Morrow and Sinclair⁽¹³⁸⁾ have examined the effect of cyclic accumulation of microplastic strain on the relaxation of the mean stress for various steel hardnesses. Coffin⁽¹³⁹⁾ has observed the remarkable effect of a small torque on cumulative permanent twist of a double-gage-length specimen subject to repeated uniaxial strain. Some of the complexity of the phenomenon associated with macro strain gradients was avoided in tests of thin wall annealed copper tubing by Moyar and Sinclair.⁽⁵⁰⁾ Inherent cycle-dependent accumulation of plastic strain is observed under steady tension and alternating torsion. The effect of periods of cyclic stress on subsequent recovery and creep rate in lead has been explored by Kennedy.⁽¹⁴⁰⁾ Periods of cyclic loading at low stress values increase the creep rate while periods at high stress decelerate subsequent creep. Also in his tests the total plastic strain accumulated in a creep test under fluctuating loads was much greater than in a creep test conducted at the highest load for the same time.

The fact that either hardening or softening can occur under cyclic conditions is reflected by cycle-dependent changes in a host of bulk material properties including indentation hardness and the mechanical hysteresis

(141, 142, 143, 144, 145) Every metal has a range of potential strength or hardness which can be achieved by cold working, annealing, and so on. Metals initially on the low end of this potential hardness spectrum cyclically harden: those on the high end soften.^(146, 147) In each case, intermediate states are approached, representing a stable condition for the particular metal and imposed cycling conditions.

The initial cyclic rate of change in properties is greatly influenced by the cyclic strain range but rapidly diminishes with repeated cycling -- the major changes occurring in the first few per cent of the fatigue life. Materials quickly adjust to a nearly stable steady state condition which is reflected by a constant terminal hardness⁽¹⁴⁸⁾ and a stable mechanical hysteresis loop.^(53, 149) Tuler and Morrow⁽⁴⁸⁾ have recently shown that the stable intermediate state can also be achieved by partially annealing cold worked OFHC copper.

A number of researchers have attempted to treat mechanistically the phenomenon of cycle-dependent hardening and softening. Notable among these is Thompson,⁽¹⁴¹⁾ who uses transmission electron microscopy observations of dislocations and other lattice defects (principally dislocation loops) to discuss the mechanism of fatigue hardening. Others have invoked annihilation of dislocations of opposite sign⁽¹⁴⁵⁾ and cyclic-induced polygonization⁽¹⁵⁰⁾ as the mechanism of fatigue softening. The subject has also been treated as a generalized Bauschinger effect^(147, 47, 151) involving the introduction, relaxation, and intensification of internal

stresses in localized weak zones.

Mechanics Analysis II-C-1: Contribution from the theory of plasticity as regards the effect of rolling on cumulative deformation is limited. There have been combined analytical and experimental investigations into the two-dimensional strip rolling process that were essentially for purposes of power calculations. However, some idea of the nature of plastic strain may be obtained from **Reference 152.** Actually, analytical plasticity research into contact problems is still concerned with treating the static indentation problem in a more realistic way. The complex stress and strain cycle induced during the passage of a rolling load, the change in surface geometry in the general three-dimensional case, and a non-Hertzian pressure distribution all combine to defy a comprehensive solution.

A contribution to the two-dimensional problem of the rolling of a rigid cylinder on an elastic-perfectly plastic half space was made by Johnson.⁽⁵⁶⁾ From an examination of the residual stress distribution he found that the shakedown limit, irrespective of yield criterion, occurs when the maximum contact stress equals four times the yield stress in pure shear. Below this limit entirely elastic behavior will eventually be established. The limit corresponds to a load 70% greater than the load necessary to initiate yielding.

However, in a particularly simple case Eldredge⁽¹⁶⁾ has made an analysis that demonstrates certain desirable features of an analytical solution in this area. Therefore, his solution will be presented in condensed

form by use of difference equation notation (subscripts refer to stress cycle). The case of a rigid ball grooving a perfectly plastic plane is treated. Perfect plasticity is defined to mean that the projected contact area for a subsequent cycle is equal to the original projected area. It should be noted that this assumption provides a means of including size effect since the "yield pressure" based on projected area can be determined as a property independent of ball size. It is assumed that in forming the groove the contact area occurs on the front half of the ball (Figure 40). The original projected area is bounded by a semicircle of diameter equal to the track width (w_1). The subsequent shape of the area is determined empirically. This gives rise to the relation

$$\ell_{n+1} w_n = 0.7 w_1^2 \quad (26)$$

Considering the transverse profile (Figure 16) of the ball, the trigonometric relation between the track width w_n (chord length) and track depth u_n (chord height) any cycle, n , yields:

$$w_n^2 = 4D u_n \quad (27)$$

Likewise, considering the longitudinal ball profile (Figure 40c) the trigonometric relation between the length of the contact area (ℓ) and the increment in track depth is

$$\Delta u_n = u_{n+1} - u_n = \frac{\ell_{n+1}^2}{4D} \quad (28)$$

From Equations 26, 27, and 28 the fundamental cyclic difference equation for track width as a function of number of cycles is

$$w_n^4 - w_{n+1}^2 w_n^2 + 0.49 w_1^4 = 0 \quad (29)$$

Thus with w_1 known as a function of ball size, load and "yield pressure," the track width at any cycle may be determined.

A similar analysis for the cycle-dependent blunting of a perfectly plastic sphere rolling between rigid platens has been performed by Reis.⁽¹⁵³⁾ The corresponding cyclic difference equation for track width is

$$w_{n+1}^4 + 2w_{n+1}^3 w_n - 2w_n^3 w_{n+1} - w_n^4 - \frac{\pi^2}{2} w_1^4 = 0 \quad (30)$$

Materials Analysis II-C-2: In view of the scant experimental data, formulation of pertinent variables into mathematical equations for a range of conditions is not available. That is, analysis of material behavior as regards rate of accumulation of plastic strain for ideal conditions has not been attempted. However, an indication of this type of analysis is given by Morrow and Sinclair in the analysis of cycle-dependent stress relaxation phenomenon.⁽¹³⁸⁾

An atomistic mechanism for the effects of combined fatigue-creep stressing has been proposed by Kennedy.⁽¹⁴⁰⁾ The intersection of screw dislocations to form a "jog" provides a source of vacancies or interstitials when moved back and forth through the crystal lattice by repeated stress, these in turn accelerating the climb process of dislocations to facilitate further polygonization (recovery) and creep.

Synthesis II-C-3: A synthesis of material behavior with regard to the mechanics of the rolling contact situation to provide a rational basis for design or estimation of service behavior is not available.

Results II-D-1: The result of this research has been isolated design information obtained directly in rolling contact tests on a few particular materials or bearing designs. Only limited indication of the mechanism responsible for failure mode has been given.

Critical Review II-D-2: Since interest in high temperature service is relatively new, there is even a lack of clear phenomenological information from service failures. Contributions from wear and plastic deformation have not been fully separated for any known range of variables or conditions. Stability to cyclic stress does not of necessity follow results of static tests for the purposes of material ranking. Purified material tests into the effect of cyclic stress and temperature on cumulative plastic deformation are lacking even for the "ideal" laboratory materials, much less the complex bearing steels. Combined stress tests also need to be conducted. Although contribution from the mechanics of solids is, of course, limited, some means is needed of extending minimum data to various rolling element configurations and of interrelating geometric variables.

C. EXCESSIVE ROLLING RESISTANCE

Description of Mode III-A-1: Usually, minimum rolling resistance is a desirable feature of all rolling contact bearings. In the case of instrument ball bearings such as those used in gyro-guidance systems, resistance to rolling is a major concern. Failure occurs when the magnitude or variation of rolling resistance produces a friction torque that interferes in an unpredictable way with instrument response. Attention is directed to the

inherent features of rolling resistance, not to other catastrophic failure types that may be manifest in extreme friction torque.

Primary Phenomenological Observations

III-A-2: Serious scientific interest in the nature of rolling friction as a phenomenon dates back at least as far as 1785 to the experiments of Coulomb. Tabor⁽¹⁵⁴⁾ summarizes the experiments of Morin and Dupuit in France around 1840, and the interesting controversy between the two over the dependence of rolling friction on wheel radius. In 1876 Reynolds⁽¹⁵⁵⁾ attributed the source of rolling friction to interfacial slip between elastic surfaces due to differential deformation. He deduced this from his observation that a metal cylinder moved forward a distance less than its circumference when rolled over a rubber surface. The experiments of Crandall⁽⁶³⁾ in 1890, which involved measurement of the force necessary to pull a plate from between loaded rollers, substantially verified Dupuit's finding that friction force is inversely proportional to the square root of roller radius. Since that time, bearing manufacturers with more practical concern have established a so-called "friction coefficient" for a wide variety of particular rolling bearings for convenience of engineering design and selection. The coefficient of friction does vary appreciably with load, however. The effect of rotational speed is negligible for most design purposes. Although there is conflict in values, empirical results of this type of research are summarized in many of the recent texts treating rolling contact bearings. (156, 157, 11, 158) The emphasis placed on instrument bearing friction torque has given rise to an effort to standardize methods and

instruments to study friction phenomena,⁽¹⁵⁹⁾ including significant changes in rolling resistance with running time and test conditions.

Full Scale Tests III-B-1: Many full scale tests have been performed on a variety of bearings under various conditions of speed, load, and lubricant to determine friction torque or coefficient of friction, but few experiments of basic significance relating to contact geometry or rolling element dynamics have been undertaken.

The research of Palmgren and Snare⁽¹⁶⁰⁾ seems to confirm that lubrication of rolling bearings is hydrodynamic at high speed and light load, turning into boundary lubrication at lower speed and heavier load. In an extensive series of tests with various types of ball and roller bearings, friction torque due to hydrodynamic lubrication shear, differential slip (Heathcote) friction and internal hysteresis were separated. For unloaded bearings, resistance moment increased with viscosity and speed of rotation to the two-thirds power. This is in keeping with hydrodynamic theory. In thrust ball bearings, friction due both to differential sliding and hysteresis depends on load to the four-thirds power; hence their effect on friction torque may be separated since sliding resistance is dependent on degree of osculation. Resistance moment in heavily loaded bearings is essentially independent of speed and lubricant as opposed to those operating in the region of hydrodynamic lubrication. In most bearings, there is a combination of both types. It is assumed in the analysis of hysteresis losses that the percentage of energy dissipated is independent of stress, but for the higher loads this does not

appear to be well founded on the basis of other material tests.

Coefficient of friction for a range of straight mineral oils, synthetic oils, and mineral oil-additive blends lubricating thrust ball bearings have been measured by Rounds⁽¹⁶¹⁾ for ball velocity speeds up to 600 ft./min.; maximum contact pressures of 300,000 psi, 400,000 psi, and 500,000 psi; and oil temperatures of 100° F, 200° F, and 300° F. In general the coefficient of friction decreases as oil temperature, ball velocity, or load increases and is independent of oil viscosity in contrast to hydrodynamic theory, indicating boundary lubrication and the importance of surface films.

Bench Rig Tests III-B-2: Bench rig tests of fundamental importance in rolling contact have been reported which explored the effect of surface roughness, established the role of internal hysteresis losses, and examined the influence of relative surface velocity on the point of application and angle of inclination of resultant contact force for very light loads. Barwell⁽¹⁶²⁾ has reviewed the results of a number of bench rig tests. An interesting theory of rolling friction based on the attractive and repulsive atomic forces of surfaces in intimate contact is proposed by Tomlinson and is shown to be consistent with his measurements of coefficient of friction for hard steel rollers oscillating on steel plates. Barwell points out limitations of the theory, especially the complications introduced by oxide films.

Tabor⁽¹⁶³⁾ performed a series of critical laboratory experiments demonstrating the significance of energy losses in rolling due to

internal material hysteresis as opposed to interfacial slip mechanisms. For rolling of a ball in a deep groove, differential slip was a dominant source and could be influenced by the presence of a lubricant, but not when rolling on a flat surface. These tests involved rolling a steel ball on either flat or pre-grooved rubber. Also, identical copper balls were rolled back and forth over each other in a special pendulum apparatus and the decrement in amplitude measured. The symmetry conditions ruled out interfacial slip, establishing material hysteresis as the major source of rolling resistance.

With a rolling friction apparatus designed to measure the force necessary to roll a ball between flat plates, Drutowski⁽¹⁶⁴⁾ determined the effect of contact stress and material on average friction force. There was, however, a great variation in friction force, with instantaneous values many times the average. Roughness of finish or orientation of lay have only a small effect on average friction force, but a more marked effect on peak values. The appreciable number of friction peaks for even the smoothest steel surfaces (1 micro-inch) seemed to indicate that the peaks were due to material inhomogeneity as well as geometrical irregularities. This was confirmed when friction force history for rolling of steel and synthetic sapphire were compared. The friction peaks for steel were still marked, but they were essentially unmeasurable for the homogeneous sapphire. Rolling force increased with the 1.2 power of load for the initial elastic range. It increased with the 2.4 power for loads above that causing observable plastic deformation. For 52100

steel hardened to Rockwell C 60, calculation based on reported data shows maximum contact stress to be approximately 350,000 psi at this transition point. Drutowski⁽³⁹⁾ also reports the reduction in average rolling friction force with decrease in retained austenite in a 52100 steel.

For elastomers, like Neoprene, and thermoplastics, like Plexiglas, Flom⁽¹⁶⁵⁾ has measured dynamic mechanical losses (rebound of a steel ball from the specimen surface) and correlated them with measurements of rolling friction (three steel balls rolling on a plastic surface) at various speeds and temperatures.

The rolling friction of a sapphire ball on single crystals of copper was shown to be strongly dependent on crystallographic direction of rolling in the experiments of Dyer⁽¹⁶⁶⁾ with the rig developed by Drutowski. The anisotropic hardening and shape of the ball tracks are studied and discussed in terms of slip systems activated and dislocation interactions.

The rolling resistance of copper discs loaded in the plastic range to produce a forward shear strain accumulation has been measured by Hamilton.⁽⁵⁴⁾ Although the sensitivity of the apparatus was limited, measurable rolling resistance was observed before the onset of forward flow. It increased rapidly with load beyond this point.

Dunk and Hall⁽¹⁶⁷⁾ have investigated the dynamics of rolling and sliding contact conditions for light loads (nominal maximum contact stress = 4,200 psi) and hydrodynamic lubrication. A single "coefficient of friction" is not sufficient to describe the situation fully,

since the resultant force at contact is only given completely by magnitude, direction (inclination angle), and point of application (offset). The apparatus consisted of a pair of disks separately mounted on low-friction bearings and independently motor driven through calibrated spiral springs. The sliding velocity was of primary importance in determining inclination, while the sum of the sweep velocities determined the offset. At higher loads (nominal maximum contact pressure = 88,500 psi) in the elasto-hydrodynamic regime, measurements of surface traction, film thickness (capacitance technique) and surface temperature at various speeds and loads are made by Crook⁽¹⁶⁸⁾ in two ingenious test rigs. The first rig involves a freely running roller between three driving peripheral rollers of equal diameter. Known amounts of braking torque may be applied to the center roller to control sliding speed. The portion of the surface traction due to rolling (determined from extrapolation of data to pure rolling) is independent of load and proportional to film thickness in this regime. As rolling speed is increased the effect of pressure and temperature on apparent viscosity diminish. This is attributed to viscoelastic effects since the oil is under stress for so brief a period of time. In the second two-roller rig relative sliding speeds are considerably increased so that an intrinsic effect of rate of shear strain upon effective viscosity (non-Newtonian behavior) occurs.

Pertinent Material Tests III-B-3: While research on phenomena associated with this failure mode (material hysteresis and surface friction phenomena) is extensive, its pertinence

has not been explored. To review even representative work on the effect of frequency, stress level, temperature, and material on mechanical hysteresis or damping capacity would lead this discussion far afield. A summary of research⁽¹⁶⁹⁾ shows that for high stress the specific damping capacity is highly dependent on stress level, while for low stresses specific damping capacity may be independent of amplitudes. Variations in energy absorbed per cycle stems from gradual material transformation or change in frequency among many other variables. The significance of stress gradients and provision for modifying specific damping energy are treated by Podnieks and Lazan.⁽¹⁷⁰⁾ For moderate to high stress levels the change in energy absorbed per cycle, or damping, is a manifestation of the cycle dependent hardening or softening discussed above (II-B-3).

The work of Bowden and Leben⁽¹⁷¹⁾ is representative of the basic material and lubricant tests to establish laws of friction and explore the intimate surface asperity and lubricant film interactions.

Mechanics Analysis III-C-1: Mechanics analysis has been undertaken which is pertinent to the hysteresis phenomenon and hydrodynamic film behavior.

Tabor⁽¹⁷²⁾ and Drutowski⁽¹⁶⁴⁾ have calculated the elastic strain energy involved in pressing a ball into a plane. The maximum elastic energy is proportional to the load raised to four-thirds power. Drutowski^(173, 174) has also defined the volume of significantly stressed material involved in the rolling of a ball with regard to an empirically determined value of strain energy density which bounds

this volume. It is experimentally verified that the constant of proportionality between rolling force and stressed volume is independent of ball diameter.

In several calculations for dynamic mechanical losses in rolling contact, such as those of Flom, only direct compression-release cycles of elements in the rolling track are considered for simplicity. In a discussion Tabor⁽¹⁶⁵⁾ emphasizes the distinction between energy dissipation under the actual complex loading cycle involving reversal of shear distortion to that under such simple cycles, concluding that actual losses may be greater by a factor of three. Flom's data supports this conclusion.

Rolling friction arising from microslip phenomena due to elastic surface compliance may be calculated from solutions such as those of Johnson⁽¹⁷⁵⁾ and dePater.⁽¹⁷⁶⁾ For a ball rolling in a straight groove Johnson compares coefficient of rolling resistance (tangential force/normal force) calculated according to theories associated with three sources of rolling resistance: microslip, Heathcote differential slip, and material hysteresis. He demonstrates that for a particular case of close ball and groove conformity, theoretical rolling resistance due to microslip is larger than that due to hysteresis.

Calculations for coefficient of friction or rolling resistance due to lubricant "pumping" and viscous shear are illustrated by the hydrodynamic theory of Kapitsa.⁽¹⁷⁷⁾ In this two-dimensional laminar flow theory the shape of the elastically deformed rollers at contact is prescribed as parabolic.

The source of rolling resistance in

elasto-hydrodynamic lubrication arises from the curvature forced upon the velocity profiles by the convergence of flow at contact entry, according to Crook.⁽¹⁶⁸⁾ He calculates this component of frictional traction for a Newtonian fluid whose viscosity varies with pressure and demonstrates that it is dependent only on film thickness. The general agreement with experiments indicates that in pure rolling the temperature due to friction is too small to significantly change viscosity.

Materials Analysis III-C-2: Mathematical and graphical description is available to the relations among variables involved in hysteresis energy dissipation in simple reversed stress states. Demer⁽¹⁷⁸⁾ has compiled a list of sources. The atomic mechanisms responsible for these phenomena have been analyzed and range from diffusion processes of various activation energies at low stress to thermoelastic coupling or simply non-reversible heat flow processes induced by cycles of mechanical work.

The work already cited concerning the effect of pressure and temperature variables on lubricant properties is pertinent in this area.

Synthesis III-C-3: Synthesis of results from the above phases of research in application to rolling contact situations is incomplete. However, the possibilities of such synthesis has been illustrated by Drutowski.⁽¹⁶⁴⁾ On the basis of measured rolling friction and elastic strain energy calculations he calculated a specific damping capacity in rolling which agreed roughly with values determined in standard tests.

Results III-D-1: In summary, resistance

to rolling may arise from a number of sources:

1. Fluid resistance offered to the rolling elements due to the presence of lubricant films.
 2. Direct interaction of the rolling surfaces and sliding due to elastic deformation (interfacial slip).
 3. Hysteresis energy dissipation in the rolling element material.
 4. Effect of rolling in producing an elastic mound ahead of a grooving element.
- This phenomenon is mentioned by Palmgren⁽¹⁵⁶⁾ and discussed more fully by Dunk.⁽¹⁷⁹⁾ The resultant effect may vary considerably with different directions of tangential force with respect to rolling direction.

Contrary to the impression perhaps created by widespread use of a constant coefficient of friction in bearing design and power loss calculation, the variation of rolling resistance with time as well as its magnitude poses a practical problem in instrument and precision rolling bearings. Small gyro bearings operate in the speed range of 10,000 to 20,000 rpm and may be subject to significant loads due to preloading in order to establish isoelastic conditions in the instrument assembly. Variation in friction torque, which is in a range less than 70 dyne-centimeters may cause serious "drift" in the instrument even without catastrophic bearing failure. This variation may come about because of transformation with time or cycles of the rolling element material, lubricant or their films, or it may develop due to changing operating conditions of speed, load, tempera-

ture, or intermittent periods of service.

Several sources of these phenomena have been explored in standard laboratory tests: variation of film thickness with time, effect of a range of variables on energy dissipation in materials, etc. Also, various rolling contact rigs have been used in determining the effect on rolling resistance of a limited range of material, speed, and load variables. There have been some efforts to separate experimentally the various sources of rolling resistance. Instruments have been recently developed to accurately measure friction torque of full scale instrument bearings.

Critical Review III-D-2: The greatest single obstacle to analysis of the phenomena and failure due to excessive or variable rolling resistance, however, is still the lack of experimental data in rolling contact in which the complete force system and kinematic variables are known and controlled. This has been attempted only for very low loads.

IX. REFERENCES CITED

1. Arthur D. Little, Inc., "Yearly Progress Report on a Study of Contact Fatigue," Sponsored by the ASME Research Committee on Contact Fatigue of Rolling Elements, 1 October 1961 — 1 October 1962.
2. G. Sachs, R. Sell, and W. F. Brown, Jr., "Tension, Compression, and Fatigue Properties of Several Steels for Aircraft Bearing Applications," Proceedings, American Society for Testing and Materials, Vol. 59 (1959), p. 635.
3. W. J. Greenert and Rawlings, "Basic Information on the Bearing Properties of Various Materials in Oil and Sodium Potassium Alloy," U. S. Naval Engineering Experiment Station Report 090014D, April, 1956.
4. G. J. Moyer, "An Analysis of the Fatigue Strength of Surfaces in Rolling Contact," M. S. Thesis, Department of Theoretical and Applied Mechanics, University of Illinois, Urbana, Illinois, 1958.
5. L. G. Johnson, "The Median Ranks of Sample Values in their Population with an Application to Certain Fatigue Studies," Industrial Mathematics, Vol. 2 (1951), p. 1.
6. G. J. Moyer and J. Morrow, Discussion of E. V. Zaretsky and W. J. Anderson, "Relation Between Rolling-Contact Fatigue Life and Mechanical Properties for Several Aircraft Bearing Steels," Proceedings, American Society for Testing and Materials, Vol 60 (1960), p. 644.
7. N. G. Kennedy, "Fatigue of Curved Surfaces in Contact Under Repeated Load Cycles," Proceedings of the International Conference on Fatigue of Metals, Institution of Mechanical Engineers, London, 1957, p. 282.
8. S. Timoshenko and J. N. Goodier, Theory of Elasticity, 2nd ed. New York: McGraw-Hill Book Co., Inc., 1951. p. 381.
9. G. Lundberg and A. Palmgren, "Dynamic Capacity of Rolling Bearings," Acta Polytechnica, Mechanical Engineering Series, Vol. 1, No. 3 (1947).
10. H. Bear and H. Butler, "Preliminary Metallographic Studies of Ball Fatigue Under Rolling-Contact Conditions," National Advisory Committee for Aeronautics, Technical Note 3925, 1957.
11. P. Eschmann et al. Ball and Roller Bearings, Their Theory, Design and Application. London: K. G. Heyden & Co., 1958.
12. J. O. Almen, "Fatigue of Metals as Influenced by Design and Internal Stresses," Surface Stressing of Metals, American Society for Metals, Cleveland, 1947, p. 76.
13. P. H. Dawson, "The Pitting of Lubricated Gear Teeth and Rollers," Power Transmission, Vol. 30 (April and May, 1961), p. 208 and p. 286. (Also published as Research Series No. 86, Associated Electrical Industries Limited, Manchester, England).
14. A. H. Cottrell. Theoretical Aspects of Fracture. New York: John Wiley and Sons, Inc., 1959. P. 20.

15. F. R. Shanley. Strength of Materials. New York: McGraw-Hill Book Co., Inc., 1957. P. 693.
16. K. R. Eldredge and D. Tabor, "The Mechanism of Rolling Friction: I. The Plastic Range," Proceedings, Royal Society of London, Vol. 229, No. 1177, (April 21, 1955), Ser. A, p. 181.
17. J. O. Almen. "Appendix I. Effects of Residual Stress on Rolling Bodies," Rolling Contact Phenomena. Amsterdam: Elsevier Pub. Co., 1962. P. 400.
18. J. O. Almen and P. H. Black, Residual Stresses and Fatigue in Metals. New York: McGraw-Hill Book Co., Inc. 1963.
19. B. Crossland, "Effect of Large Hydrostatic Pressures on the Torsional Fatigue Strength of Alloy Steel," Proceedings of the International Conference on Fatigue of Metals, Institution of Mechanical Engineers, London and New York, 1956, p. 138.
20. K. L. Johnson and J. A. Jefferis, "Plastic Flow and Residual Stresses in Rolling and Sliding Contact," Symposium on Fatigue in Rolling Contact, Institution of Mechanical Engineers, London, 1963, Paper No. 5.
21. F. B. Stulen, "A Hypothesis of Fatigue Failure of Ball and Roller Bearings," Informal Technical Note No. 569, Curtiss-Wright Corporation, Caldwell, N.J., May 25, 1962.
22. F. T. Barwell, "The Effect of Lubricant and Nature of Superficial Layer After Prolonged Periods of Running," Properties of Metallic Surfaces (Institute of Metals, Monograph and Report Series No. 13), London, 1953.
23. R. Kuguel, "The Highly Stressed Volume of Material as a Fundamental Parameter in the Fatigue Strength of Metal Members," University of Illinois Department of Theoretical and Applied Mechanics, Report No. 169, 1960. See also "A Relation Between Theoretical Stress Concentration Factor and Fatigue Notch Factor Deduced from the Concept of Highly Stressed Volume," Proceedings, American Society for Testing and Materials, Vol. 61 (1961), p. 732.
24. W. Weibull, "A Statistical Representation of Fatigue Failures in Solids," Acta Polytechnica, Mechanical Engineering Series, Vol. 1, No. 9 (1949).
25. G. M. Sinclair and T. J. Dolan, "Effect of Stress Amplitude on Statistical Variability in Fatigue Life of 75S-T6 Aluminum Alloy," Transactions, American Society of Mechanical Engineers, Vol. 75 (1953), p. 867.
26. G. Mesmer, "Vergleichende Spannungsoptische Untersuchungen und FlieBversuche unter Kongentriertem Druck," Technische Mitteilungen Thermodynamik, Vol. 1 (1930), pp. 85-100, 106-112.
27. G. Niemann and K. W. Kraupner, "Das Plastische Verhalten Umlaufender Stahlrollen bei Punktberuhung," V.D.I. Forschungsheft, No. 434 (1952), p. 5.
28. E. V. Zaretsky, W. J. Anderson, and R. J. Parker, "The Effect of Contact Angle on Rolling-Contact Fatigue and Bearing Load Capacity," Transactions, American Society of Lubrication Engineers, Vol. 5, No. 1 (April, 1962), p. 210.
29. G. J. Moyar and J. Morrow, "Relation of Fatigue to Pitting Failure of Surfaces in Rolling Contact," University of Illinois Department of Theoretical and Applied Mechanics, Report No. 565, 1958.
30. F. B. Stulen and H. N. Cummings, "A Failure Criterion for Multiaxial Fatigue Stresses," Proceedings, American Society for Testing and Materials, Vol. 54 (1954), p. 822.
31. W. N. Findley et al., "Theory for Combined Bending and Torsion Fatigue with Data for SAE 4340 Steel," Proceedings of the International Conference on Fatigue of Metals, Institution of Mechanical Engineers, London and New York, 1956, p. 150.

32. H. Sytri, "Fatigue Strength of Ball Bearing Races and Heat-Treated 52100 Steel Specimens," Proceedings, American Society for Testing and Materials, Vol. 51(1951), p. 682.
33. W. J. Greenert, "The Toroid Contact Roller Tests as Applied to the Study of Bearing Materials," Journal of Basic Engineering (Transactions of the American Society of Mechanical Engineers) Ser. D., Vol. 84 (March, 1962), p. 181.
34. E. N. Bamberger and R. A. Baughman, "Development of Fatigue Data for Bearing Materials," General Electric Report No. R57AGT712, FPLD, Nov., 1957.
35. J. Morrow, "Correlation of RC Rig Data with Full Scale Bearings," General Electric Co., Metallurgical Engineering Suboperation, Applied Research Operation, Flight Propulsion Laboratory Dept., Cincinnati, Ohio, July 15, 1959 (see also General Electric Flight Propulsion Division Report R61FPD297, May, 1961).
36. P. Lewis, "Fatigue Tests to Evaluate Ball Bearing Materials in Mil-L-7808 Oil," General Electric Report No. 58GL75, General Engineering Laboratory, 1958.
37. E. N. Bamberger, "Evaluation of L-605 (H. S. 25) for High Temperature Unlubricated Bearing Application," General Electric Co. Technical Report No. R59FPD658, Sept., 1959.
38. G. J. Moyar, "A Mechanics Analysis of Rolling Element Failures," Ph. D. thesis, Department of Theoretical and Applied Mechanics, University of Illinois, Urbana, Illinois, 1960. Also Dept. of Theoretical and Applied Mechanics Report No. 182, December, 1960.
39. R. C. Drutowski and E. B. Mikus, "The Effect of Ball Bearing Steel Structure on Rolling Friction and Contact Plastic Deformation," Journal of Basic Engineering (Transactions of the American Society of Mechanical Engineers), Vol. 82, Ser. D., No. 2 (June, 1960), pp. 302-308.
40. D. Tabor, "A Simple Theory of Static and Dynamic Hardness," Proceedings, Royal Society of London, Ser. A., Vol. 192, No. A1029 (February 4, 1948), p. 247.
41. A. B. Jones. New Departure Engineering Data, Analysis of Stresses and Deflections. New Departure (Division of General Motors Corp.), Bristol, Conn., Vol. 1 (1946).
42. E. V. Zaretsky and W. J. Anderson, "Relation Between Rolling-Contact Fatigue Life and Mechanical Properties for Several Aircraft Bearing Steels," Proceedings, American Society for Testing and Materials, Vol. 60 (1960), p. 627.
43. Personal communication with J. Lawrence, SKF Industries, Inc., Philadelphia, Pa.
44. E. N. Bamberger, "Materials for High Temperature Unlubricated Bearings," General Electric Co., Technical Report No. R59AGT54, 1959.
45. J. E. Merwin and K. L. Johnson, "Analysis of Plastic Deformation in Rolling Contact," Proceedings, Institution of Mechanical Engineers, London, Vol. 177, No. 25 (1963), p. 676.
46. G. J. Moyar, discussion of a paper by J. Akoaka in Rolling Contact Phenomena, Amsterdam: Elsevier Pub. Co., 1962. P. 296.
47. L. Bairstow, "The Elastic Limits of Iron and Steel Under Cyclical Variations of Stress," Philosophical Transaction of the Royal Society, Series A, 1911, 210, p. 35.
48. F. R. Tuler and J. Morrow, "Cycle-Dependent Stress-Strain Behavior of Metals," TAM Report No. 239, Department of Theoretical and Applied Mechanics, University of Illinois, March, 1963.

49. R. W. Smith, M. H. Hirschberg, and S. S. Manson, "Fatigue Behavior of Materials Under Strain Cycling in Low and Intermediate Life Range," NASA Technical Note D-1574, April, 1963.
50. G. J. Moyar and G. M. Sinclair, "Cyclic Strain Accumulation Under Complex Multiaxial Loading," Proceedings of the International Conference on Creep, Institution of Mechanical Engineers, London and New York, 1963, p. 47.
51. A. W. Crook, "Simulated Gear-Tooth Contact: Some Experiments Upon Their Lubrication and Subsurface," the International Conference on Creep, Vol. I, Institutional of Mechanical Engineers, London and New York, 1963, p. 47.
52. N. C. Welsh, "Structural Changes in Rubbed Steel Surfaces," Proceedings of the Conference on Lubrication and Wear, Institution of Mechanical Engineers, London, 1958.
53. P. P. Benham, "Axial-Load and Strain-Cycling Fatigue of Copper at Low Endurance," Journal, Institute of Metals, Vol. 89 (May, 1961), p. 328.
54. G. M. Hamilton, "Plastic Flow in Rollers Loaded Above the Yield Point," Proceedings, Institution of Mechanical Engineers, Vol. 177, No. 25 (1963), p. 667.
55. J. J. Bush, W. L. Grube, and G. H. Robinson, "Microstructural and Residual Stress Changes in Hardened Steel Due to Rolling Contact," Rolling Contact Phenomena. Amsterdam: Elsevier Pub. Co., 1962. P. 365.
56. K. L. Johnson, "A Shakedown Limit in Rolling Contact," Proceedings of the Fourth U. S. National Congress of Applied Mechanics, Berkeley, Calif., June, 1962.
57. J. T. Tykociner. Research as a Science-Zetetics. Urbana, Ill.: University of Illinois Electrical Engineering Research Laboratory, 1959.
58. T. Tallian and O. Gustafsson, "The Mechanics of Rolling-Element Bearing Vibrations," American Society of Mechanical Engineers, Paper No. 58-A-292, 1958. Abstract in Mechanical Engineering, March, 1959, p. 94.
59. C. C. Moore and P. Lewis, "Current Development Problems in High Temperature Aircraft Roller Bearings," Proceedings of the Conference on Lubrication and Wear, Institution of Mechanical Engineers, London, 1958, p. 438.
60. W. Radeker, "Wear Caused by Metal-Against-Metal Sliding Friction, with Special Consideration of the Effect of Temperature," Brucher translation from Archiv für das Eisenhüttenwesen, Vol. 15, No. 10 (April, 1942), p. 453.
61. H. H. Schreiber and G. Ulsenheimer, "Zur Frage der Ermüdungserscheinungen bei Wälzlagern," Wear, Vol. 3, No. 2 (March/April, 1960), pp. 122-143.
62. I. R. Stribeck, "Ball Bearings for Various Loads," Transactions, American Society of Mechanical Engineers, Vol. 29 (1907), p. 420.
63. C. L. Crandall and A. Marston, "Friction Rollers," Transactions, American Society of Civil Engineers, Vol. 32 (1894), p. 99.
64. A. Palmgren, "Die Lebensdauer von Kugellagern," Zeitschrift VDI, Vol. 68, No. 14 (1924), p. 339.
65. J. Hoshino, "Some Studies of the Pitting of Marine Reduction Gears," Proceedings of the International Conference on Fatigue of Metals, Institution of Mechanical Engineers, London and New York, 1956, p. 723.
66. W. J. Davies and K. L. Day, "Surface Fatigue in Ball Bearings, Roller Bearings, and Gears in Aircraft Engines," Symposium on Fatigue in Rolling Contact, Institution of Mechanical Engineers, London, 1963, Paper No. 3.

67. J. D. Keller, "Effect of Roll Wear on Spalling," Iron and Steel Engineer, Vol. 37, No. 12 (Dec., 1960), p. 171.
68. J. O. Almen, "Surface Deterioration of Gear Teeth," Mechanical Wear, American Society for Metals, Cleveland, 1960, p. 229.
69. A. B. Jones, "Metallographic Observations of Ball Bearing Fatigue Phenomena," Symposium on Testing of Bearings, American Society for Testing Materials, Special Technical Publication No. 70, 1947.
70. T. W. Morrison, T. Tallian, H. O. Walp, and G. H. Baile, "The Effect of Trace Element Content and Multiple Vacuum Melting on the Fatigue Life of Ball Bearings Made From AISI 52100 Steel," Symposium on Fatigue in Rolling Contact, Institution of Mechanical Engineers, London, 1963, Paper No. 7.
71. M. E. Otterbein, "The Effect of Aircraft Gas Turbine Oils on Roller Bearing Fatigue Life," Transactions, American Society of Lubrication Engineers, Vol. 1, No. 1 (1958), p. 33.
72. B. Sternlicht, P. Lewis, and P. Flynn, "Theory of Lubrication and Failure of Rolling Contacts," Journal of Basic Engineering (Transactions of the American Society of Mechanical Engineers) Ser. D., Vol. 83 (June, 1961), p. 213.
73. L. B. Sibley et al, "A Study of the Influence of Lubricant Properties on the Performance of Aircraft Gas Turbine Engine Rolling Contact Bearings," Wright Air Development Center, WADC TR 58-565 (ASTIA Document No. 204218), 1958. Also published as WADD Technical Report 60-189, June, 1960.
74. S. Way, "Pitting Due to Rolling Contact," Journal of Applied Mechanics, Vol. 2, No. 2 (June, 1935), p. A-49.
75. E. Buckingham, "Surface Fatigue of Plastic Materials," Transactions, American Society of Mechanical Engineers, Vol. 66 (1944), p. 297.
76. T. L. Carter, "Preliminary Studies of Rolling-Contact Fatigue Life of High-Temperature Bearing Materials," National Advisory Committee for Aeronautics, Research Memorandum E57K12, 1958.
77. R. A. Baughman, "Effect of Hardness, Surface Finish and Grain Size on Rolling Contact Fatigue Life of M50 Bearing Steel," Journal of Basic Engineering (Transactions of the American Society of Mechanical Engineers), Ser. D., Vol. 82, No. 2 (June, 1960), p. 287.
78. R. F. Johnson and J. R. Blank, "Fatigue in Rolling Contact: Some Metallurgical Aspects," Symposium on Fatigue in Rolling Contact, Institution of Mechanical Engineers, London, 1963, Paper No. 9.
79. R. F. Johnson and J. F. Sewell, "The Bearing Properties of 1% C-Cr Steel as Influenced by Steelmaking Practice," Journal of the Iron and Steel Institute, Vol. 196, Part IV (Dec., 1960), p. 414.
80. E. N. Bamberger, "Final Report - Heat to Heat Evaluation of M-50," General Electric Co., Applied Research Operation, Flight Propulsion Laboratory Department, Report No. DM59-156, Metallurgical Engineering Code 59MI-58, Cincinnati, Ohio, 1959.
81. F. T. Barwell and D. Scott, "Effect of Lubricant on Pitting Failure of Ball Bearings," Engineering, Vol. 182, No. 4713 (July, 1956), p. 9.
82. W. J. Anderson and E. V. Zaretsky, "Effect of Several Operating and Processing Variables on Rolling Fatigue," Rolling Contact Phenomena. Amsterdam: Elsevier Pub. Co., 1962. P. 317.
83. F. G. Rounds, "Effects of Base Oil Viscosity and Type on Bearing Ball Fatigue," Transactions, American Society of Lubrication Engineers, Vol. 5, No. 1 (April, 1962), p. 172.

84. F. G. Rounds, "Effect of Lubricants and Surface Coatings on Life as Measured on the Four-Ball Fatigue Test Machine," Rolling Contact Phenomena. Amsterdam: Elsevier Pub. Co., 1962. P. 346.
85. D. Scott, "The Effect of Material Properties, Lubricant, and Environment on Rolling Contact Fatigue," Symposium on Fatigue in Rolling Contact, Institution of Mechanical Engineers, London, 1963, Paper No. 10.
86. J. B. Martin and A. Cameron, "Effect of Oil on the Pitting of Rollers," Journal of Mechanical Engineering Science, Vol. 3, No. 2 (June, 1961), p. 148.
87. E. Buckingham and G. J. Talbourdet, "Recent Roll Tests on Endurance Limits of Materials," Mechanical Wear (Proceedings of a Conference held at Massachusetts Institute of Technology, 1948), American Society for Metals, Cleveland, 1950, p. 289.
88. T. Nishihara and T. Kobayashi, "Pitting of Steel Under Lubricated Rolling Contact and Allowable Pressure on Tooth Profiles," Transactions, Society of Mechanical Engineers (Japan), Vol. 3, No. 13 (November, 1937), p. 292. (English summary p. S-73.)
89. P. H. Dawson, "The Effect of Metallic Contact and Sliding on the Shape of the S-N Curve for Pitting Fatigue," Symposium on Fatigue in Rolling Contact, Institution of Mechanical Engineers, London, 1963, Paper No. 4.
90. W. T. Chesters, "The Effect of Material Combination on Resistance to Surface Fatigue," Symposium on Fatigue in Rolling Contact, Institution of Mechanical Engineers, London, 1963, Paper No. 8.
91. W. Wernitz, "Friction at Hertzian Contact with Combined Roll and Twist," Rolling Contact Phenomena. Amsterdam: Elsevier Pub. Co., 1962. P. 132.
92. R. E. McKelvey and C. A. Moyer, "The Relation Between Critical Maximum Compressive Stress and Fatigue Life Under Rolling Contact," Symposium on Fatigue in Rolling Contact, Institution of Mechanical Engineers, London, 1963, Paper No. 1.
93. A. A. Milne and M. C. Nally, "Some Studies of Pitting Failure in Rolling Contacts," Proceedings of the Conference on Lubrication and Wear, Institution of Mechanical Engineers, London, 1958, p. 459.
94. R. A. Burton, J. C. Tyler, and P. M. Ku, "Fundamental Studies of Contact Fatigue," Southwest Research Institute, Report RS-352 (Progress Report No. 8), June, 1962.
95. M. D. Hersey and R. F. Hopkins, "Viscosity of Lubricants Under High Pressure," Mechanical Engineering, Vol. 67, No. 12 (Dec., 1945), p. 820.
96. J. W. M. Boelhouwer and L. H. Toneman, "The Viscosity-Pressure Dependence of Some Organic Liquids," Proceedings of the Conference on Lubrication and Wear, Institution of Mechanical Engineers, London, 1957, p. 214.
97. F. P. Bowden and D. Tabor. The Friction and Lubrication of Solids (International series of monographs on physics). Oxford: Clarendon Press, 1950. Chapter 9.
98. H. R. Hertz. Miscellaneous Papers. London: Macmillan & Co. 1896.
99. H. R. Thomas and V. A. Hoersch. Stresses Due to the Pressure of One Elastic Solid Upon Another (Engineering Experiment Station Bulletin No. 212). Urbana, Ill.: University of Illinois College of Engineering, 1930.
100. H. Fessler and E. Ollerton, "Contact Stresses in Toroids under Radial Loads," British Journal of Applied Physics, Vol. 8, No. 10 (Oct., 1957) p. 387.
101. H. Poritsky, "Stresses and Deflections of Cylindrical Bodies in Contact with Application to Contact of Gears and of Locomotive Wheels," Journal of Applied Mechanics, Vol. 17 (1950), p. 191.

102. J. O. Smith and C. K. Liu, "Stresses Due to Tangential and Normal Loads on an Elastic Solid with Application to Some Contact Stress Problems," Journal of Applied Mechanics, Vol. 20, No. 2 (June, 1953), p. 157.
103. R. D. Mindlin, "Compliance of Elastic Bodies in Contact," Journal of Applied Mechanics, Vol. 16, No. 3 (Sept., 1949), p. 259.
104. M. Hetenyi and P. H. McDonald, Jr., "Contact Stresses Under Combined Pressure and Twist," Journal of Applied Mechanics, Vol. 25, No. 3 (Sept., 1958), p. 396.
105. K. L. Johnson, "The Effect of a Tangential Contact Force upon the Rolling Motion of an Elastic Sphere on a Plane," Journal of Applied Mechanics, Vol. 25, No. 3 (Sept., 1958), p. 339.
106. T. T. Loo, "Effect of Curvature on the Hertz Theory for Two Circular Cylinders in Contact," Journal of Applied Mechanics, Vol. 25, No. 1 (March, 1958), p. 122.
107. C. A. Moyer and H. R. Neifert, "A First Order Solution for the Stress Concentration Present at the End of Roller Contact," See also Reference No. 92, Transactions, American Society of Lubrication Engineers, Vol. 6, No. 4 (1963), p. 324.
108. E. H. Lee and J. R. M. Radok, "The Contact Problem for Viscoelastic Bodies," Journal of Applied Mechanics (Transactions of the American Society of Mechanical Engineers), Series E (Sept., 1960), p. 430.
109. L. W. Morland, "A Plane Problem of Rolling Contact in Linear Viscoelasticity Theory," Journal of Applied Mechanics, Series E, Vol. 29, No. 2 (June, 1962), p. 345.
110. J. Cole and J. Huth, "Stresses Produced in Half Plane by Moving Loads," Journal of Applied Mechanics, Vol. 25 No. 4 (Dec., 1958), p. 433.
111. B. W. Kelley. The Importance of Surface Temperature to Surface Damage (Handbook of Mechanical Wear, ed. C. Lipson and L. V. Colwell). Ann Arbor: University of Michigan Press, 1961. Chapter 8, p. 155.
112. D. Dowson, G. R. Higginson, and A. V. Whitaker, "Stress Distribution in Lubricated Rolling Contacts," Symposium on Fatigue in Rolling Contact, Institution of Mechanical Engineers, London, 1963, Paper No. 6.
113. L. B. Sibley and F. K. Orcutt, "Elasto-Hydrodynamic Lubrication of Rolling-Contact Surfaces," Transactions, American Society of Lubrication Engineers, Vol. 4, No. 1 (April, 1961), p. 234.
114. A. W. Crook, "The Lubrication of Rollers: III. A. Theoretical Discussion of Friction and the Temperature in the Oil Film," Philosophical Transactions of The Royal Society, Ser. A., Vol. 254, p. 237.
115. F. W. Smith, "The Effect of Temperature in Concentrated Contact Lubrication," Transactions, American Society of Lubrication Engineers, Vol. 5, No. 1 (April, 1962), p. 142.
116. F. W. Smith, "Lubricant Behavior in Concentrated Contact -- Some Rheological Problems," Transactions, American Society of Lubrication Engineers, Vol. 3, No. 1 (1960), p. 18.
117. Tokio Sasaki, Haruo Mori, and Norio Okino, "Fluid Lubrication Theory of Roller Bearing, Parts I and II," Journal of Basic Engineering (Transactions of the American Society of Mechanical Engineers) Ser. D., Vol. 84, 1962, p. 166 and p. 175.
118. R. A. Burton, "An Analytical Investigation of Viscoelastic Effects in the Lubrication of Rolling Contact," Transactions, American Society of Lubrication Engineers, Vol. 3, No. 1 (1960), p. 1.

119. H. Block, "Hydrodynamic Effects on Friction in Rolling with Slippage," Rolling Contact Phenomena. Amsterdam: Elsevier Pub. Co., 1962. P. 186.
120. N. F. Mott, "Work-Hardening and the Initiation and Spread of Fatigue Cracks," Proceedings, Royal Society of London, Ser. A., Vol. 242, No. 1229 (Oct. 29, 1957), p. 145.
121. W. A. Wood and H. M. Bendler, "Effect of Superimposed Static Tension on the Fatigue Process on Copper Subjected to Alternating Torsion," Transactions, Metallurgical Society of American Institute of Mining and Metallurgical Engineers, Vol. 224, No. 1 (Feb., 1962), p. 18.
122. R. A. Burton, "Progress Report No. 1 on Analytical Studies of Lubricant Films" (Institute sponsored project 12-823-8) Department of Engines, Fuels, and Lubricants, Southwest Research Institute, San Antonio, Texas, 1959.
123. B. V. Deryaguin et al, "Mechanism of Boundary Lubrication and Properties of Lubricating Film -- Short-and-Long-Range Action in Theory of Boundary Lubrication," Wear, Vol. 1, No. 4 (Feb., 1958), p. 277.
124. W. Davey and E. D. Edwards, "Extreme-Pressure Lubricating Properties of Some Sulphides and Di-Sulphides in Mineral Oil, As Assessed by Four-Ball Machine," Wear, Vol. 1, No. 4 (Feb., 1958), p. 291.
125. E. H. Loeser and S. B. Twiss, "Analysis of Films Formed by Radioactive E-P Additives," Lubrication Engineering, Vol. 14, No. 8 (Aug., 1958), p. 343.
126. E. I. Radzimovsky. Stress Distribution and Strength Condition of Two Rolling Cylinders Pressed Together (Engineering Experiment Station Bulletin No. 408). Urbana, Ill.: University of Illinois College of Engineering, 1953.
127. E. Ollerton and J. W. W. Morey, "Fatigue Strength of Rail Steel in Rolling Contact," Symposium on Fatigue in Rolling Contact, Institution of Mechanical Engineers, London, 1963, Paper No. 2.
128. V. Hopkins and A. D. St. John, "Development and Evaluation Techniques for Determination of the Lubricity and Stability of New High-Temperature Lubricants and Hydraulic Fluids," Wright Air Development Center, WADC TR 58-297 (ASTIA Document No. 203382), 1958.
129. F. W. v. Hackewitz, "The Influence of Kapitsa's Viscosity on the Hydrodynamic Lubrication of a Cylindrical Roller Bearing as Affecting Contact Pressure and Oil-Film Thickness," Journal of Applied Mechanics, Vol. 25, No. 4, (Dec., 1958), p. 620.
130. W. Weibull, "Efficient Methods for Estimating Fatigue Life Distributions of Roller Bearings," Rolling Contact Phenomena. Amsterdam: Elsevier Pub. Co., 1962. p. 252.
131. T. Tallian, "Weibull Distribution of Rolling Contact Fatigue Life and Deviations Therefrom," Transactions, American Society of Lubrication Engineers, Vol. 5, No. 1 (April, 1962), p. 183.
132. R. E. Cramer and R. S. Jensen. Progress Reports of Investigation of Railroad Rails and Joint Bars (Engineering Experiment Station Reprint No. 54). Urbana, Ill.: University of Illinois College of Engineering, 1955.
133. W. A. Glaeser et al, "The Development of Oscillatory Rolling Contact Bearings for Airframe Application in the Temperature Range 300°F to 600°F," Wright Air Development Center, WADC TR59-145, 1959.
134. C. C. Moore, "Wear of Haynes 25 Roller Bearings (Stator)," General Electric Co., Technical Report No. 59FPD917, 1959.

135. J. Akaoka, "Some Considerations Relating to Plastic Deformation Under Rolling Contact," Rolling Contact Phenomena. Amsterdam: Elsevier Pub. Co., 1962. P. 266.
136. G. J. Moyer and G. M. Sinclair, "Cumulative Plastic Deformation in Rolling Contact," Journal of Basic Engineering (Transactions of the American Society of Mechanical Engineers), Ser. D., Vol. 85, No. 1 (March, 1963), p. 105.
137. G. K. Bhat and A. E. Nehrenberg, "A Study of the Metallurgical Properties That Are Necessary for Satisfactory Bearing Performance and the Development of Improved Bearing Alloys for Service up to 1000°F," Wright Air Development Center, WADC TR57-343 (ASTIA Document No. 142117), 1957.
138. J. Morrow and G. M. Sinclair, "Cycle-Dependent Stress Relaxation," Symposium on Basic Mechanisms of Fatigue, American Society for Testing Materials, Special Technical Publication No. 237, 1959.
139. L. F. Coffin, Jr., "The Stability of Metals Under Cyclic Plastic Strain," Journal of Basic Engineering (Transactions of the American Society of Mechanical Engineers), Ser. D., Vol. 82, No. 3 (Sept., 1960), p. 671.
140. A. J. Kennedy, "The Effect of Fatigue Stresses on Creep and Recovery," Proceedings of the International Conference on Fatigue of Metals, Institution of Mechanical Engineers, London and New York, 1956, p. 401.
141. N. Thompson, "Metal Fatigue," Z. Metallkunde, Vol. 53, No. 1 (June, 1962), pp. 71-78, (In English).
142. P. P. Benham, "Fatigue of Metals Caused by a Relatively Few Cycles of High Load or Strain Amplitudes," Metallurgical Review, Vol. 3, No. 11 (1958), pp. 203-234.
143. L. F. Coffin, Jr., "Low Cycle Fatigue: A Review," Applied Materials Research, Vol. 1, No. 3 (Oct., 1962), pp. 129-141.
144. B. J. Lazan and T. Wu, "Damping, Fatigue and Dynamic Stress-Strain Properties of Mild Steel," Proceedings of American Society for Testing and Materials, Vol. 51 (1951), p. 649.
145. L. F. Coffin, Jr., and J. F. Tavernelli, "The Cyclic Straining and Fatigue of Metals," Transactions of the Metallurgical Society of American Institute of Mining and Metallurgical Engineers, Vol. 215 (October, 1959), pp. 794-806.
146. T. Broom and R. K. Ham, "The Hardening and Softening of Metals by Cyclic Stressing," Proceedings of the Royal Society, A242, 1957, pp. 166-179.
147. N. H. Polakowski and A. Palchoudhuri, "Softening of Certain Cold-Worked Metals Under the Action of Fatigue Loads," Proceedings of the American Society for Testing and Materials, Vol. 54 (1954), pp. 701-716.
148. R. B. Davies, J. Y. Mann and D. S. Kemsley, "Hardness Changes During Fatigue Tests on Copper," International Conference on Fatigue of Metals, The Institution of Mechanical Engineers, London, 1956, pp. 551-556.
149. P. P. Benham and H. Ford, "Low Endurance Fatigue of a Mild Steel and an Aluminum Alloy," Journal of Mechanical Engineering Science, Vol. 3, No. 2 (June, 1961), pp. 119-132.
150. R. K. Ham and T. Broom, "The Mechanism of Fatigue Softening," Philosophical Magazine, Vol. 7, No. 73 (Jan., 1962), pp. 95-103.
151. D. S. Kemsley, "The Behavior of Cold-Worked Copper in Fatigue," Journal of the Institute of Metals, Vol. 87 (Sept., 1958), pp. 10-15.
152. C. W. MacGregor and L. F. Coffin, "The Distribution of Strains in the Rolling Process," Journal of Applied Mechanics, Vol. 10, No. 1 (March, 1943), p. A-13.
153. E. E. Reiss, "Cyclic Deformation and Rolling Resistance of Perfectly Plastic Spheres," (Third Student Symposium

- on Engineering Mechanics), TAM Report No. 218, Department of Theoretical and Applied Mechanics, University of Illinois, June, 1962.
154. D. Tabor, "Introductory Remarks," Rolling Contact Phenomena. Amsterdam: Elsevier Pub. Co., 1962. P. 1.
 155. O. Reynolds, "On Rolling-Friction," Philosophical Transactions, Royal Society of London, Vol. 166, Part I (1876), p. 155.
 156. A. Palmgren. Ball and Roller Bearing Engineering. SKF Industries, Inc., Philadelphia, Penn., 1945.
 157. D. F. Wilcock and E. R. Booser. Bearing Design and Application. New York: McGraw-Hill Book Co., Inc., 1957.
 158. M. C. Shaw and F. Macks. Analysis and Lubrication of Bearings. New York: McGraw-Hill Book Co., Inc., 1949.
 159. A. B. Asch, "Antifriction Instrument — Bearing Torque Testing and Resistance to Motion of Such Bearings," Journal of Basic Engineering (Transactions, American Society of Mechanical Engineers) Ser. D., Vol. 81 (1959), p. 46.
 160. A. Palmgren and B. Snare, "Influence of Load and Motion on the Lubrication and Wear of Rolling Bearings," Proceedings of the Conference on Lubrication and Wear, Institution of Mechanical Engineers, London, 1958, p. 454.
 161. F. G. Rounds, "Effect of Lubricant Composition on Friction as Measured with Thrust Ball Bearings," Journal of Chemistry and Engineering Data, Vol. 5 (1960), p. 499.
 162. F. T. Barwell, "Friction and its Measurement," Metallurgical Reviews, Vol. 4, Part 14 (1959), The Institute of Metals, London, p. 141.
 163. D. Tabor, "The Mechanism of Rolling Friction: II. The Elastic Range," Proceedings, Royal Society of London, Series A, Vol. 229, No. 1177 (April 21, 1955), p. 198.
 164. R. C. Drutowski, "Energy Losses of Balls Rolling on Plates," Paper presented at technical session on the Instrument Ball Bearing Conference sponsored by New Departure (Division of General Motors Corp.), 1958.
 165. D. G. Flom, "Dynamic Mechanical Losses in Rolling Contacts," Rolling Contact Phenomena. Amsterdam: Elsevier Pub. Co., 1962. P. 97.
 166. L. D. Dyer, "Rolling Friction on Single Crystals of Copper in the Plastic Range," Rolling Contact Phenomena. Amsterdam: Elsevier Pub. Co., 1962. P. 76.
 167. A. C. Dunk and A. S. Hall, Jr., "Resistance to Rolling and Sliding," Transactions, American Society of Mechanical Engineers, Vol. 80 (1958), p. 915.
 168. A. W. Crook, "The Lubrication of Rollers: IV. Measurements of Friction and Effective Viscosity," Philosophical Transactions of the Royal Society, Series A, Vol. 255, No. 1056 (Jan. 17, 1963), p. 281.
 169. C. E. Feltner, "Strain Hysteresis, Energy and Fatigue Fracture," University of Illinois Department of Theoretical and Applied Mechanics, Report No. 146, Urbana, Illinois, June, 1959.
 170. E. R. Podnieks and B. J. Lazan, "Analytical Methods for Determining Specific Damping Energy Considering Stress Distribution," Wright Air Development Center, WADC TR 56-44, 1957.
 171. F. P. Bowden and L. Leben, "The Nature of Sliding and the Analysis of Friction," Proceedings, Royal Society of London, Series A, Vol. 169, No. A938 (Feb. 7, 1939), p. 371.

172. D. Tabor, "Elastic Work Involved in Rolling a Sphere on Another Surface," British Journal of Applied Physics, Vol. 6 (1955), p. 79.
173. R. C. Drutowski, "The Volume of Stressed Material Involved in the Rolling of a Ball," Journal of Basic Engineering (Transactions of the American Society of Mechanical Engineers), Series D, June, 1961, p. 162.
174. R. C. Drutowski, "The Linear Dependence of Rolling Friction on Stressed Volume," Rolling Contact Phenomena. Amsterdam: Elsevier Pub. Co., 1962. P. 113.
175. K. L. Johnson, "Tangential Traction and Micro-Slip in Rolling Contact," Rolling Contact Phenomena. Amsterdam: Elsevier Pub. Co., 1962. P. 6.
176. A. D. de Pater, "On the Reciprocal Pressure Between Two Elastic Bodies," Rolling Contact Phenomena. Amsterdam: Elsevier Pub. Co., 1962. P. 29.
177. P. L. Kapitsa, "The Hydrodynamic Theory of Lubrication During Rolling Friction," Translation No. TIL/T4585, prepared by Technical Information and Library Services (Great Britain), 1956, from Zhurnal Technicheskoi Fizik, Vol. 25 (1955), p. 747. (ASTIA Document No. 113729).
178. L. J. Demer, "Bibliography of Material Damping Field," Wright Air Development Center, WADC TR 56-180, 1956.
179. A. C. Dunk, "Resistance to Rolling and Sliding Contact," Ph.D. Thesis, Purdue University, 1955.
180. R. H. Butler and T. L. Carter, "Stress Life Relation of Rolling-Contact Fatigue Spin Rig," National Advisory Committee for Aeronautics, Technical Note No. 3930, 1957.
181. R. A. Baughman, "Experimental Laboratory Studies of Bearing Fatigue," American Society of Mechanical Engineers, Paper No. 58-A-235, 1958.
182. C. P. Bacha, "An Apparatus for Fatigue Testing Roller Bearing Rollers," (unpublished) Rutgers University, 1956.

Abstract in Mechanical Engineering, Vol. 81, No. 3 (March, 1959), p. 94.

X. INDEX

- Aluminum
 - bending fatigue strength of, 12
 - trace element in bearings, 45
- Anisotropy, copper single crystal rolling, 66
- Bauschinger effect related to cyclic hardening and softening, 62
- Bauschinger natural elastic limit, 31
- Bearings
 - ball, 5,20,23,44,57,60,65
 - instrument, 42,64,69
 - needle, 58
 - roller, 44,53,56,58,65
 - thrust ball, 23,65
- Bench rig, 46-50
 - divergence of data from, 5
 - tests of rolling resistance, 65-67
 - types: cone and three ball, 50; five ball, 49,59; four ball, 48; G.E.rolling contact, 5, 47; geared roller, 9; Macks spin, 5, 47, 48; repeated contact, 50; U.S. Naval Eng. Exp. Sta. (Annapolis), 5; Univ. of Ill., 7
- Blunting
 - analysis of perfectly plastic, 63
 - brass toroids, 27
 - inner race in "hourglass" roller bearings, 58
 - profile in hard steel, 27,30
- Brass, tensile and tension-torsion tests, 32
- Brass toroid rolling element, 7,26,27
- Bridge rollers, 44, 58
- Carbide cemented balls, 28, 59
- Carbide particles in bearing steels, 47
- Case hardened steel, 4,7,50
- Characteristic life, influence of contact stress and size on, 11
- Chemical effects: in fatigue, 10; lubricant on surface crack initiation, 48, 55
- Chromium segregation in bearing steels, 47
- Coefficient of friction in rolling, 64-66
- Coefficient of pressure viscosity, 48,51,53,65,66
- Cold worked metals
 - effect of cyclic loading on, 62
 - grooving of, 28
 - rate of cumulative deformation in rolling contact, 34,60
- Complex loading
 - cycle in rolling contact, 25,31,39
 - energy losses under, 68
 - tension-torsion tests, 32,55
- Conformity influence on rolling resistance, 61
- Conformity of ball and groove, 27
- Contact
 - angle, effect on pitting life, 49
 - area, 5,12,15,28,63
 - ellipse: eccentricity, 7,15; orientation, 5; width increase, 22,63
 - stress reduction due to plastic deformation, 13, 28
- Copper
 - balls, rolling resistance of, 66
 - blister on rolling track in, 10
 - one-directional loading of, 32
 - plastic grooving of, 28,66
 - single crystal, 66
 - stable cyclic state in OFHC, 62
 - tension-torsion cyclic tests of, 55,61
 - trace element in bearing steels, 45
- Correlation equation, 22, 24
- Correlation of data
 - bench rig and bearing failures, 4,20-24,48,56,57
 - elastic limit for tension, compression, and rolling contact, 29
 - on basis of maximum contact stress, 50
 - pitting and standard material tests, 4,10,17,47,49,50,51
 - pitting life for various rolling element geometries, 19
 - statistical method, 56
- Crack
 - due to repeated contact, 9
 - initiation, 9,10
 - longitudinal subsurface, 9
 - propagation, 10
 - radial subsurface in steel rolls, 10
 - subsurface, effect on stress distribution, 12
 - surface vs. subsurface, 50,55,57
- Creep
 - high temperature, in rolling contact, 60
 - subsurface tangential, due to rolling, 33
 - under fluctuating loads, 61,63
- Crown of rollers, effect on pitting strength, 50
- Cumulative plastic deformation in rolling
 - analysis summary, 37
 - possible sources of, 31
 - literature review summary, 36
- Cycle-dependent
 - hardening and softening, 62
 - mechanism, 62
 - reduction of deformation resistance in rolling contact, 32
 - related to rolling resistance, 67
 - softening of hard steels, 32
 - stress relaxation, 63
- Cyclic
 - difference equation for track width, 63
 - material properties, 31
 - stress-strain behavior, 32, 61
- Cylinders, pitting strength of, 15,17,18
- Cylinders, residual stresses in, 10,34,35
- Damping capacity, relation to rolling friction, 68
- Damping capacity, dependence on stress level, 67
- Dielectric oil film measurements, 46
- Dimensional instability: metallurgical, 25; tests in steels, 61
- Dimensionless forms for grooving of hard steel, 28
- Dimensionless forms from Grubin's lubrication theory, 53
- Dislocation interactions in fatigue, 62
- Dislocation interactions in rolling, 32,66
- Dynamic
 - capacity of bearings, 44
 - information, need for in bench rig tests, 58
 - peak pressure in rotating bearing, 56
 - photoelastic tests, 57
- Elasticity, crack stress model, 12
- Elasticity, solution for contact stresses, 7, 52
- Elastohydrodynamic
 - analysis of lubricated rolling contact, 53
 - source of rolling resistance, 68
- Elastomers, 66
- Electron micrographs, 59
- Endurance formula for ball bearings, 44
- Endurance limit, surface, 55
- Endurance tests of deep groove ball bearings, 45
- Energy
 - dissipation associated with offset of normal force in rolling, 33,65
 - elastic, in rolling and indentation, 67
 - equation in lubrication theory, 54
 - losses (hysteresis) in rolling contact, 37,65
- Failure, definition of modes in rolling contact, 41
- Failure, noise level at, 7
- Fatigue
 - creep mechanism, 63
 - criteria, 16,18,55
 - low-cycle data, 56
 - mechanism of, 10,18,54
 - process, associated with statistical parameters, 57
- Fatigue strength
 - effect of specimen size on, 11
 - relation of bending and torsion, 17
- Flaking, incipient, 10
- Fluid mechanics survey, pertinent to bearing lubrication, 53
- Forging ratio influence on plastic deformation and pitting life, 60

- Friction
 - coefficient in rolling bearings, 64
 - force, influence on surface distortion in grooving, 34
 - laws of, 67
 - torque in bearings: analysis, 56; due excessive deformation, 58; due lubricant deterioration, 42; measurement, 65
- Gears
 - comparison of pitting strength to roller bearings, 45
 - failures in service, 44
 - pitting tests of materials used in, 50
 - surface crack initiation in, 10
 - tests of through hardened and carburized, 45
- General Electric rolling contact rig, 5
- Grain size, 20
- Grooving
 - analysis of perfectly plastic, 63
 - of ball bearing races, 60
 - profile in hard steel, 30
 - trigonometric relations for, 27
- Hardness
 - hot, 61
 - influence on pitting, 47
 - relation to plastic deformation in rolling contact, 28, 59
 - relation to tensile, compressive and fatigue properties, 51
 - relative, of roller pairs in pitting tests, 50
 - surveys in ball bearing races, 45
- Hertz contact pressure modification
 - due finite size bodies, 52
 - due hydrodynamic film, 33,53
 - due viscoelastic effects, 52
- Hertz pressure distribution, 9,52
- High temperature
 - acceleration of lubricant-surface reactions, 48
 - effect on cumulative plastic deformation, 25,33,34, 39,58
 - effect on pitting, 20,46,47
 - in contact zone as a pitting criterion, 46
 - steels, 47
- Hydrodynamic
 - film, modification of Hertzian pressure and influence on plastic deformation, 33,46
 - propagation of surface cracks, 10
 - theory applied to roller bearing lubrication, 56,65
- Hydrogen embrittlement due to water in lubricants, 48
- Hydrostatic compressive stress
 - influence on crack initiation, 10
 - influence on fatigue strength, 16
 - torsion fatigue tests under, 10,16
- Hysteresis
 - atomic mechanisms of, 68
 - mechanical, 61
 - losses and rolling friction, 65
- Inclusions
 - detrimental types, 47
 - in vacuum melted steel, 50
 - photoelastic study needed, 57
 - role in fatigue crack initiation, 10
- Indentation
 - repeated, 29
 - tests for static load capacity, 59
 - types of imprints, 26
- Index
 - of bearing life, 46
 - plastic deformation, 38
 - pressure viscosity, 48
 - research classification, 41
 - stress and strain, 28
- Induction vacuum melting, 51
- Kinematic conditions of rolling elements in bench rig, 50
- Kinematic variables lacking in rolling contact tests, 69
- Lead, cyclic recovery and creep rate in, 61
- Lead, grooving of, 28
- Lubricant
 - contamination by water, 48
 - effect of rate of shear on viscosity, 51
 - effect on contact stress distribution, 53
 - effect on pitting, 20,24,45,48,49
 - effect on rolling resistance, 68
 - environmental contaminants, 55
 - film temperature, 53
 - film thickness measurements, 46,53
 - types: ester-based, 54; extreme pressure additives, 48; mineral oil, 65; MIL-L-7808, 24,46,47; MIL-L-6081, 24; of various chemical classes or composition, 48,51; polymer, 55; sodium potassium (NaK), 5,49; synthetic oil, 65; water, 56;
- Lubrication
 - boundary, 51,65
 - dimensionless forms in Grubin's theory, 53
 - theory of roller, 54
- Martensite tempering, 61
- Materials, screening of, in bench rig tests, 46,50
- Mechanics analyses of pitting failure, 55-56
- Metallographic examination of pitting failure, 45,47
- Metallurgical structure
 - change with temperature, 47
 - transformation due rolling, 45,59
- Microplastic deformation, 59
- Microresidual stress,
 - role in crack initiation at inclusions, 10
- Microslip, 68
- Microstructure, 60; altered by rolling, 59
- N.A.S.A. five ball tester, 49
- Neoprene, dynamic mechanical losses in, 66
- Noise due bearing imperfections, 41
- Noise level at pitting failure, 7
- Non-Newtonian effects in lubricants, 51,53
- Normal stress influence factor, 17
- Octahedral shear stress
 - for initiation of plastic deformation, 29
- Orthogonal shear stress
 - dependence on contact geometry, 9,15,20
 - depth to maximum, 15
 - elastic solution for, 52
 - for asymmetrical pressure distribution, 33
 - role in cumulative plastic deformation, 32
- Photoelastic tests, 53,57
- Pitting failures, 4
 - definition of, 44
 - initiation and propagation of, 9
 - list of variables influencing, 20
 - mechanism of, 9
 - metallographic observation of, 9
 - S-N curves, 21
 - summary: of analysis, 37; of literature review, 36
- Pitting life
 - adjustment for stress level, 5
 - correlation with plastic deformation, 60
 - dependence on stress level, 5,9,21,22,45,50
 - effect of: rolling element geometry or configuration, 4,7,19; rolling element size, 4; sliding, 49; temperature, 47
 - list of variables affecting, 20,46
 - scatter or dispersion in, 21,57
- Pitting strength, affected by
 - relative hardness of roller pairs, 50
 - rolling element configuration and size, 4,5,9
- Plastic shearing of lubricants, 54
- Plastic nucleus, 29
- Plastic deformation in rolling contact
 - contact stress reduction due to, 12,13,15,17,21,28
 - elastically restrained, 26
 - increase in track width, 21,22
 - index of, 38
 - initiation, 12, 28-29, 59,60
 - mechanism, 32
 - pronounced, 26
 - residual stresses due to, 10
 - rolling element geometry changes due to, 12
- Plasticity
 - effects in solidified oils, 51
 - loading and yielding surface, 31
 - Prandtl-Reuss relations, 34
 - three-dimensional solution for rolling, 36
 - two-dimensional solution, 34,36,62
- Preload, 34
- Probability: multiplicative law of, 15; of failure, 5,57; of survival, 11,15; paper, 5
- Profile radius
 - changes due: blunting, 60; grooving, 26
 - effect on pitting, 50
 - elastic relations based on deformed, 13,26
- Rail heads, cumulative plastic deformation, 58
- Rail steels, pitting tests of, 56
- Rate of cumulative deformation in rolling, 31,33,39,60
- Rate of strain accumulation, 63
- Repeated contact: compared to rolling, 9; tests, 50
- Repeated tensile tests, 31,32
- Research classification, 41-43
- Residual stress
 - circumferential, in steel rolls, 10
 - effect of preload on, 34
 - in three-dimensional contact, 10,35
 - influence on crack propagation, 10

- intensification due cumulative plastic strain, 25,34,59
- measurement of, 59
- micro-, at inclusions, 10
- tensile, in a cylindrical roller, 34
- Retained austenite
 - effect on initiation of plastic deformation, 28,59
 - effect on pitting, 47
 - transformation of, 61
- Reversal of shear stress, relation to: rolling contact
 - energy losses, 68; pitting and cumulative plastic deformation, 32,37
- Rheological behavior of lubricants in rolling and sliding, 54
- Rheological models in lubrication theory: Bingham, 54; Maxwell, 54
- Rolling element configuration (geometry) effect
 - pitting, 4-7,9,19,37; plastic deformation, 28,31,36
- Rolling resistance (friction)
 - comparison of theories, 68
 - due to lubricant "pumping", 68
 - experiments, 64
 - manifestation of cycle-dependent hardening or softening, 67
 - needed investigations, 40
 - of copper discs in plastic range, 66
 - summary of literature review, 36
 - theory based on atomic forces in surface, 65
- Sapphire balls in rolling, 66
- Shakedown applicability to cumulative plastic deformation in rolling contact, 32
- Shakedown limit for two dimensional rolling, 62
- Size effect
 - in cumulative deformation, 36
 - on fatigue strength, 11,15,56
 - volume of significantly stressed material, 11,15,17,19, 21,67
- Skew angle in rolling contact, 7,39
- Skew effect on asymmetrical plastic deformation, 30
- Sliding, influence on
 - formation of "oyster shell" flake on gears, 45; pitting life, 49; surface initiated pitting, 10
- Sliding, resistance losses in rolling, 65,67
- Sliding, thermal stresses caused by, 53
- Slip
 - differential, in deep grooves, 34,66,68
 - due to combined roll and spin, 49
 - effect on pitting strength, 49
 - free rolling, 54
 - in single crystal copper, 66
 - interfacial, in rolling, 66
 - lines in subsurface material, 45
- Spalling of steel mill rolls, 45
- Specific damping capacity, 68
- Speed effects
 - in hydrodynamic lubrication, 46,67
 - in plastic deformation, 25,61
 - on elastic stress distribution, 52
 - on friction coefficient in rolling bearings, 64,65,67
 - on lubricant film thickness, 56,67
- Spin velocity effect
 - on pitting life in five ball bench rig, 49
 - on pitting strength (with combined roll), 49
 - on surface strains and ball motion, 52
- Statistical life variability, 5
 - distribution function for, in ball bearings, 57
 - in vacuum melted steels, 50
 - influence of specimen size on, 11
 - influence of stress level on, 11,39,57
- Steel
 - air melt, 45
 - making process, effect on pitting, 47
 - mild low carbon, 12
 - rail, 56
 - stainless bearing balls, 48
 - types: 52100—5,14,15,17,45,47,51,60,61,66; 4620—7; 4340—7; Halmo—51; M-50—21,22,47,61; M-1—24,44,51, 59; MV-1—5,14; 440 C stainless—58; M-2—58
- Strain
 - accumulation: under cyclic loading, 34; related to fatigue life, 56
 - cyclic plastic, 61
 - nature of distribution in rolling, 62
 - rate of accumulation, 63
- residual shear, 34
- uniaxial repeated, 61
- Stress
 - at surface due subsurface crack, 10,12
 - complimentary normal, 16,17
 - concentration at roller ends, 50,52
 - critical in rolling contact, 7,16,17,18,45
 - cycles per bearing revolution, 23
 - essential shear, 16,18
 - maximum contact, 7,13,16,19
 - state of, 29
- Stress distribution: due partial load on infinite strip, 12; effect of plastic flow on, 12
- Subsurface
 - cracks, 9,10,45,50,55
 - distortion and plastic flow, 9,58,33,61
 - metallurgical transformation, 45
 - microhardness surveys, 58
- Surface
 - asperity, 67
 - compliance, 68
 - corrugation, 61
 - cracks, 9,10,49
 - distortion due to rolling, 33
 - finish, 20,66
 - tensile stress, 9
- Tangential traction or friction
 - effect on cumulative plastic deformation, 52
- Thermal stress, 53
- Thermoplastics, 66
- Timken plastic deformation data, 13,15
- Tin, 28
- Toroid rollers, 5,7,16,18
- Torsion fatigue data, 10,18,19,50; tests under hydrostatic fluid pressure, 10,16,17
- Trace elements, 45
- Trigonometric relations
 - original and deformed dimensions for elastically restrained plastic deformation, 27
 - perfectly plastic grooving, 59
 - pronounced plastic deformation, 26
- U.S.Naval Eng. Exp. Sta. (Annapolis)
 - specimens and materials, 14
 - toroid and cylinder bench rig tests, 4,18,19,22
 - track width data, 13
- Vacuum melting, 50
- Vanadium trace element, 45
- Velocity profile in lubricant film, 68
- Vibration: due "run-out", 58; from original imperfections, 41
- Viscosity
 - effect on: coefficient of friction (rolling), 65; pitting fatigue limit, 49; pitting life, 46,48
 - index, 48
 - variation with: pressure, 48,55; with temperature, 55, 67
- Viscoelastic
 - body, fundamental equations for, 54
 - effects in lubricating oils, 67
 - indentation solution, 52
 - two-dimensional rolling solution, 52
- Viscometer, 51
- Water contamination in mineral oil lubricants, 48
- Water lubrication of rail steels, 56
- Wear, 25; contrasted to plastic deformation, 27,30,31, 58,59; effect of hardness on, 59
- Weibull
 - analysis of material strength, 15
 - cumulative distribution function, 11
 - deviations from, 57
 - presentation of bearing pitting data, 11,23,47,51
 - probability paper, 5
 - slope, 11,19,22
 - "weakest link" concept, 11
- Work hardening in copper by rolling, 28
- X-ray measurement of film thickness, 53
- Yield criterion, 62
- Yield strength of rolling bodies, 26
- Yield stress, 29
- Yielding at high contact stress, 21

This page is intentionally blank.

PUBLICATIONS OF THE COLLEGE OF ENGINEERING

Bulletins from the University of Illinois College of Engineering are detailed reports of research results, seminar proceedings, and literature searches. They are carefully reviewed before publication by authorities in the field to which the material pertains, and they are distributed to major engineering libraries throughout the world. They are available at a charge approximately equal to the cost of production.

The annual *Summary of Engineering Research* is available in the fall of each year. It contains a short report on every research project conducted in the College during the past fiscal year, including the names of the researchers and the publications that have resulted from their work. It is available free of charge.

Engineering Outlook, the College's monthly newsletter, contains short articles about current happenings, new research results, recent technical publications, and educational practices in the College of Engineering. Free subscriptions are available upon request.

The Seminar and Discussion Calendar, which is published and distributed weekly, lists current meetings, lectures, and other events on the engineering campus that are open to the public. Free subscriptions are available upon request.

Requests for a catalog of available technical bulletins or for any of the above publications should be addressed to the Engineering Publications Office, College of Engineering, University of Illinois, Urbana, Illinois 61803.

